Responses and proposed changes to referees for gmd-2016-301

Matthias Forkel, Wouter Dorigo, Gitta Lasslop, Irene Teubner, Emilio Chuvieco and Kirsten Thonicke

Note to formatting: *We repeat referee comments in italics and orange*. Author responses are in normal font. Our proposed changes to the manuscript are coloured blue. Cross-references to figures in the initial discussion manuscript and in the response letter are indicated as Figure # and Figure R#, respectively. References to line numbers refer to the initial discussion manuscript.

1 Response to Anonymous Referee #1

Our response to Anonymous Referee #1 is published online in the interactive discussion at https://www.geosci-model-dev-discuss.net/gmd-2016-301/.

In response to referee 1, we include Figure A1 in the appendix of the manuscript and add a paragraph on the pre-selection of predictor variables in chapter 2:

"We used datasets of global monthly burned area as response variable and several datasets on land cover, climate, soil moisture, vegetation state, and socioeconomic factors as predictor variables in model development. To make pre-selection of relevant predictor variables, we first tested the predictive performance of various candidate variables such as absolute values, anomalies, or long-term precedent mean values of precipitation, wet days, soil moisture, or vegetation state (Figure A1). We generally found a higher importance of the absolute variables than of the anomalies. For the development of SOFIA models, we finally selected the set of predictor variables based on their importance, their interpretability, and based on how closely they are related to fire activity (by avoiding variables that account for indirect effects) (Table 1)."

2 Response to Anonymous Referee #2

The authors simulate fraction burned area at the global scale using a flexible modelling approach that is fed by climate and satellite-derived data. The topic is relevant because fire is an important component of the Earth System, and improving our estimates of fire activity can improve our capability of the Earth System itsefl. Nevertheless, I have serious doubts that the way the study is designed will help move the body of knowledge of fire in the Earth System forward.

Dear Referee 2, we are grateful for the critical review that will help to improve the quality of the manuscript. Given the contrasting assessments of our study from referees 1 and 2, apparently the scientific community does not unanimously question the contribution of our approach to moving forward the body of knowledge of fire in the Earth system. However, we also acknowledge that we may have given the wrong impression that our approach aims to provide a complete and detailed assessment of controlling factors of fire activity in the Earth system. Such an assessment is beyond the scope of our study and also beyond the primary scope of model description papers in GMD. Thus, to avoid overambitious claims and to make the aims of our study more clearly we propose to rewrite the sentence at line 94-98 as follows:

"Here we aim to describe and apply a flexible data-driven fire modelling approach, called SOFIA (Satellite Observations for FIre Activity). The SOFIA approach provides a framework to identify the importance and the functional relationships between observational datasets and the spatial and temporal variability of burned area while revealing model formulations that could be easily adapted for more complex vegetation-fire models. We test the approach using observational datasets of land cover, climate conditions, soil moisture, vegetation state, and socioeconomics."

At some point in the work it seems like the authors are adding variables to a box without clearly understanding their relation \ interaction with fire activity. In my opinion, this does not move the body of knowledge forward. In- stead this is an exploratory approach that could be used to identify important variables and relation forms (or structures), although I don't think it will ever "identify required model structures". In my opinion the work would benefit by a more constrained anal- ysis instead of adding too many things to a box and trying to make sense of it in the end.

We fully agree with the referee that our study did not "identify required model structures". Instead, our study proposes a data-driven modelling approach that can be used as a tool to reach this goal. Therefore, we intentionally used the term "identifying" instead of "identification" in the title. Indeed, we follow an exploratory or data-driven approach to identify important variables and their relationships with burned area. We would like to point out that we follow a different paradigm in model development than in classical model development. Classical model development follows phases of data acquisition (measurements or data collection), and the development of conceptual, mathematical, and computational models (Gupta et al., 2012). Thereby, the development of the mathematical and computational models are based on the conceptual model, i.e. based on assumptions or theories about how a system works. In contrary, we are here following a data-driven approach (also referred as reverse approach or reverse engineering) (Solomatine and Ostfeld, 2008). In the data-driven approach, the conceptual model is developed after adequate mathematical and computational models have been inferred from the data (Gupta et al. 2012). Adequate models as identified by data-driven approaches or in model optimization experiments are also referred to as "behavioural" models within the GLUE approach (Beven and Binley, 2014). Thus, the derived mathematical and computational models possibly allow generating new hypotheses about the system. Previously, data-driven approaches based on machine learning methods have been successfully used to identify controlling factors for fire (Aldersley et al., 2011; Archibald et al., 2009; Bistinas et al., 2014). Our work builds on these approaches but aims to go a step further by identifying relations between single variables and burned area (we call this model structures), which could be adopted within more complex fire models or which could form the basis for a new empirical fire model. Of course, such relations cannot be directly transferred to more complex models but likely require re-calibration because ecosystem state variables such as FAPAR or VOD follow different definitions than in the observations or are not available in vegetation models. Following the data-driven paradigm, we intentionally did not (further) constrain our analysis approach. However, we agree with the referee that fire model development could potentially benefit from a hybrid approach, which includes expert knowledge or existing theories and models within the data-driven modelling procedure (Solomatine and Ostfeld, 2008). This is however beyond the scope of our study.

We propose to make clearer that we aim to describe and apply a data-driven approach of model development but that we don't aim to provide a complete understanding of controls and mechanisms for fire activity. First, we suggest changing the title of the manuscript:

"A data-driven approach to identify controls on global fire activity from satellite and climate observations (SOFIA V1)"

Secondly, we propose to rewrite lines 63-77 of the Introduction:

"Despite such recent model developments, it is not clear which functional relationships, complexity, and model parametrizations are most adequate to represent fire activity (Hantson et al., 2016).

Satellite observations of fire activity can be further integrated with fire models to estimate model parameters or to assess the adequacy of functional relationships (Knorr et al., 2014; Lasslop et al., 2015; Le Page et al., 2015). For example, parameters of empirical relations were optimized in SIMFIRE (simple fire model) to predict annual fire frequency from vegetation conditions, fire weather conditions, and population density (Knorr et al., 2014). Such parameter optimization approaches are one aspect of model-data integration or model-data fusion that encompasses a continuous cycle from the definition of model structures (i.e. predictor variables and functional relationships), estimation of model parameters, generalization or upscaling of the model, evaluation of model results, to model application and potentially back to a reformulation of the model structure (Keenan et al., 2011; Williams et al., 2009). However, a full model-data integration cycle has been rarely applied in the development of global fire models.

In comparison to process-oriented global vegetation-fire models, data-driven approaches provide an alternative framework to understand and model climate, vegetation, and socioeconomic controls on fire activity. While the development of mathematical and computational process-oriented vegetation-fire models usually starts from a conceptual model (Gupta et al., 2012), data-driven approaches aim to derive mathematical and computational models directly from the data (Solomatine and Ostfeld, 2008). In data-driven approaches, algorithms from artificial intelligence (e.g. neural networks), machine learning (e.g. random forest), or evolutionary algorithms (e.g. genetic optimization) are applied to predict a response variable (here burned area, or fire counts) from a set of potential predictor variables (Solomatine and Ostfeld, 2008). If an adequate data-driven model has been derived, the importance of individual variables and the sensitivities of the response variable to the predictor variables allow to develop a conceptual model about the studied system (Solomatine and Ostfeld, 2008). In global fire modelling, data-driven fire models have been developed using machine learning algorithms such as generalized linear models (Bistinas et al., 2014), maximum entropy (Parisien et al., 2016), or random forest (Aldersley et al., 2011; Archibald et al., 2009) mainly to identify controls on fire activity. However, such machine learning models often have complex structures, are seen as "black boxes", and thus cannot be easily adapted or even implemented within process-oriented global vegetation/fire models. Alternatively, empirical fire models like SIMFIRE (Knorr et al., 2014) could be generalized to integrate several different candidate predictor variables and to then assess the importance and functional relationships. Consequently, such a flexible data-driven but functional fire modelling approach would allow exploring different predictor variables similar as in machine learning algorithms while potentially revealing model structures that can be more easily adapted for process-oriented vegetation-fire models."

Some major comments:

1) The equifinality in the modelling approach is clear. Choosing 1 model from a bunch of good candidate models and identifying the controls of fire activity just misses the whole point. It gets more critical if you think that not all combinations were tested. What would make sense in my opinion would be analyze all valid models and trying to extract relevant information on the most important variables and influential controlling factors. Not sure on how you could do that but perhaps it would be worthwhile to take a look at Keith Beven's work and the GLUE methodology (references below).

Equifinality, i.e. the presence of multiple adequate models and parameter sets that result in very similar responses, is a general problem in environmental modelling (Beven, 2006). It is obvious that equifinality is relevant in our study where we optimize model structures to predict fire activity. Equifinal "behavioural" models can be identified by assessing and comparing the adequacy of model structures (Gupta et al., 2012) and by assessing parameter covariances (Beven and Binley, 2014). General approaches to identify behavioural models and to avoid equifinal models are the use of multiple datasets of the same variable to account for errors or uncertainties in model forcing or reference data, the testing of different cost functions to constrain certain parameters, the inclusion of prior parameter uncertainties in the cost function, or the application of models to new observational data or under different conditions (Beven, 2006; Beven and Binley, 2014; Williams et al., 2009). The GLUE methodology is a likelihood-based approach to identify behavioural models and to quantify uncertainty in model predictions. Thereby, uncertainty quantification usually depends on the optimization of model parameters using global search algorithms such as Monte Carlo or evolutionary algorithms. Similarly, we also used an evolutionary algorithm (i.e. genetic optimization using derivatives (Mebane and Sekhon, 2011)) to train each SOFIA candidate model. Within GLUE, prior parameter uncertainties are often used to constrain the likelihood of each model. Contrary, we intentionally did not use prior parameter uncertainties in the estimation of SOFIA model parameters because #1 we intentionally did not want to constrain the analysis and #2 because prior parameter values and uncertainties were not available for SOFIA models. However, our results allow extracting parameter values and ranges for each functional relationship that could be used as prior parameter values in a potentially more constrained analysis. For example, parameters that control the functional relationship to NLDI, to DTR and WET in shrublands, and to VOD were well constrained in the SOFIA model SF.124421 (Figure R 2).

Besides the use of prior parameter uncertainties, we indeed applied all the approaches to avoid equifinality: We first generated several candidate models and assessed their global adequacy using a sample of grid cells (Table A2). From this analysis, we identified four adequate models that represent global fire dynamics ("best" models, Table 2). We then applied and evaluated these best models based on all global burned area data and by using both the GFED and CCI burned area datasets as reference (i.e. accounting for observational uncertainty) (Fig. 4 and 5). This analysis helped to identify only one model that is adequate in all regions. However, it is true that in savannas, tropical croplands and tropical forests the four best SOFIA models perform relatively equally, i.e. all are adequate models in these regions (Fig. 5). Therefore, controls on fire activity can be analysed from all four models in these regions. As an example, we additionally analysed the controls from all best SOFIA models for Africa and the Mediterranean (Figure R 1).

We propose to include a more detailed discussion on equifinality (from line 704 onwards) and to change the title of chapter 5.1:

"5.1 Performance and equifinality of SOFIA models"

"The four best SOFIA models reached similar performances in savannas and tropical croplands, and in tropical forests which demonstrates the equifinality in fire modelling. Equifinality, i.e. the presence of multiple adequate models and parameter sets that result in very similar responses, is a general problem in environmental modelling (Beven, 2006). General approaches to avoid equifinal models are the use of multiple datasets of the same variable to account for errors or uncertainties in model forcing or reference data, the testing of different cost functions to potentially constrain certain parameters, the inclusion of prior parameter uncertainties in the cost function, or the application of models to new observational data or under different conditions (Beven, 2006; Beven and Binley, 2014; Williams et al., 2009). In our analysis, we were able to rule out three from four initially equifinal SOFIA models based on the application of these models to the full global data and by regional comparisons against two burned area datasets. The presence of equifinality in SOFIA model structures suggests to also include prior parameter uncertainties for each functional relationship to better constrain SOFIA models. However, prior parameter estimates and uncertainties were not available as we here applied the SOFIA approach for the first time. The results from the optimized SOFIA models allow extracting parameter values and ranges for each functional relationship. For example, parameters that control the functional relationship to socioeconomic development (NLDI), to diurnal temperature range and to the number of wet days in shrublands, and to VOD were well constrained in the SOFIA model SF.124421 (Figure A3). These parameters could be potentially used as prior parameter values in a more constrained analysis."

We will include Figure R 2 as Figure A 3 in the main text.

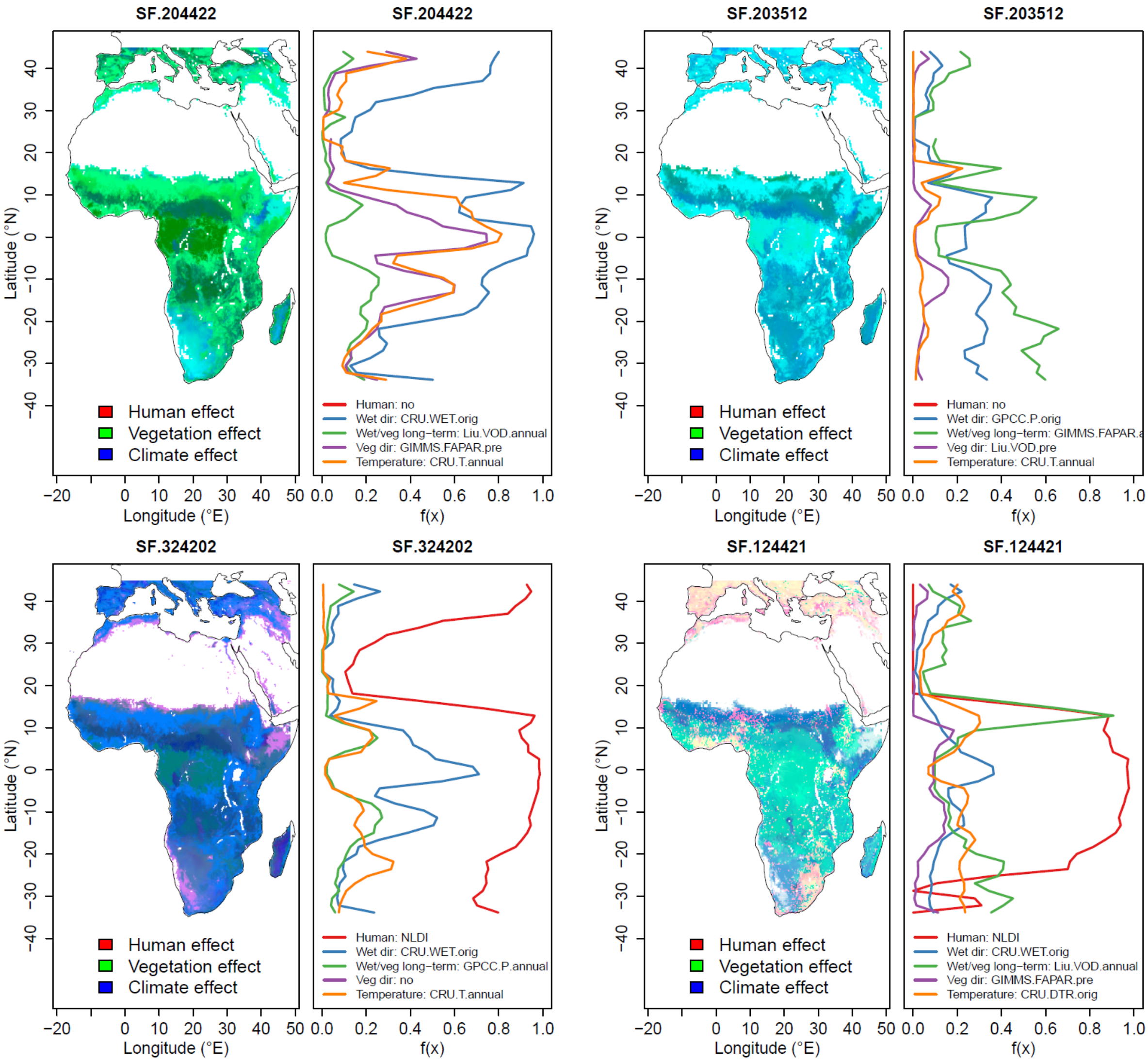

Figure R 1: Equifinality in controls on fire activity from the four best SOFIA models. The maps are RGB composites of the human influence (red), the vegetation effects (green, mean of direct and long-term vegetation effect), and the climate effect (blue, mean of wetness and temperature effect). The spatial variability of each controlling factor is shown as latitudinal gradient where f(x) = 0 and f(x) = 1 indicate fully constrained and maximum fire activity, respectively.

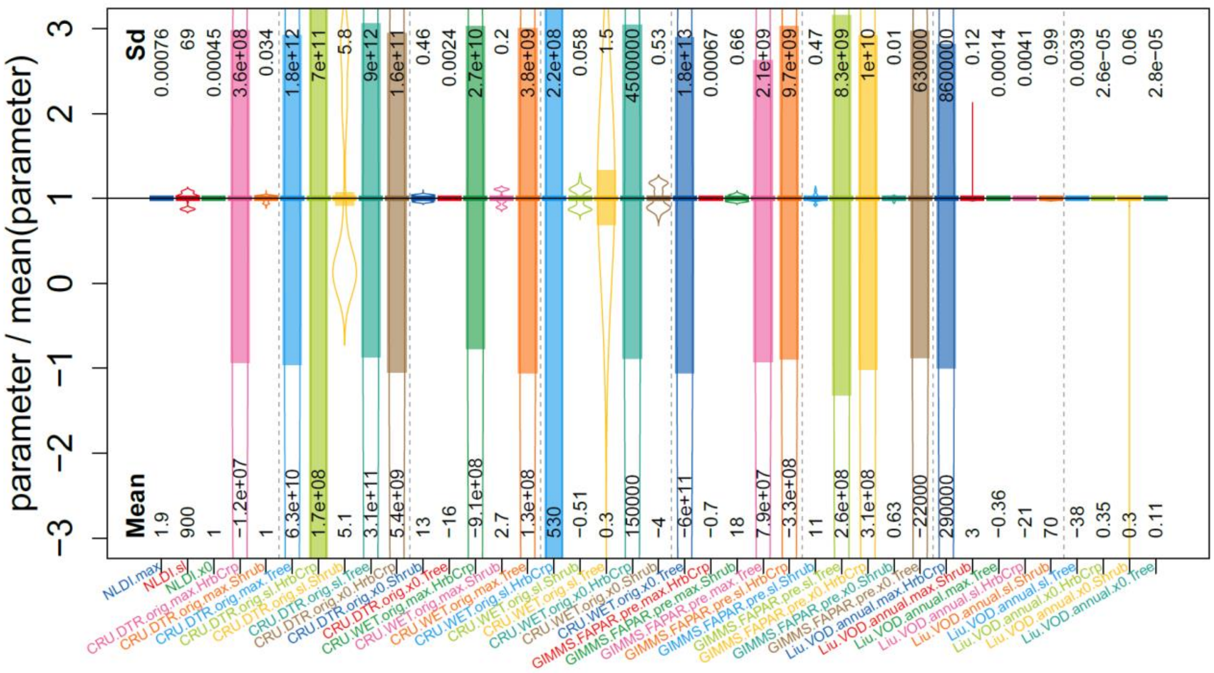

*Figure R 2: Uncertainty in parameters of SF.124421 after genetic optimization. Shown are distributions (outlines), mean values (= 1), and confidence intervals (bars) for mean values for each parameter in SF.124421. Plotted are parameters from equally good-performing parameter sets (i.e. > 0.8 * normalized likelihood NLL, NLL = LL / max(LL) with LL = exp(-cost)).*

2) The spatial resolution is a problem, as you correctly mentioned (L693-698). You are modelling fire closer to the landscape scale than the fire regime scale. To model fire activity at such a fine scale you would need other type of information and confine your analysis to specific regions. I think the work would gain a lot by doing the analysis at coarser resolutions.

Here we used a spatial resolution of 0.25°. This resolution is common to many of the used datasets (e.g. GFED.BA, CCI.SM, VOD) and only slightly higher than that of the highest-resolution global vegetation/fire models (0.5°). We intentionally applied the analysis at the 0.25° resolution because predictor variables need to be spatially averaged for coarser resolution and thereby the variability in land cover and temporal dynamics of weather or vegetation conditions will be reduced as well. Thus using higher resolution data potentially helps to better identify underlying relationships than using coarse resolution data.

3) The work needs a more solid background on how environmental and human factors influence fire patterns. This is absolutely crucial, frames the entire work and I suggest you do this at the beggning of the Introduction. The "effects" described in 3.2 need this background information. Your work assumptions should be clear and supported by the correct literature.

First, we would like to point out again that, according to the data-driven approach of model development we intentionally aim to avoid too many assumptions. We shortly summarized the factors for fire at the beginning of the Introduction (lines 35-39) and describe how different satellite datasets can potentially represent controls on fire (lines 78-93). We hope that with explaining our motivation better, e.g. the main purpose is the description of the SOFIA model approach, this concern is also partly addressed.

4) The work is lacking many important references of relevant past works. Please see the list at the bottom of this document.

Many thanks for these references. Although we were aware about some of these references, we did not include them in the first version of the manuscript to focus on the most relevant for global process-oriented and data-driven fire modelling. We will include the reference at appropriate places. See also our reply to comment #1 where we now refer to the GLUE approach and to comment #5 were we now include references for the importance of agriculture.

5) A proper analysis on the importance of crop inclusion is not made. It seems that there is a compensation between adding explicitly "crops" and adding a "human-related variable". This is strange for several reasons, since fire is used as a tool in croplands all over the globe (see Korontzi et al 2006) both in poor and rich countries, as well in dense or sparsely populated regions (see Li et al. 2013). Mmost importantly you need to better support and investigate this result.

Fires in croplands are mainly used to remove harvest residues or to fertilize soils and thus are indeed an important tool in agriculture. However, 89% to 92% of all global fires occur outside of croplands (Korontzi et al., 2006). Burned area decreased globally with increasing cropland area (Bistinas et al., 2014) and croplands have rather small fire sizes than non-agricultural regions (Hantson et al., 2015). Thus our approach was maybe not sufficiently able to discover the role of agricultural fires because we were using the GFED4 datasets without the correction for small fires. Many global vegetation/fire models do not account for agricultural fires (Hantson et al., 2016; Rabin et al., 2015) because regional practices of agricultural fire use are diverse and cannot be easily parameterized, and because agricultural fires do not directly affect natural vegetation and carbon cycle dynamics (unless agricultural fires escape to nearby forests). Accordingly, we never had the aim to describe mechanisms of fire use within agricultural stands but used the fractional coverage of croplands as predictor for the overall burned area within a grid cell. As the referee correctly states, in this sense the use of either croplands in the land cover grouping scheme or the use of NLDI as human effect on fire activity result in similar model performances. To further investigate the relation between cropland cover and burned area, we analysed the partial dependency of the burned area on the coverage of croplands as predicted by a random forest model (Figure R 5). We found that the relationships between cropland cover and burned area is non-monotonic, non-linear, and varies per biome (Figure R 5, right panel). These patterns are the reason why cropland cover does not add to model performance in SOFIA models that rely on monotonic functional relationships.

We propose to improve the discussion on the role of agricultural fires (lines 707-714):

"The derived SOFIA models and the spatial patterns of sensitivities show a sharp decline of burned area with increasing socioeconomic development or population density and thus agree with previous studies that show a primarily negative effect of human activities, population density, or croplands on burned area (Andela et al., 2017; Archibald et al., 2013; Bistinas et al., 2014; Chuvieco and Justice, 2010; Knorr et al., 2014). Strikingly, our results suggest that human effects on global burned area can be expressed by either cropland area, NLDI, or population density but the combination of these factors did not improve the performances of SOFIA models. These variables serve all as proxies for the negative relationship between humans and burned area but do not directly describe human activities of fire use or suppression. For example, regional studies have shown that various information on infrastructure, land use, and other relevant socioeconomic indicators are important to predict fire activity (Archibald et al., 2009; Arndt et al., 2013; Parisien et al., 2016). However such spatially- and temporally-resolved datasets and assessments are missing for the global scale. Certainly, our results do not imply that croplands are unimportant for the global variability of burned area. Agricultural fires account for around 10% of all global fires (Korontzi et al., 2006) and for around 5% of global burned area (Giglio et al., 2013) and are used to remove harvest residues or to fertilize soils. However croplands show more small fires than large fires (Hantson et al., 2015b). As we here used the GFED burned area datasets that was not corrected for small fires (Giglio et al., 2013), small agricultural fires are likely misrepresented in this dataset and thus cannot be accurately analysed within the SOFIA approach. The representation of agricultural fires in a global fire model needs to account for various land use patterns and practices that go far beyond natural climate-vegetation relationships (Le Page et al., 2015; Magi et al., 2012; Rabin et al., 2015). By taking into account this complexity, agricultural fires are often not represented in global vegetation-fire models because they do not directly affect natural vegetation and carbon cycle dynamics (Hantson et al., 2016), unless agricultural fires escape to nearby forests (Cano-Crespo et al., 2015). In summary, an improved representation of human effects on fire in global vegetation-fire models is currently lacking since globally consistent, temporally and spatial resolved, relevant information on infrastructure and socioeconomics is not available."

Additionally, as you mention in the Discussion, you do not mimic the shape of the function that relates pop. Density with ignitions (e.g. Pechony & Schindell 2009), therefore excluding pop. density is most likely the problem of the model rather the problem of the variable. This in fact trou- bles me because I can make the same question for several other "effects": is the lack of importance of an effect \ variable the consequence of having bad variables and \ or models?

We read the reviewer's statement carefully, but unfortunately cannot agree and see the constellation rather different. In fact, we did not mention this in the Discussion. Indeed, we identified a global decrease of burned area with increasing population density which is in agreement with independent studies (Andela et al., 2017; Bistinas et al., 2014; Knorr et al., 2014) (Figure R 3). Please also note that the SOFIA approach does not explicitly separate fire ignition.

The importance of a variable in our analysis based on SOFIA models is affected by the usage of a variable within a certain model structure, by the observational error of this variable, and by the real-world relevance of this variable for fire activity. The effect of model structures on variable importance is compensated by comparing an ensemble of different model structures. The effects of observational error and real-world relevance of a certain variable on the importance of a variable for model performance is a general challenge in environmental modelling (Beven, 2007; Gupta et al., 2012; Jakeman et al., 2006; Williams et al., 2009) and is not specific to our analysis. We referred to these issues already in our previously proposed changes in response to comments #1 and #5.

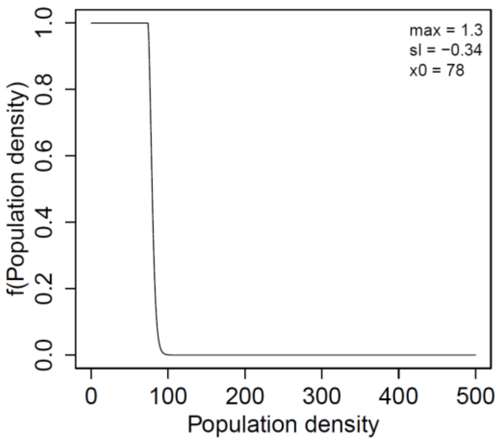

Figure R 3: The response function from the best SOFIA model including population density (SF.314511) globally shows a decline of fire activity with increasing population density, a finding which is in agreement with independent studies (Andela et al., 2017; Bistinas et al., 2014; Knorr et al., 2014).

6) The comparisons of the impact of controlling effects and predictor variables on model performance made along the work are troublesome. I highlight one clear example. The land cover grouping scheme \ classes is especially relevant for your modelling approach, since it controls model performance and model complexity. The analysis that you made does not help the reader to reach a clear conclusion. In one hand, PFTs lead to the best IoAs, on the other hand the additional complexity is extremely penalized. Why don't you make a simple a robust comparison with the same (or similar) degree of complexity? Do you need all classes in all land cover schemes?

Unfortunately, we do not fully understand this comment and the provided example. Contrary to the statement of the referee, our results show that IoA does not depend on the used land cover grouping scheme but we found good performing models in all land cover grouping schemes (Fig. 2 a, Fig. 3 a).

However, the referee is right that our analysis does currently not provide much insight on the question how land cover should be grouped or what land cover classes are required to accurately estimate fire activity. To address this question, we computed another random forest (RF) model only based on the PFT grouping scheme (RF.PFT, i.e. without any variables that account for weather conditions, vegetation conditions, or human influences). With RF.PFT we aim to predict spatial patterns (but not temporal dynamics) of burned area from the spatial distribution of vegetation types. The importance of variables in this RF model provides insight which land cover classes are most important to predict global patterns of burned area. Globally, the most important land cover variables were the coverage of broad-leaved deciduous shrubs (Shrub.BD), broad-leaved evergreen trees (Tree.BE), and broad-leaved deciduous trees (Tree.BD) (Figure R 4). Of lowest importance were the coverages of crops (Crop), needle-leave deciduous trees (Tree.ND), and the ratio of croplands to other vegetation (CropRatio). Again, the low importance of croplands in the RF model might be surprising given the real importance of fire use in croplands but it is a result of the complex, non-monotonic, relations between cropland cover and burned area (Figure R 5). On the contrary, the dependency of burned area on the coverage of broad-leaved deciduous shrubs (which were of highest importance) was mostly monotonic and similar among biomes (Figure R 5). These patterns suggest that cropland cover is an insufficient predictor variable to represent agricultural fire use.

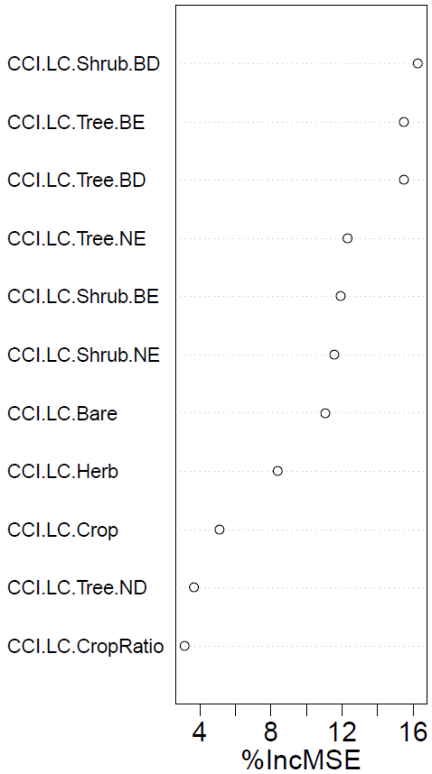

Figure R 4: Importance of variables in a random forest model to predict burned area only from the spatial distribution of land cover classes as expressed by PFTs (RF.PFT). Variables with a higher percentage increment in mean squared error are of higher importance.

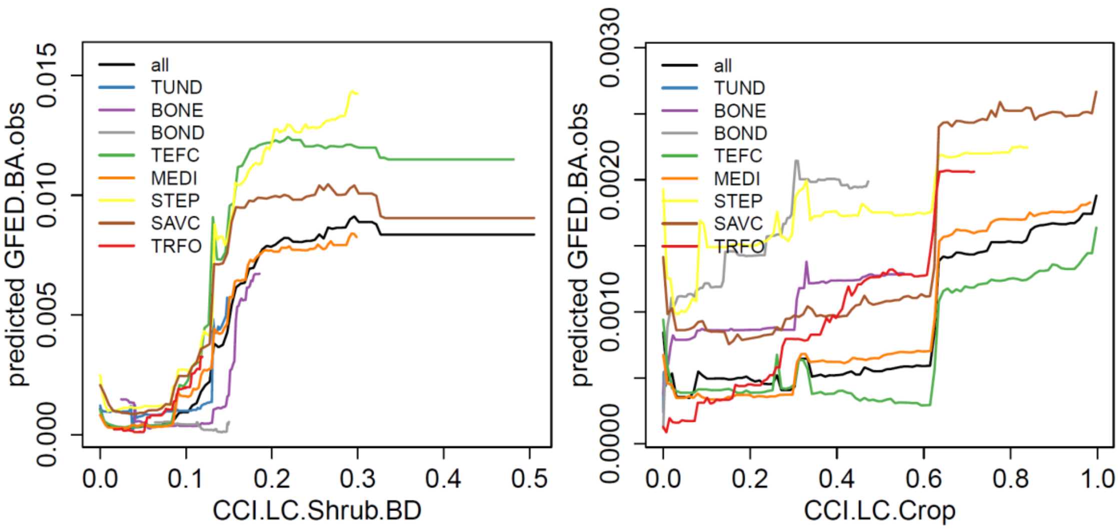

Figure R 5: Partial dependencies of burned area to the fractional coverage of broad-leaved deciduous shrubs (left) and croplands (right) based on a random forest model that is only based on PFTs (RF.PFT). Colours refer to biome-based regions as shown in Figure A1 of the manuscript.

7) The way conclusions are drawn needs to be moderated. You have a "virtual lab" called SOFIA that can help make some experiments, it will not inform you about the truth, certaintly not about what really determines fire activity at the global scale. An example (there are many) is related with the way you interpret the importance or not of separating crops from herbaceous. The only implication is on model performance...not on reality itself. Fires occur in croplands and in herbaceous areas for different reasons, independently of what the importance of the variables or controlling functions points out.

The term "virtual lab" is a very nice description of the SOFIA approach. Sometimes variables might be a good proxy for something that is not well observed. The cropland fraction for instance has been suggested in a linear modelling approach to be an indicator of landscape fragmentation and therefore increases in cropland fraction can reduce fire occurrence (Bistinas et al., 2014). Although such relations are maybe not "true", as it is not the cropland itself that is reducing the fire, it can still be valuable for improving the model's performance. However, our results modify this finding because we show the complexity of cropland-burned area relations by using non-linear modelling approaches. As models are always a simplification of reality, we fully agree that the SOFIA approach or specific SOFIA models cannot inform us about the reality of fire activity. However, we also never claimed that our SOFIA-based results are a description of fire in reality. Especially throughout chapter 4.4 and 5.1, we mention that results are based on the SOFIA model SF.124421 and thus model-dependent.

8) Some contraditory results : RF is better globally although you state that SOFIA outperforms both RF and JBACH. Fig 2 shows clear improvements depending on land cover grouping scheme which is contradicted in L523-524.

The referee likely misunderstood our results. With respect to the first example, RF is only better than SOFIA models because it can use a lot of variables or datasets. However only the RF model RF.124421 is comparable with a SOFIA model because they use the same set of predictor variables (RF.124421 and SF.124421). In this comparison, RF.124421 and SF.124421 reached similar IoA but SF.124421 reached slightly better FV in optimization (Tab. 2). SF.124421 also better reproduced spatial-temporal patterns of annual total burned area at regional scales than RF.124421 (Figure 5). Moreover, the regional comparisons also demonstrate that SOFIA models better reproduce means, distributions, and had higher IoA than more complex RF models (RF2) in many regions (Figure 5). Based on these results, we indeed conclude that SOFIA outperforms the RF models considered in this study.

Also the reviewer's comment on Figure 2 is not quite correct. We cannot see any clear dependency of the SOFIA performance on the used land cover grouping scheme (Fig. 2a).

9) The stratified sampling is necessary and interesting, but confusing. It looks like you stratified in space, per biome (which biomes??), and then on the level of fire activity. Finally you sample in time, correct? I am not sure I totally understood the methodology I suggest you improve the way it is written and take a look at Boschetti et al 2015.

We first computed for all grid cells the maximum annual burned area for all grid cells to stratify the sampling. We then used the regions (biomes) as shown in Fig. A1 (a) to further stratify the sampling. For each region, we determined a number of grid cells that we want to sample based on the area of the region. Then, we computed quantiles ((minimum = q0) < q0.01 < q0.02 < … < q0.99 < (q1 = maximum), increment by 0.01) of the regional annual maximum burned area. We assigned a quantile class (100 classes, e.g. first class for q0 to q0.01) to each grid cell of a region. We then randomly sampled grid cells for each quantile class. These sampled grid cell were then divided into subsets for model training and evaluation as described at lines 355-363. We rewrote the paragraph at lines 343-354:

"We sampled several grid cells from the global datasets (0.25° resolution) to optimize and evaluate all candidate SOFIA models. A sampling of grid cells is necessary to retain enough independent data for evaluation of SOFIA models and because optimization of all SOFIA models on the entire global datasets with 0.25° spatial resolution, monthly time steps, and 15 years was computationally not feasible. However the sampling needs to represent the global spatial patterns and the entire statistical distribution of burned area, including extreme fire events. Therefore, we performed a sampling of grid cells stratified by regions (representing biomes) and by the statistical distribution of burned area. We first computed the maximum annual burned area for all grid cells in 1997-2011 to represent the spatial distribution of extreme fire years. Regions were defined based on land cover and climate zone (Kottek et al., 2006) (Figure A 2). For each region, we classified the annual maximum burned area of each 0.25° grid cell into 100 classes according to regional quantiles of the maximum annual burned area (e.g. class 1 covers quantile 0 (minimum) to quantile 0.01 and the last class covers quantile 0.99 to 1 (maximum) of regional annual maximum burned area). We then randomly sampled grid cells for each regional quantile class. In total, 3161 grid cells were sampled with most of the cells in savannahs and tropical croplands (n = 953, largest region) and fewest cells in boreal needle-leaved deciduous forests (n = 135, smallest region) (Figure A 2 b). Consequently, the sampled grid cells are representative for the global statistical distributions (Figure A 2 c-e) and for spatial patterns of fire activity (Figure A 2 f)."

10) The abstract needs to be completely rewriten, so that the reader can undersand the relevance of the problem, what limitations you identified and are going to tackle, how are you going to tackle these limitations (really missing this one), your major results and finally implications for the evolution of the body of knowledge on this area.

We acknowledge that the abstract is not written in a style that is common for most research articles and therefore may be a bit confusing. This is because our study is a model description paper, where we describe the SOFIA modelling approach, compare it to other models and show a particular application. An increase in the scientific knowledge is not required for articles in GMD. However, we propose to rewrite the abstract in the following way to make the aims of our study more clear:

"Vegetation fires affect human infrastructures, ecosystems, global vegetation distribution, and atmospheric composition. However, the climatic, environmental and socioeconomic factors that control global fire activity in vegetation are only poorly understood and in various complexities and formulations represented in global process-oriented vegetation-fire models. Data-driven model approaches such as machine learning algorithms have successfully been used to identify and better understand controlling factors for fire activity. However, such machine learning models cannot be easily adapted or even implemented within process-oriented global vegetation/fire models. To overcome this gap between machine learning-based approaches and process-oriented global fire models, we here introduce a new flexible data-driven fire modelling approach (Satellite Observations to predict FIre Activity, SOFIA approach version 1). SOFIA models can use several functional relationships between predictor variables and burned area that can be easily adapted with more complex process-oriented vegetation-fire models. We created an ensemble of SOFIA models to test the importance of several predictor variables. Models result in the highest performance in predicting burned area if they account for a direct restriction of fire activity at wet conditions and if they include a land cover-dependent restriction or allowance of fire activity by vegetation density and biomass. The use of vegetation optical depth data from microwave satellite observations, a proxy for vegetation biomass and water content, reaches higher model performance than commonly used vegetation variables from optical sensors. We further analyse spatial patterns of the sensitivity between human, climate, and vegetation predictor variables and burned area . We finally discuss how multiple observational datasets on climate, hydrological, vegetation, and socioeconomic variables together with data-driven modelling and model-data integration approaches can guide the future development of global process-oriented vegetation-fire models."

Some Minor Commnts

11) There are Several terms in the text need to be revised: - fire suppression: Moisture does not suppress fires, it contrains \ reduces \ restricts fire activity (see Bradstock et al 2010) Firefighters suppress fires. - You mention several times "before a fire". You are modeling the occurrence of a fire, if it doesn't happen you still need predecent conditions, so I suggest you drop the term.

We will use the terms "precedent months" and "restriction".

12) NLDIg adds extra parameters depending on the number of land cover groups. Did you consider this in your 100 parameters threshold? Did you consider this in the AIC calculation? Is the calculation shown in L302-303 correct?

The number of extra parameters in NLDI.g were considered in the threshold and in the computation of AIC. The calculation of the number of parameters is correct.

13) Figure 2: Number of variables or number of controlling factors? Maybe I missed something, but each controlling actor can have multiple variables? (e.g. temperature can have both DTR and annual temp?). If not, as I originally understood, then I don't understand that does "number of variables" mean in Figure 2.

Each controlling factor can have only one predictor variable. This implies that the "number of variables" equals the "number of controlling factors".

Some suggestions:

- A pairwise plot between estimated and GFED \ CCI burned area

Pairwise or scatterplots are an intuitive approach for the evaluation of a single model against a reference dataset. However, we need to compare two burned area datasets with four best-performing SOFIA models, two random forest models, and with JSBACH-SPITFIRE. This already results in 14 scatterplots. Additionally, we also want to compare model performance for different regions which further increases the number of scatterplots (14 scatterplots * 7 regions = 98 scatterplots). Thus scatterplots are not an adequate approach for model evaluation given this complexity. Therefore we developed the plot type as in Figure 5 (based on (Phillips, 2017)) which allows us to compare regional statistical distributions, mean values, and the IoA.

- Maps of differences in estimated-observed burned area - A map showing disagreements between GFED and CCI would help frame the evaluation better. (low expectation on areas where both disagree)

Maps can either visualize disagreements in spatial patterns (i.e. difference in mean annual burned area between two datasets), temporal dynamics (i.e. correlation or IoA between two datasets), or statistical distributions (e.g. Kolmogorov-Smirnov statistic or FV between two datasets). We already combined all of this information in Figure 5 that does not only serve for the evaluation of SOFIA models but also clearly highlights regional disagreements between the GFED and CCI datasets.

At this stage I don't think it makes since to go into gramar details.

Copernicus provides a professional language correction service.

The references I mentioned previsouly:

Le Page et al. 2010. Seasonality of vegetation fires as modified by human action: observing the deviation from ecoãA˘Rclimatic fire regimes

Magi et al 2012. Separating agricultural and non-agricultural fire seasonality at regional scales

Le Page et al 2015. HESFIRE: a global fire model to explore the role of anthropogenic and weather drivers.

Li et al 2013 Quantifying the role of fire in the Earth system – Part 1: Improved global fire modeling in the Community Earth System Model (CESM1),.

Bradstock 2010. A biogeographic model of fire regimes in Australia: current and future implications (the "switches" that control fire);

Boschetti et al 2016. A stratified random sampling design in space and time for regional to global scale burned area product validation

Beven & Binley, 1992. The future of distributed models: model calibration and uncertainty pre- diction.

Beven, 2002. Towards a coherent philosophy for modelling the environment.

Beven & Binley, A., 2014. GLUE: 20 years on.

Pettinari & Chuvieco 2016. Generation of a global fuel data set using the Fuel Characteristic Classification System

Rabin et al. 2015 Quantifying regional, time-varying effects of cropland and pasture on vegetation fire (the effects of crops on burned area)

Broxton et al. 2014. A Global Land Cover Climatology Using MODIS Data (for Discussion)

Korontzi et al. 2006. Global distri- bution of agricultural fires in croplands from 3 years of Moderate Resolution Imaging Spectroradiometer (MODIS) data.

References

Aldersley, A., Murray, S. J. and Cornell, S. E.: Global and regional analysis of climate and human drivers of wildfire, Sci. Total Environ., 409(18), 3472–3481, doi:10.1016/j.scitotenv.2011.05.032, 2011.

Andela, N., Morton, D. C., Giglio, L., Chen, Y., Werf, G. R. van der, Kasibhatla, P. S., DeFries, R. S., Collatz, G. J., Hantson, S., Kloster, S., Bachelet, D., Forrest, M., Lasslop, G., Li, F., Mangeon, S., Melton, J. R., Yue, C. and Randerson, J. T.: A human-driven decline in global burned area, Science, 356(6345), 1356–1362, doi:10.1126/science.aal4108, 2017.

Archibald, S., Roy, D. P., Van Wilgen, B. W. and Scholes, R. J.: What limits fire? An examination of drivers of burnt area in Southern Africa, Glob. Change Biol., 15(3), 613–630, doi:10.1111/j.1365-2486.2008.01754.x, 2009.

Archibald, S., Lehmann, C. E. R., Gómez-Dans, J. L. and Bradstock, R. A.: Defining pyromes and global syndromes of fire regimes, Proc. Natl. Acad. Sci., 110(16), 6442–6447, doi:10.1073/pnas.1211466110, 2013.

Arndt, N., Vacik, H., Koch, V., Arpaci, A. and Gossow, H.: Modeling human-caused forest fire ignition for assessing forest fire danger in Austria, IForest - Biogeosciences For., 6(5), 315–325, doi:10.3832/ifor0936-006, 2013.

Beven, K.: A manifesto for the equifinality thesis, J. Hydrol., 320(1–2), 18–36, doi:10.1016/j.jhydrol.2005.07.007, 2006.

Beven, K.: Towards integrated environmental models of everywhere: uncertainty, data and modelling as a learning process, Hydrol Earth Syst Sci, 11(1), 460–467, doi:10.5194/hess-11-460-2007, 2007.

Beven, K. and Binley, A.: GLUE: 20 years on, Hydrol. Process., 28(24), 5897–5918, doi:10.1002/hyp.10082, 2014.

Bistinas, I., Harrison, S. P., Prentice, I. C. and Pereira, J. M. C.: Causal relationships versus emergent patterns in the global controls of fire frequency, Biogeosciences, 11(18), 5087–5101, doi:10.5194/bg-11-5087-2014, 2014.

Chuvieco, E. and Justice, C.: Relations Between Human Factors and Global Fire Activity, in Advances in Earth Observation of Global Change, edited by E. Chuvieco, J. Li, and X. Yang, pp. 187–199, Springer Netherlands, Dordrecht. [online] Available from: http://link.springer.com/10.1007/978-90-481-9085-0_14 (Accessed 24 October 2016), 2010.

Chuvieco, E., Giglio, L. and Justice, C.: Global characterization of fire activity: toward defining fire regimes from Earth observation data, Glob. Change Biol., 14(7), 1488–1502, doi:10.1111/j.1365-2486.2008.01585.x, 2008.

Giglio, L., Randerson, J. T. and van der Werf, G. R.: Analysis of daily, monthly, and annual burned area using the fourth-generation global fire emissions database (GFED4), J. Geophys. Res. Biogeosciences, 118(1), 317–328, doi:10.1002/jgrg.20042, 2013.

Gupta, H. V., Clark, M. P., Vrugt, J. A., Abramowitz, G. and Ye, M.: Towards a comprehensive assessment of model structural adequacy, Water Resour. Res., 48(8), W08301, doi:10.1029/2011WR011044, 2012.

Hantson, S., Pueyo, S. and Chuvieco, E.: Global fire size distribution is driven by human impact and climate: Spatial trends in global fire size distribution, Glob. Ecol. Biogeogr., 24(1), 77–86, doi:10.1111/geb.12246, 2015.

Hantson, S., Arneth, A., Harrison, S. P., Kelley, D. I., Prentice, I. C., Rabin, S. S., Archibald, S., Mouillot, F., Arnold, S. R., Artaxo, P., Bachelet, D., Ciais, P., Forrest, M., Friedlingstein, P., Hickler, T., Kaplan, J. O., Kloster, S., Knorr, W., Lasslop, G., Li, F., Mangeon, S., Melton, J. R., Meyn, A., Sitch, S., Spessa, A., van der Werf, G. R., Voulgarakis, A. and Yue, C.: The status and challenge of global fire modelling, Biogeosciences, 13(11), 3359–3375, doi:10.5194/bg-13-3359-2016, 2016.

Jakeman, A. J., Letcher, R. A. and Norton, J. P.: Ten iterative steps in development and evaluation of environmental models, Environ. Model. Softw., (21), 602–614, 2006.

Knorr, W., Kaminski, T., Arneth, A. and Weber, U.: Impact of human population density on fire frequency at the global scale, Biogeosciences, 11(4), 1085–1102, doi:10.5194/bg-11-1085-2014, 2014.

Korontzi, S., McCarty, J., Loboda, T., Kumar, S. and Justice, C.: Global distribution of agricultural fires in croplands from 3 years of Moderate Resolution Imaging Spectroradiometer (MODIS) data, Glob. Biogeochem. Cycles, 20(2), GB2021, doi:10.1029/2005GB002529, 2006.

Kottek, M., Grieser, J., Beck, C., Rudolf, B. and Rubel, F.: World Map of the Köppen-Geiger climate classification updated, Meteorol. Z., 15(3), 259–263, doi:10.1127/0941-2948/2006/0130, 2006.

Lasslop, G., Hantson, S. and Kloster, S.: Influence of wind speed on the global variability of burned fraction: a global fire model's perspective, Int. J. Wildland Fire, doi:10.1071/WF15052, 2015.

Le Page, Y., Morton, D., Bond-Lamberty, B., Pereira, J. M. C. and Hurtt, G.: HESFIRE: a global fire model to explore the role of anthropogenic and weather drivers, Biogeosciences, 12(3), 887–903, doi:10.5194/bg-12-887-2015, 2015.

Li, F., Levis, S. and Ward, D. S.: Quantifying the role of fire in the Earth system – Part 1: Improved global fire modeling in the Community Earth System Model (CESM1), Biogeosciences, 10(4), 2293–2314, doi:10.5194/bg-10-2293-2013, 2013.

Mebane, W. R. and Sekhon, J. S.: Genetic Optimization Using Derivatives: The rgenoud Package for R, J. Stat. Softw., 42(11), 2011.

Moritz, M. A., Parisien, M.-A., Batllori, E., Krawchuk, M. A., Van Dorn, J., Ganz, D. J. and Hayhoe, K.: Climate change and disruptions to global fire activity, Ecosphere, 3(6), 1–22, doi:10.1890/ES11-00345.1, 2012.

Parisien, M.-A., Miller, C., Parks, S. A., DeLancey, E. R., Robinne, F.-N. and Flannigan, M. D.: The spatially varying influence of humans on fire probability in North America, Environ. Res. Lett., 11(7), 075005, doi:10.1088/1748-9326/11/7/075005, 2016.

Phillips, N.: yarrr: A Companion to the e-Book "YaRrr!: The Pirate's Guide to R." [online] Available from: https://cran.r-project.org/web/packages/yarrr/index.html (Accessed 5 September 2017), 2017.

Rabin, S. S., Magi, B. I., Shevliakova, E. and Pacala, S. W.: Quantifying regional, time-varying effects of cropland and pasture on vegetation fire, Biogeosciences, 12(22), 6591–6604, doi:10.5194/bg-12-6591-2015, 2015.

Solomatine, D. P. and Ostfeld, A.: Data-driven modelling: some past experiences and new approaches, J. Hydroinformatics, 10(1), 3–22, doi:10.2166/hydro.2008.015, 2008.

Williams, M., Richardson, A. D., Reichstein, M., Stoy, P. C., Peylin, P., Verbeeck, H., Carvalhais, N., Jung, M., Hollinger, D. Y., Kattge, J., Leuning, R., Luo, Y., Tomelleri, E., Trudinger, C. M. and Wang, Y. P.: Improving land surface models with FLUXNET data, Biogeosciences, 6(7), 1341–1359, doi:10.5194/bg-6-1341-2009, 2009.

A data-driven approach to identify controls on global fire activity from satellite and climate observations (SOFIA V1)

Matthias Forkel[1], Wouter Dorigo[1], Gitta Lasslop[2], Irene Teubner[1], Emilio Chuvieco[3] and Kirsten Thonicke[4]

[1] Remote Sensing Research Group, Department of Geodesy and Geoinformation, Technische Universität Wien, Gusshausstraße 27-29, 1040 Vienna, Austria
[2] Max Planck Institute for Meteorology, Bundesstr. 53, 20146 Hamburg, Germany
[3] Department of Geology, Geography and the Environment, University of Alcalá, Colegios 2, 28801 Alcalá de Henares, Spain
[4] Potsdam Institute for Climate Impact Research, Telegraphenberg A62, 14412 Potsdam, Germany

Correspondence to: Matthias Forkel (matthias.forkel@geo.tuwien.ac.at)

Abstract

Vegetation fires affect human infrastructures, ecosystems, global vegetation distribution, and atmospheric composition. However, the climatic, environmental and socioeconomic factors that control global fire activity in vegetation are only poorly understood, and in various complexities and formulations represented in global process-oriented vegetation-fire models. Data-driven model approaches such as machine learning algorithms have successfully been used to identify and better understand controlling factors for fire activity. However, such machine learning models cannot be easily adapted or even implemented within process-oriented global vegetation/fire models. To overcome this gap between machine learning-based approaches and process-oriented global fire models, we here introduce a new flexible data-driven fire modelling approach (Satellite Observations to predict FIre Activity, SOFIA approach version 1). SOFIA models can use several predictor variables and functional relationships to estimate burned area that can be easily adapted with more complex process-oriented vegetation-fire models. We created an ensemble of SOFIA models to test the importance of several predictor variables. SOFIA models result in the highest performance in predicting burned area if they account for a direct restriction of fire activity at wet conditions and if they include a land cover-dependent restriction or allowance of fire activity by vegetation density and biomass. The use of vegetation optical depth data from microwave satellite observations, a proxy for vegetation biomass and water content, reaches higher model performance than commonly used vegetation variables from optical sensors. We further analyse spatial patterns of the sensitivity between anthropogenic, climate, and vegetation predictor variables and burned area. We finally discuss how multiple observational datasets on climate, hydrological, vegetation, and socioeconomic variables together with data-driven modelling and model-data integration approaches can guide the future development of global process-oriented vegetation-fire models.

1 Introduction

Wildland fires are important disturbances in the Earth system which affect ecosystems, global vegetation distribution, infrastructures and human assets, and contribute to atmospheric composition through the release of aerosols, reactive trace gases, and greenhouse gases (Bowman et al., 2011). The ignition and spread of fires in ecosystems depend on the availability and properties of fuel (i.e. biomass and litter loads, composition, and moisture content), weather conditions, and human activities (Krawchuk and Moritz, 2011; Moritz et al., 2012). Human activities have a predominant role in fire ignition, and affect fire behaviour either directly through fire restriction or indirectly through land management and landscape structure (Bowman et al., 2011). Burned area is a key variable to describe fire impacts on ecosystems and vegetation distribution (Bond, 2005), and to estimate fire emissions (Seiler and Crutzen, 1980). Recent estimates of average yearly global burned area range from 3.3 to 3.8 million km^2 (Chuvieco et al., 2016; Giglio et al., 2013) which is around 4 % of the global vegetated area

Deleted: Identifying required model structures
Deleted: predict
Deleted: data
Formatted: Font color: Auto
Deleted: In particular, extreme fire conditions can cause devastating impacts on ecosystems and human society and dominate the year-to-year variability in global fire emissions.
Deleted: and consequently it is unclear which components, structures, and
Deleted: are required
Deleted: vegetation/fire models to accurately predict fire activity at a global scale. Here we introduce the SOFIA
Deleted: for
Deleted:) modelling
Deleted: , which integrates
Deleted: satellite
Deleted: climate datasets and different empirical model structures to systematically identify required structural components in global vegetation/fire models to predict
Deleted: . Models
Deleted: the spatial patterns and temporal variability of
Deleted: suppression
Deleted: suppression
Deleted: new
Deleted: The SOFIA approach implements and confirms conceptual models where fire activity follows a biomass gradient and is modulated by moisture conditions. The use of datasets on population density or socioeconomic development do not improve model performances, which indicates that the complex interactions of human fire usage and management cannot be realistically represented by such datasets. However, the best SOFIA models outperform a highly flexible machine learning approach and the state-of-the art global process-oriented vegetation/fire model JSBACH-SPITFIRE. Our results suggest using
Deleted: to
Deleted: /fire models and to better understand the interactions between fire and hydrological, ecological, and atmospheric Earth system components
Formatted: Font color: Auto
Deleted: (Bowman et al., 2009).
Deleted: suppression

(Randerson et al., 2012). On a global scale, burned area shows only a small inter-annual variability which is stabilized by the annual recurrent patterns of very large burned areas in African savannahs (Giglio et al., 2013). However, in boreal, temperate and tropical regions, burned area has a very high inter-annual variability which is strongly linked to the variability in atmospheric circulation patterns, e.g. to El Niño events (Andela and van der Werf, 2014; Balzter et al., 2005; Giglio et al., 2013; Hess et al., 2001). Such years with extreme fire activity in forests can cause large emissions of greenhouse gases (Kasischke and Bruhwiler, 2002; Vinogradova et al., 2015), dominate together with peatland fires the inter-annual variability of global fire emissions (Page et al., 2002; van der Werf et al., 2006, 2010), and thus strongly affect atmospheric composition (Langenfelds et al., 2002; Simpson et al., 2006). Consequently, a realistic simulation of the spatial and temporal variability of burned area is necessary in Earth System Models (ESMs) and Dynamic Global Vegetation Models (DGVMs) to adequately assess current and future fire impacts on the Earth system.

Satellite observations of burned area or of active fires can be used to develop, evaluate, or improve process-oriented global vegetation-fire models (Poulter et al., 2015b). The first fire modules within DGVMs like GlobFIRM (global fire model, Thonicke et al. (2001)) were developed in the late 1990s and early 2000s in absence of global burned area datasets as reference. Later, regional satellite-derived burned area datasets were used to evaluate new developed global fire models such as SPITFIRE (SPread and InTensity of FIRE, Thonicke et al. (2010)). The first global burned area datasets were derived in the mid-2000s from several optical satellite sensors such ATSR (Simon et al., 2004), MODIS (Roy et al., 2005), and SPOT (Grégoire et al., 2003; Tansey et al., 2008). The increasing temporal coverage of satellite observations enables to derive multi-year harmonized burned area datasets like the products from the Global Fire Emissions Database (GFED) (Giglio et al., 2010, 2013) or from the European Space Agency (ESA) Climate Change Initiative (CCI) on fire (Fire CCI) (Chuvieco et al., 2016). Consequently, global burned area datasets are nowadays commonly used within model benchmarking systems (Kelley et al., 2013) or to evaluate further developments in process-oriented vegetation-fire models (Kloster et al., 2010; Lasslop et al., 2014; Yue et al., 2014). Despite such recent model developments, it is not clear which functional relationships, complexity, and model parametrizations are most adequate to represent fire activity (Hantson et al., 2016).

Satellite observations of fire activity can be further integrated with fire models to estimate model parameters or to assess the adequacy of functional relationships (Knorr et al., 2014; Lasslop et al., 2015; Le Page et al., 2015). For example, parameters of empirical relations were optimized in SIMFIRE (simple fire model) to predict annual fire frequency from vegetation conditions, fire weather conditions, and population density (Knorr et al., 2014). Such parameter optimization approaches are one aspect of model-data integration or model-data fusion that encompasses a continuous cycle from the definition of model structures (i.e. predictor variables and functional relationships), estimation of model parameters, generalization or upscaling of the model, evaluation of model results, to model application and potentially back to a reformulation of the model structure (Keenan et al., 2011; Williams et al., 2009). However, a full model-data integration cycle has been rarely applied in the development of global fire models.

In comparison to process-oriented global vegetation-fire models, data-driven approaches provide an alternative framework to understand and model climate, vegetation, and socioeconomic controls on fire activity. While the development of mathematical and computational process-oriented vegetation-fire models usually starts from a conceptual model (Gupta et al., 2012), data-driven approaches aim to derive mathematical and computational models directly from the data (Solomatine and Ostfeld, 2008). In data-driven approaches, algorithms from artificial intelligence (e.g. neural networks), machine learning (e.g. random forest), or evolutionary algorithms (e.g. genetic optimization) are applied to predict a response variable (here burned area, or fire counts) from a set of potential predictor variables (Solomatine and Ostfeld, 2008). If an adequate data-driven model has been derived, the importance of individual variables and the sensitivities of the response variable to the predictor variables allow to develop a conceptual model about the studied system (Solomatine and Ostfeld, 2008). In global fire modelling, data-driven fire models have been developed using machine learning algorithms such as generalized linear models (Bistinas et al., 2014), maximum entropy (Parisien et al., 2016), or random forest (Aldersley et al., 2011; Archibald et al., 2009) mainly to

Deleted: such as

Deleted: (Andela and van der Werf, 2014; Balzter et al., 2005; Giglio et al., 2013; Hess et al., 2001)

Formatted: Complex Script Font: Times New Roman, 12 pt, English (United Kingdom)

Deleted: Consequently, to realistically assess current and future fire impacts on the Earth system it is necessary to realistically simulate

Deleted: system models

Deleted: or dynamic global vegetation models

Deleted:).

Formatted: Font: +Body (Times New Roman)

Deleted: /

Deleted: in order to better simulate fire impacts on terrestrial vegetation distribution and global carbon cycling

Deleted: spread

Deleted: intensity

Deleted: fire

Deleted: , e.g.

Deleted: (Kloster et al., 2010; Lasslop et al., 2014; Yue et al., 2014)

Deleted: Additionally, satellite and other observation-based datasets on climate, vegetation, and socioeconomic factors

Deleted: increasingly used

Deleted: identify controls on

Deleted: and to develop and parameterize empirical fire models (Aldersley et al., 2011; Archibald et al., 2009; Bistinas et al., 2014; Chuvieco et al., 2008; Lasslop et al., 2015; Lehsten et al., 2010; Moritz et al., 2012).

Formatted: Font: Times New Roman, English (United Kingdom)

Formatted: Font: (Default) Times New Roman, Complex Script Font: Times New Roman, 12 pt

Formatted: Font: (Default) Times New Roman, Complex Script Font: Times New Roman, 12 pt

Deleted: uses empirical relations

Formatted: Font: (Default) Times New Roman, Complex Script Font: Times New Roman, 12 pt

Deleted: (Knorr et al., 2014). The development of SIMFIRE followed for the first time in global fire modelling a

Formatted: Font: (Default) Times New Roman, Complex Script Font: Times New Roman, 12 pt

Deleted: (

Formatted: Font: (Default) Times New Roman, Complex Script Font: Times New Roman, 12 pt

Deleted:) approach where model parameters are estimated based on observations within a formal framework (Keenan et al., 2011; Williams et al., 2009). Moreover, model-data integration

Formatted: Font: (Default) Times New Roman, Complex Script Font: Times New Roman, 12 pt

Deleted: relations

Formatted: Font: (Default) Times New Roman, Complex Script Font: Times New Roman, 12 pt

Deleted: (Williams et al., 2009). Global process-oriented vegetation/fire models use currently various model structures and ...

Deleted: Satellite observations

Formatted ...

Deleted: several datasets on vegetation and moisture conditions ...

Formatted ...

identify controls on fire activity. However, such machine learning models often have complex structures, are seen as “black boxes”, and thus cannot be easily adapted or even implemented within process-oriented global vegetation/fire models. Alternatively, empirical fire models like SIMFIRE (Knorr et al., 2014) could be generalized to integrate several different candidate predictor variables and to then assess the importance and functional relationships. Consequently, such a flexible data-driven but functional fire modelling approach would allow exploring different predictor variables similar as in machine learning algorithms while potentially revealing model structures that can be more easily adapted for process-oriented vegetation-fire models.

Satellite observations provide several datasets on vegetation and moisture conditions that can be used as predictor variables in data-driven fire models. Time-variant biomass datasets would be the first choice to represent fuel loads in empirical fire models because the availability of fuel is a prerequisite for fire activity (Krawchuk and Moritz, 2011). However, current global biomass maps are static (Avitabile et al., 2016; Saatchi et al., 2011; Thurner et al., 2014) and thus provide only limited information for fire modelling. Consequently, other proxies of vegetation biomass such as model-based net primary production (NPP) (Bistinas et al., 2014; Moritz et al., 2012), satellite-derived vegetation cover (Bistinas et al., 2014; Lehsten et al., 2010), or the fraction of absorbed photosynthetic active radiation (FAPAR) (Knorr et al., 2014) have been used as proxies for fuel loads in global empirical fire models. As an alternative, satellite retrievals of vegetation optical depth (VOD) might be used as proxy for fuel loads. VOD is a vegetation variable that is derived from active or passive microwave satellite observations and is related to vegetation density and water content (Liu et al., 2011b, 2013a, Vreugdenhil et al., 2016a, 2016b). VOD has a higher sensitivity to forest biomass than FAPAR (Andela et al., 2013) and was used to estimate temporal changes in biomass (Liu et al., 2015). Thus VOD might be a valuable predictor variable for the biomass-driven variability in fire activity. Satellite datasets of surface soil moisture might be valuable proxies for the moisture of surface fuels in empirical fire models (Krueger et al., 2015, 2016) because they represent the top ~3 cm of the soil (Dorigo et al., 2015). Such datasets might potentially provide useful information for empirical fire models to represent fuel loads, fuel moisture, or fire weather conditions.

Here we aim to describe and apply a flexible data-driven fire modelling approach, called SOFIA (Satellite Observations for FIre Activity). The SOFIA approach provides a framework to identify the importance and the functional relationships between observational datasets and the spatial and temporal variability of burned area while revealing model formulations that could be easily adapted for more complex vegetation-fire models. We test the approach using observational datasets of land cover, climate conditions, soil moisture, vegetation state, and socioeconomics. Based on the philosophy of model-data integration, we generated several different candidate model structures and optimized and evaluated each model against observed burned area time series. Additionally, we simulated global burned area with the random forest machine learning approach and with a process-oriented vegetation-fire model (JSBACH-SPITFIRE) to compare the performance of the derived SOFIA models with two independent state-of-the art data-driven and process-oriented modelling approaches, respectively. We used random forest to test if a more flexible modelling approach than SOFIA results in higher performances. In comparison to random forest, SOFIA has the advantage that it could be easily transferred to or implemented in global process-oriented vegetation-fire models. The SPITFIRE fire module within the JSBACH (Jena scheme for biosphere-atmosphere coupling in Hamburg) land surface model (Lasslop et al., 2014; Rabin et al., 2016) was used to compare SOFIA results with a global process-oriented vegetation-fire model.

We first describe the observational datasets and the derived variables that we used to develop SOFIA models (Sect. 2). Secondly, we describe the SOFIA approach and the JSBACH-SPITFIRE and random forest modelling approaches (Sect. 3). In Section 4, we first present the global performance and complexity of SOFIA models (Sect. 4.1) and how several predictor variables contribute to model performance (Sect. 4.2). Then we compare the best performing SOFIA models globally against random forest and JSBACH-SPITFIRE (Sect. 4.3) and apply the best SOFIA model to explore spatial patterns of the sensitivity between predictor variables and burned area (Sect. 4.4). Finally, we discuss the performance and equifinality of our results (Sect. 5.1), the importance of certain predictor variables for global fire modelling (Sect 5.2), and suggest the use of multiple

Deleted: in global empirical fire models. Although time
Deleted: ,
Deleted: (Avitabile et al., 2016; Saatchi et al., 2011; Thurner et al., 2014)
Deleted: So far, it has not yet been systematically tested what variables provide the best
Deleted: In this study,
Formatted: Font: (Default) Times New Roman, Complex Script Font: Times New Roman, 12 pt
Deleted: identify what model structures
Formatted: Font: (Default) Times New Roman, Complex Script Font: Times New Roman, 12 pt
Deleted: complexities are required to predict global spatial patterns and temporal dynamics of burned area. For this purpose, we develop
Formatted: Font: (Default) Times New Roman, Complex Script Font: Times New Roman, 12 pt
Deleted: new, simple empirical
Formatted: Font: (Default) Times New Roman, Complex Script Font: Times New Roman, 12 pt
Deleted: concept
Formatted: Font: (Default) Times New Roman, Complex Script Font: Times New Roman, 12 pt
Deleted:) where
Formatted: Font: (Default) Times New Roman, Complex Script Font: Times New Roman, 12 pt
Deleted: on
Formatted: Font: (Default) Times New Roman, Complex Script Font: Times New Roman, 12 pt
Deleted: (population density and an indicator of socioeconomic development) are used to predict spatial patterns and temporal dynamics of burned area.
Formatted: Font: (Default) Times New Roman, Complex Script Font: Times New Roman, 12 pt
Deleted: „
Deleted: an alternative
Deleted: (random forest)
Deleted: /
Deleted: . The
Deleted: approach was used
Deleted: concept that allows more flexible model structures
Deleted: However
Deleted: over random forest
Deleted: be
Deleted: to
Deleted: /
Deleted: /
Deleted: and to provide suggestions for further model development
Deleted: modelling concept
Deleted: structural components
Deleted: controlling factors for fire activity
Deleted: with respect to previous work about controls on fire
Deleted:)

datasets, data-driven modelling and model-data integration approaches to improve global process-oriented vegetation-fire models (Sect. 5.3).

2 Datasets and predictor variables for model development

We used datasets of global monthly burned area as response variable and several datasets on land cover, climate, soil moisture, vegetation state, and socioeconomic factors as predictor variables in model development. To make a pre-selection of relevant predictor variables, we first tested the predictive performance of various candidate variables such as absolute values, anomalies, or long-term precedent mean values of precipitation, wet days, soil moisture, or vegetation state using random forest (Figure A1). We generally found a higher importance of the absolute variables than of the anomalies. For the development of SOFIA models, we finally selected a set of candidate predictor variables based on their importance, their interpretability, and based on how closely they are related to fire activity (by avoiding variables that account for indirect effects) (Table 1).

We based the analysis mostly on long-term harmonized or multi-satellite merged datasets in order to derive appropriate SOFIA models for long-term (i.e. decadal) variability in burned area that is covered for the period 1995–2015 of the GFED burned area dataset (Giglio et al., 2013). Although state-of-the-art single satellite sensors may provide information in higher quality, the use of such datasets would restrict the temporal coverage of the analysis. Given the common coverage of the used predictor datasets, the analysis was consequently performed for the period 1997–2011, on monthly time steps, and on a 0.25° spatial resolution. This is also comparable to common application domains of state-of-the art global process-oriented vegetation-fire models (Rabin et al., 2016). Datasets were temporally and spatially aggregated or interpolated if they originally differed from these temporal and spatial resolutions (details in the following sections for each dataset).

Table 1: Description of used datasets and derived predictor variables.

Dataset	Derived variables	Description
Burned area (response variable)		
	GFED burned area version 4 (Giglio et al., 2013), http://www.globalfiredata.org	
	GFED.BA	Fractional burned area of a 0.25° grid cell, used for optimization of SOFIA models
	ESA Fire CCI burned area version 4.1 (Chuvieco et al., 2016), http://cci.esa.int/data	
	CCI.BA	Fractional burned area of a 0.25° grid cell, independent dataset in evaluation
Predictor variables		
Land cover / plant functional types (PFTs)		
	ESA land cover_cci version 1.6.1, http://maps.elie.ucl.ac.be/CCI/viewer/index.php Land cover classes were translated to fractional coverages of plant functional types (PFTs) in 0.25° grid cells (Poulter et al., 2015a) (Table A 1).	
	CCI.LC.Tree.BE	Broadleaved evergreen trees
	CCI.LC.Tree.BD	Broadleaved deciduous trees
	CCI.LC.Tree.NE	Needle-leaved evergreen trees
	CCI.LC.Tree.ND	Needle-leaved deciduous trees
	CCI.LC.Shrub.BE	Broadleaved evergreen shrubs
	CCI.LC.Shrub.BD	Broadleaved deciduous shrubs
	CCI.LC.Shrub.NE	Needle-leaved evergreen shrubs
	CCI.LC.Herb	Natural grass and herbaceous vegetation
	CCI.LC.Crop	Cropland and managed grass
	CCI.LC.HrbCrp	Natural and managed grass and croplands = Herb + Crop
	CCI.LC.Tree	Coverage of trees = Tree.BE + Tree.BD + Tree.NE + Tree.ND
	CCI.LC.Shrub	Coverage of shrubs = Shrub.BE + Shrub.BD + Shrub.NE
	CCI.LC.Broadleaf	Coverage of broadleaved vegetation = Tree.BE + Tree.BD + Shrub.BE + Shrub.BD
	CCI.LC.Needleleaf	Coverage of needle-leaved vegetation = Tree.NE + Tree.ND + Shrub.NE
Climate and soil moisture		
	CRU TS3.23 climate data (Harris et al., 2014), https://crudata.uea.ac.uk/cru/data/hrg/cru_ts_3.23	
	CRU.T.orig	Mean monthly air temperature (°C)
	CRU.T.annual	Mean air temperature in the actual month and the 12 precedent months
	CRU.WET.orig	Monthly number of wet day
	CRU.WET.annual	Mean number of wet days in the actual month and the 12 precedent months
	CRU.DTR.orig	Mean monthly diurnal temperature range (K)
	GPCC precipitation version 7, http://dx.doi.org/10.5676/DWD_GPCC/FD_M_V7_050	
	GPCC.P.orig	Monthly total precipitation (mm)

Deleted: /
Deleted: 2
Deleted: derived
Formatted: Font color: Auto
Formatted: Font color: Auto
Deleted: We used various satellite and climate datasets to predict burned area using SOFIA. Therefore we
Deleted: (Table 1). Several other
Deleted: were derived from each dataset
Deleted: pre-fire annual
Deleted: climate
Deleted: and
Deleted: , or aggregated land cover properties because these variables might provide more predictive power for fire modelling
Deleted: instantaneous values (
Deleted: model structures
Deleted: /
Formatted: Font color: Auto, Complex Script Font: Times New Roman, 12 pt
Formatted: Font color: Auto, Complex Script Font: Times New Roman, 12 pt
Formatted: Font color: Auto, Complex Script Font: Times New Roman, 12 pt
Formatted: Font color: Auto, Complex Script Font: Times New Roman, 12 pt
Formatted: Font color: Auto, Complex Script Font: Times New Roman, 12 pt
Formatted: Font color: Auto, Complex Script Font: Times New Roman, 12 pt
Deleted: CRU TS3.23 climate data (Harris et al., 2014),
Formatted: Font color: Auto, Complex Script Font: Times New Roman, 12 pt
Formatted: Font color: Auto, Complex Script Font: Times New Roman, 12 pt
Deleted: before a fire
Deleted: before a fire
Formatted: Font color: Auto, Complex Script Font: Times New Roman, 12 pt
Formatted: Font color: Auto, Complex Script Font: Times New Roman, 12 pt

	GPCC.P.annual	Total precipitation in the actual month and the 12 precedent months
	ESA soil moisture_cci version 02.3, http://cci.esa.int/data	
	CCI.SM.orig	Mean monthly surface soil moisture
	CCI.SM.annual	Mean surface soil moisture in the actual month and the 12 precedent months
Vegetation state		
	GIMMS fraction of absorbed photosynthetic active radiation version 3g (Zhu et al., 2013), http://cliveg.bu.edu/modismisr/lai3g-fpar3g.html	
	GIMMS.FAPAR.orig	Mean monthly FAPAR
	GIMMS.FAPAR.pre	FAPAR in the precedent month
	GIMMS.FAPAR.annual	Mean FAPAR in the 12 precedent months
	Multi-sensor harmonized vegetation optical depth (Liu et al., 2011b, 2015), provided by Y. Liu	
	Liu.VOD.orig	Mean monthly VOD
	Liu.VOD.pre	VOD in the precedent month
	Liu.VOD.annual	Mean VOD in the 12 precedent months
Socioeconomics		
	GRUMP population density version 1 (years 1990, 1995, 2000) (Balk et al., 2006), http://dx.doi.org/10.7927/H4R20Z93	
	PD.med	Population density (individuals km-2), median estimate of three methods for temporal inter- and extrapolation (spline interpolation, linear interpolation, interpolation with last value as constant)
	Night light development index (year 2006) (Elvidge et al., 2012), http://ngdc.noaa.gov/eog/dmsp/download_nldi.html	
	NLDI	Night light development index, but grid cells without night lights or population set to 1.01

2.1 Burned area

Global monthly burned area data was taken from the Global Fire Emissions Database (GFED) (Giglio et al., 2013) and the ESA Fire CCI datasets (Chuvieco et al., 2016). GFED version 4 provides monthly burned area time series on a 0.25° spatial resolution for the period 1995-2015 based on a combination of the MODIS burned area product (from 2000 onwards) with active fire observations from VIRS (Visible and Infrared Scanner) and ATSR (Along-Track Scanning Radiometer) (before 2000) (Giglio et al., 2013). Fire CCI version 4.1 provides burned area time series on 0.25° spatial resolution for the period 2005-2011 based on a combination of MERIS data and MODIS thermal anomalies (Alonso-Canas and Chuvieco, 2015; Chuvieco et al., 2016). Because of the longer temporal coverage, the GFED dataset was used as the response variable in model development and for model evaluation. The Fire CCI dataset was used as an independent burned area dataset in model evaluation. Differences between the two datasets reflect the uncertainty in satellite-derived burned area. For both datasets burned area is expressed as the fractional burned area of a 0.25° grid cell.

2.2 Land cover

Land cover data was taken from the ESA land cover CCI product which provides three global land cover maps at 300 m spatial resolution covering the epochs 1998-2002, 2003-2007, and 2008-2012. We did not use the original land cover classification of the maps but translated land cover classes into plant functional types (PFTs) to be comparable with the classification used in global vegetation models (Poulter et al., 2011). The translation followed largely the rules by Poulter et al. (2015a) with some modifications to avoid coverage of broad-leaved evergreen trees and shrubs in boreal and arctic regions (Table A 1). The following nine PFTs were derived: broadleaved evergreen tree and shrub (Tree.BE, Shrub.BE), broadleaved deciduous tree and shrub (Tree.BD, Shrub.BD), needle-leaved evergreen tree and shrub (Tree.NE, Shrub.NE), needle-leaved deciduous tree (Tree.ND), natural grass or herbaceous vegetation (Herb), and managed grasslands or crops (Crop). The land cover maps were spatially aggregated and expressed as the fractional coverage of PFTs within a 0.25° grid cell.

We further aggregated the coverage of PFTs within each 0.25° grid cell to the total coverages of trees (Tree = sum of all tree PFTs, Table 1), shrubs (Shrub), and herbaceous vegetation including croplands (HrbCrp = Herb + Crop). To potentially characterise fuel types based on the dominant leaf type, PFTs were further aggregated into needle-leaved (Needleleaf) and broadleaved vegetation (Broadleaf) vegetation.

As land cover distribution is affected by fires, the land cover maps may regionally contain effects of past fires. Consequently, it can happen that fire activity is explained with the impact of the actual fire activity already present in a land cover map. We tried to reduce this effect by shifting the land cover maps by 2 years. This means that the map for the epoch 1998–2002 is used

Deleted: before a fire

Formatted: Complex Script Font: Times New Roman, 12 pt, French (France)

Formatted: Font color: Auto, Complex Script Font: Times New Roman, 12 pt, French (France)

Formatted: Font color: Auto, Complex Script Font: Times New Roman, 12 pt, French (France)

Formatted: Complex Script Font: Times New Roman, 12 pt, French (France)

Field Code Changed

Deleted: before a fire

Formatted: Font color: Auto, Complex Script Font: Times New Roman, 12 pt

Formatted: Font color: Auto, Complex Script Font: Times New Roman, 12 pt

Deleted: before a fire

Deleted: before a fire

Deleted: before a fire

Deleted: before a fire

Formatted: Font color: Auto, Complex Script Font: Times New Roman, 12 pt

Formatted: Font color: Auto, Complex Script Font: Times New Roman, 12 pt

Formatted: Font color: Auto, Complex Script Font: Times New Roman, 12 pt

Formatted: Font color: Auto, Complex Script Font: Times New Roman, 12 pt for the years ≤ 2004, the map for the epoch 2003–2007 for the period 2005–2009, and the map for the period 2008–2012 for the years ≥ 2010. However the three maps have only marginal temporal differences so that the impact of assigning land cover maps to certain years is rather small.

2.3 Climate

We used monthly data of mean air temperature, diurnal temperature range (DTR), and monthly number of wet days from the Climate Research Unit (CRU) TS3.2 dataset (Harris et al., 2014). DTR has been long used as predictor for fire weather conditions because it is sensitive to stable weather conditions that are usually associated to low humidity and are supportive for fire activity (Bistinas et al., 2014; Venevsky et al., 2002). These datasets provide monthly climate time series at 0.5° resolution based on spatially interpolated weather station observations. Precipitation was taken from the Global Precipitation Climatology Center (GPCC) version 7 dataset (Schneider et al., 2015). All climate datasets were resampled to 0.25° using the nearest neighbour method in order to avoid smoothing of climate anomalies through alternative resampling methods such as bilinear interpolation.

Deleted: Monthly data of mean air temperature, diurnal temperature range (DTR), and monthly number of wet days was taken from the Climate Research Unit (CRU) TS3.2 dataset (Harris et al., 2014). These datasets provide monthly climate time series at 0.5° resolution based on spatially interpolated weather station observations. Precipitation was taken from the Global Precipitation Climatology Center (GPCC) version 7 dataset (Schneider et al., 2015). All climate datasets were resampled to 0.25° using the nearest neighbour method in order to avoid smoothing of climate anomalies through alternative resampling methods such as bilinear interpolation.

We used the monthly values and long-term conditions of climate datasets as predictor variables (Table 1). As long-term conditions, we computed the mean temperature, mean diurnal temperature range, mean number of wet days, and the total precipitation of the actual month and the 12 precedent months.

Deleted: before a fire

2.4 Soil moisture

Surface soil moisture was taken from the ESA CCI soil moisture dataset (version 02.3 COMBINED) which is based on a merging of soil moisture products from various active and passive satellite sensors (Dorigo et al., 2015; Liu et al., 2011a, 2012). The dataset represents the upper soil layer (~ 2cm) and is available on a 0.25° spatial resolution and daily time step for the period 1979-2015. The long-term dynamic of the soil moisture dataset is consistent and environmentally plausible as demonstrated in a comparison with precipitation, soil moisture, and normalized difference vegetation index trends from independent datasets or land surface models (Albergel et al., 2013; Dorigo et al., 2012).

As soil moisture cannot be accurately retrieved underneath dense (tropical) forests, estimates are not available in all regions and thus the dataset has spatial gaps. We excluded such grid cells in the full analysis. Soil moisture time series were aggregated to monthly mean values. Temporal gaps in soil moisture time series were filled using a season-trend regression model as described in Forkel et al. (2013) and based on Verbesselt et al. (2010a, 2010b) but without accounting for breakpoints. However, some years in some grid cells were excluded from the entire analysis if soil moisture estimates were only available for less than 3 months within this year.

We used the monthly soil moisture values and long-term soil moisture conditions as predictor variables (Table 1). Long-term soil moisture conditions were computed as the mean soil moisture of the actual month and the 12 precedent months.

Deleted: before a fire

2.5 Vegetation state

To account for effects of vegetation phenology, biomass, or vegetation water content on fire activity, we used the GIMMS3g FAPAR (Zhu et al., 2013) and a VOD dataset (Liu et al., 2011b). GIMMS3g FAPAR is a long-term multi-sensor merged dataset of FAPAR and is based on the GIMMS3g NDVI (Normalized Difference Vegetation Index) dataset with a spatial resolution of 1/12° and a temporal resolution of 16 days for the period 1981 to 2012 (Pinzon and Tucker, 2014). GIMMS3g FAPAR was aggregated to 0.25° spatial resolution and averaged to monthly time steps. VOD by Liu et al. (2011b) is a long-term harmonized dataset from several passive microwave sensors. The VOD dataset has a spatial resolution of 0.25° and a monthly temporal resolution for the period 1988-2012.

Permanent gaps in FAPAR or VOD time series (mostly gaps occurring in winter in northern latitudes) were filled with the minimum value of each time series (Forkel et al., 2015) and remaining gaps were filled using the season-trend regression model (Forkel et al., 2013).

We used the monthly FAPAR or VOD values of the precedent month as predictor variables because vegetation of the actual month is likely affected by the fire event which we aim to explain. Additionally, we computed mean FAPAR and VOD of the 12 precedent months as long-term vegetation state predictor variables.

Deleted: before a fire

Deleted: before a fire

2.6 Socioeconomic variables

We used satellite-based datasets on population density and socioeconomic development as predictor variables for burned area. Population density (PD) was taken from the Global Rural-Urban Mapping Project (GRUMP) V1 dataset (Balk et al., 2006). This dataset is based on (sub-)national population statistics, satellite observations of night-time lights, and the spatial distribution of cities to provides estimates of population density on a 1 km grid for the years 1990, 1995, and 2000. The dataset was aggregated to 0.25°. The dataset was temporally interpolated between 1990 and 2000 and extrapolated between 2000 and 2011 for each grid cell to achieve a full coverage for the period 1997-2011. The interpolated time series is the median estimate from three interpolation methods (repeating last value as a constant, linear interpolation, spline interpolation). This allowed to make use of the temporal information of the population density dataset.

As an indicator for socioeconomic development, we used the night light development index (NLDI) (Elvidge et al., 2012). NLDI is derived from satellite observations of light emissions during night and an independent estimate of population density. NLDI ranges between 0 (light emissions equally distributed among people, highest development) and 1 (light emissions concentrated at one person, lowest development). NLDI is highly correlated with electrification rates and the human development index (Elvidge et al., 2012). The dataset is available on a 0.25° spatial resolution for the year 2006. NLDI is not available for grid cells without population or without detected night lights, which introduces gaps in the global NLDI map. We filled these gaps with a value of 1.01 (indicating very low development or natural ecosystems) in order to not introduce spatial gaps of the NLDI dataset in the empirical modelling of burned area.

3 Modelling approaches and model-data analysis

Formatted: Font color: Auto

3.1 SOFIA modelling approach

Deleted: concept

SOFIA is a data-driven fire model approach that allows to test several alternative functional relationships and associated variables to predict fractional burned area. The basic structure of SOFIA fire models is inspired by SIMFIRE (simple fire model) which uses empirical relationships to estimate fire frequency from vegetation (i.e. FAPAR), fire weather conditions, and socioeconomic variables (Knorr et al., 2014). In SOFIA we generalize the SIMFIRE approach by using and testing several alternative predictor variables as controls for fire activity. Each SOFIA model structure is based on the assumption that potentially the entire vegetated area can burn but burning is actually restricted by several functional relationships to controlling factors:

Deleted: an empirical modelling concept

Deleted: model structures

Deleted: suppressed

$$BA_t = \sum_{g=1}^{g=N} A_g * f_{g,t} \quad (1)$$

where *BA* is the fractional burned area of a grid cell at time step *t*, A_g is the fractional coverage of land cover group *g*, and f_g is a factor that controls fire spread [0 = fully restricted burning and 1 = un-constrained burning] for a specific land cover group. Land cover groups *g* can for example be classified according to growth forms (trees, shrubs, grasses, crops), plant functional types (PFTs), or any other potentially meaningful separation of land cover. The factor f_g is a product of individual functions that represent climatic, environmental, and socioeconomic controls on fire:

Deleted: suppressed

$$f_g = \prod_{i=1}^{i=N} f(x_{i,g}) \quad (2)$$

$$f(x_{i,g}) = \min\left[1, \frac{max_{g,i}}{1+e^{\left(-sl_{i,g} \times \left(x - x0_{i,g}\right)\right)}}\right] \quad (3)$$

where x is the value of an environmental or socioeconomic variable i; and *max*, *sl* and *x0* are parameters of a logistic function. We used the minimum value from 1 and the logistic function, and included *max* as a free parameter to allow the representation of exponential relationships within the basic structure of logistic functions. Parameters of the logistic functions can be either defined per vegetation cover group or as global parameters. Variables x can be for example vegetation state variables such as FAPAR or VOD to represent fuel loads, climate variables such as the number of wet days or diurnal temperature range to represent fire weather conditions, and socioeconomic variables such as population density or NLDI to represent human effects on fire activity. Consequently, the development of an actual SOFIA model requires two steps, namely the definition of a model structure (i.e. selection of candidate predictor variables, Sect. 3.2) and the estimation of the model parameters (Sect. 3.3). SOFIA models allow to reproduce the typical right-tailed distribution of burned area (i.e. many grid cells and months with no burned area in comparison to relatively few grid cells and months with fire activity). The underlying functional relationships can take step-wise, linear, sigmoidal, or exponential shapes depending on the parameters of the logistic functions (Figure 1). Similar model structures like SOFIA where a response variable is controlled by a product of several functions have been previously applied in environmental modelling for example in light-use efficiency models to simulate NPP (Cai et al., 2014; Nemani et al., 2003) or in phenology models to simulate leaf development (Forkel et al., 2014; Jolly et al., 2005; Stöckli et al., 2011). The response value of the functional relationship can also be used to map sensitivities of burned area to environmental or socioeconomic variables. Such a mapping of controls was previously done for plant productivity (Nemani et al., 2003) and phenology (Forkel et al., 2014; Jolly et al., 2005) based on red-green-blue (RGB) composite maps. Here we will demonstrate how this approach can be used to investigate spatial patterns of sensitivities between burned area and climatic, environmental and socioeconomic controls on fire activity.

Deleted: potentially appropriate

Deleted: allows

Deleted:) and to explore

Deleted: response functions of fire activity to environmental or socioeconomic variables that

Deleted: (Cai et al., 2014; Nemani et al., 2003)

Deleted: values

Deleted: control functions

Deleted: the spatial covariation

Deleted: with

Deleted: (Nemani et al., 2003)

Formatted: Danish

Field Code Changed

Formatted: Danish

Formatted: Danish

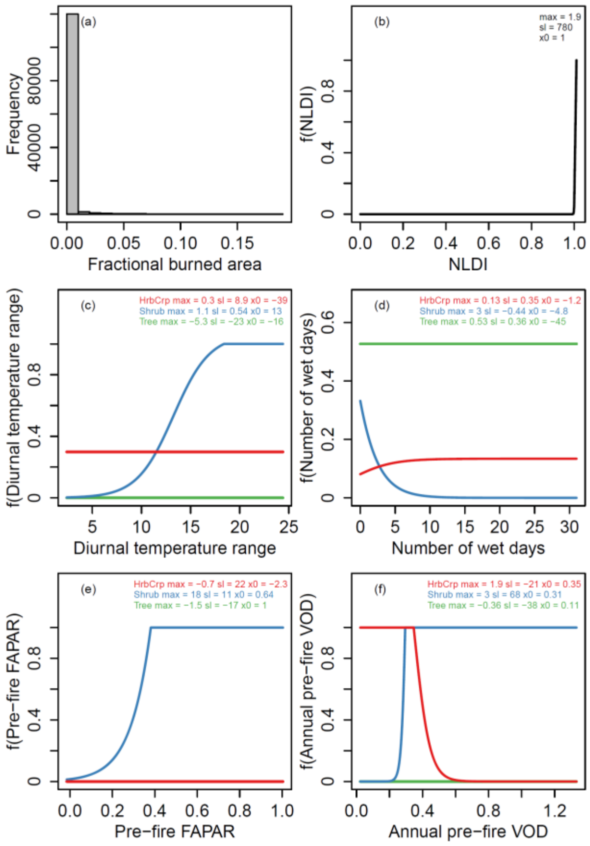

Figure 1: Example of a SOFIA model structure with three land cover groups (i.e. herbaceous vegetation and crops, shrubs, trees) and five controlling factors on fire activity. The example is taken from the SOFIA model SF.124421 (Table 2). (a) Histogram of the simulated fractional burned area. Response functions of fractional burned area on (b) night light development index, (c) diurnal temperature range, (d) number of wet days, (e) fraction of absorbed photosynthetic active radiation in the month before a fire, and (f) mean vegetation optical depth in the 12 precedent months. max, sl, and x0 are parameters of the logistic functions.

Deleted: controls

Deleted: before a fire

3.2 Testing controlling factors and predictor variables in SOFIA models

Deleted: Structural components for

To test appropriate controlling factors and related predictor variables in SOFIA models, we defined several alternative model structures. Each SOFIA model uses a specific land cover grouping scheme and several functional relationships for fire activity. We tested different land cover grouping schemes to assess the required complexity of SOFIA models to regionalize model parameters. As grouping schemes we either used growth forms (“GrowthForm” including the variables *Tree*, *Shrub*, and *HrbCrp*; Table 1), growth forms with crops separated from herbaceous vegetation (“GrowthFormCrop” including *Tree*, *Shrub*, *Herb*, *Crop*), leaf types (“LeafType” including *Needleleaf*, *Broadleaf*, *Herb*, *Crop*), or PFTs (“PFT” using the nine PFTs). Differences between GrowthForm and GrowthFormCrop will allow assessing if a separation of croplands from herbaceous vegetation is necessary to explain fire activity. The LeafType grouping scheme may potentially be useful because needles usually decompose slower than broadleaves and thus form larger pools of litter fuel. Differences between GrowthFormCrop and LeafType allow assessing if model parameters should be separated rather by growth form or by leaf type. The PFT land

Deleted: Several

Deleted: need to be defined in order to identify appropriate components of SOFIA models to predict burned area.

Deleted: controlling factors

Deleted: to assess

Deleted: to assess

cover grouping scheme is finally used to assess if the interaction of growth forms and leaf types is required to regionalize model parameters.

We defined five controlling factors on fire activity and assigned several corresponding predictor variables to each controlling factor to evaluate required components of SOFIA models:

1. *Human influences* represent potential relations between socioeconomic indicators and burned area. As predictor variables we used either population density with a global parameter set (PD), NLDI with a global parameter set (NLDI), or NLDI with parameters that vary per land cover group (NLDI.g).
2. *Temperature effects* represent potential relations between diurnal temperature range (CRU.DTR.orig) or long-term air temperature (CRU.T.annual) and burned area.
3. *Direct wetness effects* represent the obvious restriction of fire activity by wet conditions. We included either the actual-month number of wet days (CRU.WET.orig), precipitation (GPCC.P.orig), or surface soil moisture (CCI.SM.orig).
4. *Direct vegetation effects* represent potential relations between the precedent vegetation state and burned area. Therefore we either used previous-month FAPAR (GIMMS.FAPAR.pre) or VOD (Liu.VOD.pre) as predictor variables.
5. *Long-term wetness or vegetation effects* represent potential relations between long-term averaged precedent conditions of wetness or vegetation variables and burned area. Several reasons exist to test long-term averaged predictor variables as structural components of SOFIA models. Firstly, long-term conditions of precipitation and soil moisture are strongly linked to plant productivity especially in semi-arid ecosystems and thus might represent variations in vegetation and fuel loads. Secondly, long-term conditions of FAPAR and VOD are more closely related to vegetation coverage or biomass and thus might better represent fuel loads than the actual monthly values. As predictor variables for long-term conditions, we used aggregated values from the 12 precedent months for the number of wet days (CRU.WET.annual), precipitation (GPCC.P.annual), soil moisture (CCI.SM.annual), FAPAR (GIMMS.FAPAR.annual), or VOD (Liu.VOD.annual).

We also allowed that a certain controlling factor is not included in a model to test if this controlling factor is generally needed in the SOFIA model. This setup of controlling factors and associated predictor variables allows the definition of several candidate model structures (Table A 2). For example, the SOFIA model SF.124421 (the coding is described in Table A 2) used growth forms as land cover grouping scheme, NLDI for human influences, diurnal temperature range as temperature effect, the number of wet days as direct wetness effect, previous-month FAPAR as direct vegetation effect, and long-term precedent VOD as long-term vegetation effect (Figure 1). The model structure determines the complexity which we assess here based on the number of controlling factors within a SOFIA model and on the number of parameters N in a model (N = number of controlling factors * number of land cover groups * 3 parameters). We required that SOFIA models included at least 3 controlling factors and have less than 100 parameters. This results in 2712 candidate SOFIA models. We optimized and evaluated 95 randomly selected models from the set of candidate models (Table A 2). Although this selection does not allow a full factorial assessment of controlling factors and predictor variables in SOFIA models, it is a trade-off between computational feasibility and an assessment of the tendency of a factor regarding model performance.

3.3 Optimization and evaluation of SOFIA models

3.3.1 Model optimization

After the definition of candidate SOFIA models, parameters for each controlling function need to be estimated for each model to achieve an optimal performance. The parameters p of the logistic functions of each controlling factor were estimated by minimizing the sum-of-squared error (SSE) between the monthly observed (*obs*) and simulated (*sim*) fractional burned area:

$$SSE = \sum_{i=1}^{i=N} (sim_i - obs_i)^2 \quad (4)$$

where i is an index over grid cells and months. We also tested alternative cost functions in the optimization which transform burned area data, explicitly account for variance or which were based on burned area anomalies instead of absolute area in order to potentially better predict the variability of observed burned area (Table A 3).

Deleted: structural

Deleted: suppression

Deleted: pre-fire

Deleted: pre-fire

Deleted: controlling factors

Deleted: before a fire

Deleted: SOFIA

Deleted: pre-fire

Deleted: structures for

The minimization of SSE was performed by applying a genetic optimization algorithm. The used algorithm (GENOUD, genetic optimization using derivatives) combines a global search algorithm (i.e. genetic optimization) with a local search algorithm (i.e. BFGS) (Mebane and Sekhon, 2011). GENOUD was already previously used to estimate parameters in a dynamic global vegetation model (Forkel et al., 2014). Here we applied GENOUD by using 500 individuals (i.e. parameter sets) per generation, and allowed the algorithm to run for maximum 30 generations. The parameter sets of the first generation were generated randomly. The second generation is generated by using several operators to clone, mutate, and crossover the best parameter sets of the first generation (Mebane and Sekhon, 2011). The BFGS local search algorithm was first used starting from the best parameter set that evolved in the 28^{th} generation in order to avoid a too fast convergence of the algorithm towards a local optimum.

3.3.2 Model selection and evaluation

We selected the best performing SOFIA models from all optimized candidate models based on the Akaike Information Criterion (AIC) (Burnham and Anderson, 2002). AIC is a metric to empirically infer appropriate model structures from several candidate models based on performance (in terms of SSE) and by penalizing for model complexity (in terms of the number of model parameters *N*):

$$AIC = 2 \times N - 2 \times log(e^{-SSE}) \tag{5}$$

Given a certain performance threshold, the best model has the lowest AIC value (Burnham and Anderson, 2002).

To evaluate the simulated spatial-temporal patterns and temporal dynamics of fractional burned area, we used the index of agreement (IoA) and the fractional variance (FV) (Janssen and Heuberger, 1995):

$$IoA = 1 - \frac{\sum_{i=1}^{i=N}(obs_i - sim_i)^2}{\sum_{i=1}^{i=N}(|sim_i - \overline{obs}| + |obs_i - \overline{obs}|)^2} \tag{6}$$

$$FV = \frac{\sigma_{sim} - \sigma_{obs}}{0.5 \times (\sigma_{sim} + \sigma_{obs})} \tag{7}$$

where $\overline{obs}$, $\overline{sim}$ and σ_{obs}, σ_{sim} are the means and variances of the observations and simulations, respectively. IoA ranges between 0 (worst fit) and 1 (best fit) and is an overall efficiency metric that is sensitive to correlation and bias. FV ranges between -2 and 2 (best agreement at 0) where negative values indicate an underestimation and positive values an overestimation of the observed variance.

3.3.3 Data sampling for model optimization and evaluation

We sampled several grid cells from the global datasets (0.25° resolution) to optimize and evaluate all candidate SOFIA models. A sampling of grid cells is necessary to retain enough independent data for evaluation of SOFIA models and because optimization of all SOFIA models on the entire global datasets with 0.25° spatial resolution, monthly time steps, and 15 years was computationally not feasible. However the sampling needs to represent the global spatial patterns and the entire statistical distribution of burned area, including extreme fire events. Therefore, we performed a sampling of grid cells stratified by regions (representing biomes) and by the statistical distribution of burned area. We first computed the maximum annual burned area for all grid cells in 1997-2011 to represent the spatial distribution of extreme fire years. Regions were defined based on land cover and climate zone (Kottek et al., 2006) (Figure A 2). For each region, we classified the annual maximum burned area of each 0.25° grid cell into 100 classes according to regional quantiles of the maximum annual burned area (e.g. class 1 covers quantile 0 (minimum) to quantile 0.01 and the last class covers quantile 0.99 to 1 (maximum) of regional annual maximum burned area). We then randomly sampled grid cells for each regional quantile class. In total, 3161 grid cells were sampled with most of the cells in savannahs and tropical croplands (n = 953, largest region) and fewest cells in boreal needle-leaved deciduous forests (n = 135, smallest region) (Figure A 2 b). Consequently, the sampled grid cells are representative for the global statistical distributions (Figure A 2 c-e) and for spatial patterns of fire activity (Figure A 2 f).

Deleted: each grid cell (representing

Deleted:) (Figure A 1).

Deleted: computed

Deleted: to cover the regional statistical distribution of fire activity. For

Deleted: (e.g. quantiles 0.01 to 0.02), we sampled randomly grid cells while maximizing the spatial distance between sampled grid cells to cover a wide geographic range.

Deleted: (Figure A 1 b).

Deleted: (Figure A 1

Deleted: (Figure A 1

Deleted:

The sampled grid cells were further divided into a subset for optimization (60% of the sampled grid cells) and for evaluation (40% of the sampled grid cells). The time periods in both subsets was further divided according to years for which the monthly data was used for optimization (even years in 1998 to 2010) and for which the monthly data was used for evaluation (uneven years in 1997 to 2011). We used every second year for optimization or evaluation to avoid that potential temporal changes in the quality of multi-sensor satellite datasets (e.g. burned area, soil moisture, FAPAR, and VOD) affect the evaluation of model results. Based on this sampling scheme, 1817 grid cells (= 152.628 monthly observations in even years) were used for optimization and 1212 grid cells (= 116.352 monthly observations in uneven years) were used for evaluation. Note that fewer observations were used in the optimization and evaluation subsets for the comparison against the Fire CCI burned area dataset because this dataset starts only in 2005.

We applied the best-performing SOFIA models to all global 0.25° grid cells to compare them globally with the GFED and CCI burned area datasets and with JSBACH-SPIFIRE. From these global results, we compared maps of mean annual burned area and regional statistical distributions and temporal dynamics of annual burned area for the period 2005 to 2011. Therefor we aggregated burned area from the datasets and from the best SOFIA models to the coarse spatial resolution of JSBACH (1.875*1.875°).

3.4 Data-driven fire modelling with random forest

We used the random forest machine learning approach to evaluate if the basic structure of SOFIA models is flexible enough to predict burned area or if a more flexible modelling approach can reach higher performances. Random forest is a regression approach that can consider non-linear, non-monotonic and abrupt, and non-additive relations between multiple predictor variables and a response variable (Breiman, 2001). Random forest is an ensemble of multiple regression trees that are trained based on the response variable. Each tree uses a randomly selected set of predictor variables and data points (Breiman, 2001). Random forest was already previously applied to identify controls on vegetation dynamics and on fire activity (Aldersley et al., 2011; Archibald et al., 2009). We used 500 trees per random forest. For the training of the random forest, we used the same data subset that was also used to optimize SOFIA models (Sect. 3.3.3). The analysis was performed using the randomForest package in R (Liaw and Wiener, 2002).

We performed three different random forest model experiments. The model experiment RF1 used all predictor variables from Table 1 to explore the potential performance of the used datasets to predict burned area. The model experiment RF2 used all predictor variables except the variables from the soil moisture dataset in order to apply random forest globally and to compare the results with SOFIA independent of the spatial gaps of the soil moisture dataset. The model experiment RF.124421 uses the same predictor variables as the SOFIA model SF.124421 (i.e. CCI.LC.Tree/Shrub/HrbCrp, NLDI, CRU.WET.orig, Liu.VOD.annual, GIMMS.FAPAR.pre, CRU.DTR.orig) in order to compare the performance of the two model approaches based on the same predictor variables.

3.5 Process-oriented fire modelling with JSBACH-SPITFIRE

We simulated burned area with the SPITFIRE (spread and intensity of fire) fire module within the JSBACH (Jena Scheme for Biosphere-Atmosphere Coupling in Hamburg) land surface model in order to compare the performance of SOFIA models to a state-of-the art global vegetation-fire model. This comparison potentially allows us to provide suggestions for the further development of global vegetation-fire models.

Deleted: /

Deleted: /

JSBACH is the land component of the MPI (Max Planck Institute for Meteorology) Earth system model (Raddatz et al., 2007). SPITFIRE is a physically based fire module that simulates fire ignitions (based on lightning and population density), fire spread, and fire effects depending on weather conditions, vegetation type and structure, fuel moisture, and fuel size (Thonicke et al., 2010). SPITFIRE was originally developed for the LPJ (Lund-Potsdam-Jena) dynamic global vegetation model (Thonicke et al., 2010). For the implementation of SPITFIRE in JSBACH, two parameters in SPITFIRE were adjusted, one related to human ignitions and the other related to the drying of fuels (Lasslop et al., 2014). Additionally, the relation between wind speed and the rate of fire spread was modified (Lasslop et al., 2015) and a decrease of fire duration with increasing population density was implemented (Hantson et al., 2015a).

JSBACH was applied on a spatial resolution of 1.875°*1.875°. JSBACH runs on a half-hourly time step, while the SPITFIRE module is called at daily time steps. A detailed description of the simulation setup is given in the FireMIP (fire model inter-comparison project) protocol from which we use the JSBACH baseline simulation SF1 (Rabin et al., 2016). Following a spinup period to equilibrate carbon pools (continued until the slow carbon pool varied less than 1% between consecutive 50-year periods), a transient simulation was started in 1700. Data on land use (Hurtt et al., 2011) and population density (Goldewijk et al., 2010) were used starting in 1700 and interpolated to annual resolution. The CO_2 concentration of the atmosphere was provided starting from 1750 at annual resolution (Le Quéré et al., 2014). CO_2 concentration before 1750 was set to the value of 1750. Climate forcing is based on the CRUNCEPv5 dataset (1901-2013) (Wei et al., 2014). Climate data was recycled over the years 1901-1920 before 1901.

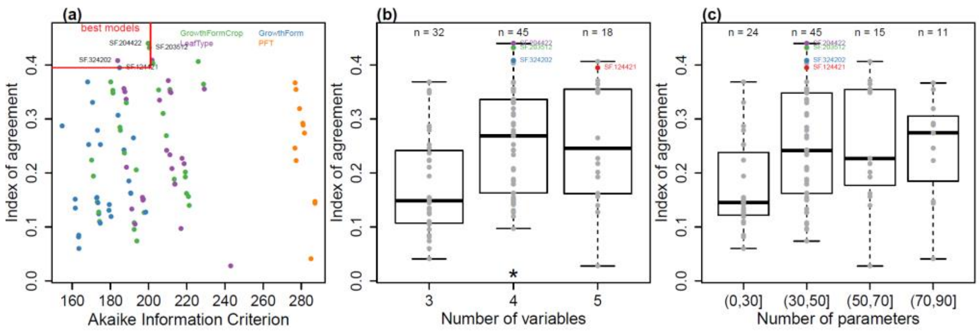

Figure 2: Effect of complexity of SOFIA models on the performance. Model performance is expressed as the index of agreement between simulated and observed (GFED) monthly burned area time series in the optimization data subset. (a) Scatterplot of the index of agreement against AIC classified by the used land cover grouping scheme. (b and c) Effect of the number of variables (= number of controlling factors) and parameters on model performance, respectively. The star symbol in (b) indicates a significantly higher IoA of models with 4 variables than the other groups (Wilcoxon rank sum test, p ≤ 0.05). The four best SOFIA models (IoA ≥ 0.395 and AIC ≤ 200) are highlighted by a red box in (a) and by coloured points in (b) and (c).

Deleted: Effects

Deleted: model

Deleted: of SOFIA models.

4 Results

Formatted: Font color: Auto

4.1 Performance and complexity of SOFIA models

The optimized candidate SOFIA models covered wide ranges of complexities and performances (Figure 2, Table 2). The best-performing SOFIA models reasonably explained the monthly spatial-temporal patterns of fractional burned area (i.e. up to IoA = 0.45 for SF.230512, Table 2) but underestimated the observed variance (i.e. negative FV, best FV = -1.44 for SF.204422). Although the comparison of the GFED and Fire CCI burned area datasets showed only a moderate agreement (IoA = 0.85 and FV = 0.06), the performance of SOFIA models was similar for both datasets (Table 2). The performance of SOFIA models was very similar for the optimization and evaluation data subsets which shows that SOFIA models can be robustly applied to different spatial and temporal domains. The SOFIA model with the lowest AIC considered only three controlling factors and had 21 parameters (SF.124002, Table A 2). However, this model reached only a poor performance (IoA = 0.29 and FV = -1.68 in the optimization subset). Consequently, this model is not suited to simulate global fire activity. Therefore we selected the best SOFIA models according to both performance (IoA ≥ 0.4) and AIC (AIC ≤ 200) (Figure 2 a). The four best SOFIA models had different combinations of predictor variables which demonstrates the equifinality in predicting global burned area.

Deleted: reasonable

Deleted: indicates

However the results show that SOFIA models were robust enough to predict global monthly fractional burned area for different spatial and temporal domains and using different datasets.

Table 2: Performance of the best SOFIA and of random forest models in predicting global distributed monthly burned area time series in the optimization and evaluation data subsets, respectively. Results for all SOFIA models are provided in Table A2. Please note that results for JSBACH-SPITFIRE are not included in this table because of its coarser spatial resolution.

Name	Model structure and included predictor variables	GFED.BA as reference (1997-2011)						CCI.BA as reference (2005-2011)			
		Optimization subset (1817 cells, even years) (data used for optimization)				Evaluation subset (1212 cells, uneven years)		Optimization subset (even years)		Evaluation subset (uneven years)	
		SSE	AIC	IoA	FV	IoA	FV	IoA	FV	IoA	FV
GFED	Comparison of GFED.BA with CCI.BA	-	-	-	-	-	-	0.78	-0.19	0.85	0.06
Best SOFIA models											
SF.204422	GrowthFormCrop, CRU.WET.orig, Liu.VOD.annual, GIMMS.FAPAR.pre, CRU.T.annual	51.88	199.8	0.44	-1.44	0.39	-1.55	0.42	-1.53	0.41	-1.53
SF.203512	GrowthFormCrop, GPCC.P.orig, GIMMS.FAPAR.annual, Liu.VOD.pre, CRU.T.annual	52.17	200.3	0.43	-1.45	0.42	-1.54	0.45	-1.49	0.45	-1.51
SF.324202	LeafType, NLDI, CRU.WET.orig, GPCC.P.annual, CRU.T.annual	52.92	183.8	0.41	-1.49	0.37	-1.65	0.39	-1.59	0.35	-1.65
SF.124421	GrowthForm, NLDI, CRU.WET.orig, Liu.VOD.annual, GIMMS.FAPAR.pre, CRU.DTR.orig	53.40	184.8	0.40	-1.51	0.39	-1.51	0.39	-1.59	0.41	-1.51
Random forest models											
RF1	Random forest based on all variables as in Table 1	8.36	-	0.95	-0.59	0.58	-1.24	0.77	-0.76	0.58	-1.24
RF2	Like RF1 but without CCI.SM variables	8.58	-	0.95	-0.60	0.58	-1.26	0.77	-0.77	0.58	-1.26
RF.124421	Random forest using the same variables as the SOFIA model SF.124421	24.05	-	0.81	-1.23	0.41	-1.69	0.65	-1.35	0.40	-1.70

We also tested if alternative cost functions in the optimization of SOFIA models would reduce the underestimation of the observed variance of burned area. The tested alternative cost functions explicitly accounted for variance, burned area anomalies, or were based on transformed burned area values (Table A 3). Although a cost function based on IoA and FV reached better performances in terms of IoA (best IoA = 0.45 against CCI.BA in the evaluation subset) and reproduced the observed variance of burned area (FV = 0 against GFED in the training subset), the resulting model overestimated mean fractional burned area which is reflected by a high SSE (Table A 3). Other alternative cost functions resulted in weaker performances than the default SSE cost function. Consequently, we used the SSE-based cost function for the optimization of all SOFIA models.

The performance of SOFIA models varied with model complexity. SOFIA models that used a higher number of controlling factors (n = 4 or 5) had in average a better performance than models with only three factors (Figure 2b). However, very complex SOFIA models with a high number of parameters (n = 70-90) did not necessarily result in higher performances than models with an average number of parameters (n = 30-70, Figure 2c). Models with a low number of parameters (n < 30) had in average low performances but we also found some SOFIA models with few parameters that reached good performances (e.g. SF.124021 with only 30 parameters, Table A 2). The four best SOFIA models had between 30 and 50 parameters. The number of parameters in SOFIA models was mostly affected by the choice of a certain land cover grouping scheme to regionalize model parameters. Models that used the GrowthForm (3 groups), GrowthFormCrop or LeafType (both 4 groups) grouping schemes reached much lower AIC values than models that used the PFT grouping scheme (with 9 PFTs) (Figure 2a). These results demonstrate that SOFIA models with a higher number of predictor variables but a medium amount of model parameters reached the best performances in predicting global monthly spatial-temporal patterns of burned area.

Random forest models reached slightly better performances than the best performing SOFIA models. The random forest model based on all variables reached very good performance in training (IoA = 0.95 for RF1) and moderate performances in the evaluation subset (IoA = 0.58 for RF1, Table 2). The random forest models with (RF1) and without soil moisture variables (RF2) reached similar performances. Similar as for the SOFIA models, the employed random forests underestimated the observed variance. However when using random forest with the same set of predictor variables as SOFIA (RF.124421 vs. SF.124421), random forest reached even weaker performances (IoA = 0.4, FV= -1.7 in evaluation against CCI burned area)

Formatted: Font color: Auto, Complex Script Font: Times New Roman, 12 pt

Formatted: Font color: Auto, Complex Script Font: Times New Roman, 12 pt

Formatted: Font color: Auto, Complex Script Font: Times New Roman, 12 pt

Formatted: Font color: Auto, Complex Script Font: Times New Roman, 12 pt

Formatted: Font color: Auto, Complex Script Font: Times New Roman, 12 pt

Formatted: Font color: Auto, Complex Script Font: Times New Roman, 12 pt

Formatted: Font color: Auto, Complex Script Font: Times New Roman, 12 pt

Moved down [1]: Similar as for the SOFIA models, the employed random forests underestimated the observed variance.

Deleted: The

Moved (insertion) [1]

Deleted: model

Deleted: slightly

than the corresponding SOFIA model. Thus the highly flexible structure of the random forest machine learning approach did not necessarily result in a much better performance than the best-performing SOFIA models. Consequently, the SOFIA approach offers enough flexibility to assess different controlling factors and its functional relationships to predict burned area.

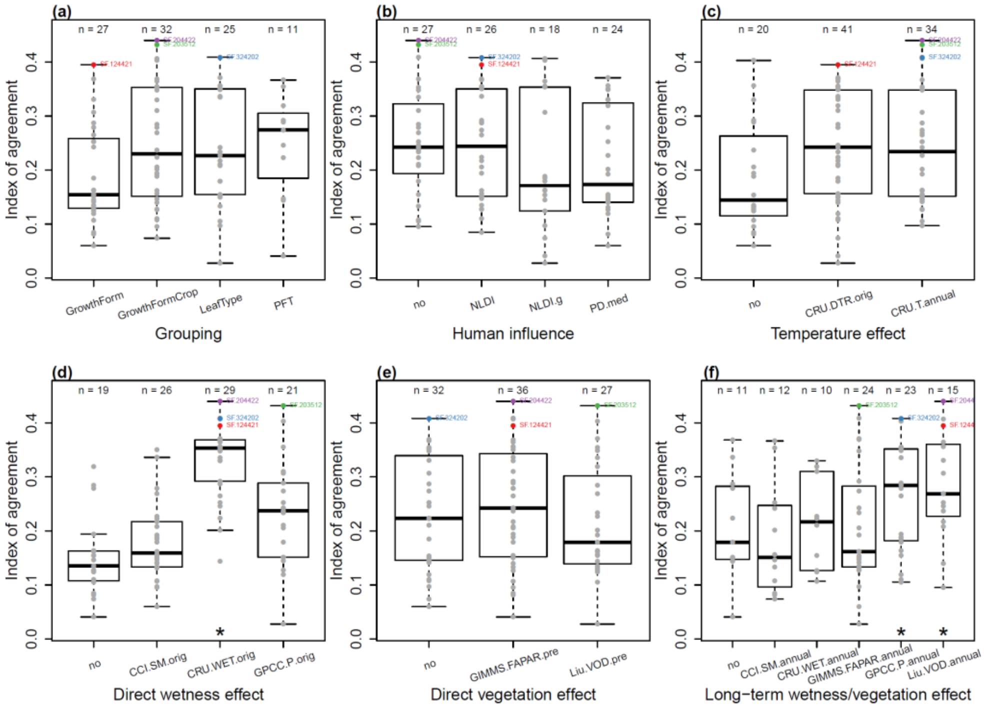

Figure 3: Effect of controlling factors and associated predictor variables in SOFIA models on the performance in simulating global monthly burned area dynamics. Performance is expressed as the index of agreement between simulated and observed (GFED) monthly burned area for the training data subset. Boxplots show the distribution of IoA based on all SOFIA model experiments that include the respective variable. Star symbols indicate a significantly higher IoA of a variable in comparison to the "no" group of each controlling factor (Wilcoxon rank sum test, $p \leq 0.05$). Distribution of IoA depending on the used (a) land cover grouping scheme; and variables to account for (b) human influence; (c) temperature effects; (d) direct wetness effects; (e) direct vegetation effects; and (f) long-term wetness or vegetation effects. The best models (IoA > 0.4 and AIC < 200) are highlighted with coloured dots.

4.2 Required controlling factors and adequate predictor variables in SOFIA models

The performance of SOFIA models depended on the controlling factor and associated predictor variables that were used in model structures (Figure 3). The choice of a certain land cover grouping scheme in SOFIA models to regionalize model parameters had only weak effects on model performance (Figure 3a). Although models based on the GrowthForm scheme had on average weaker performances than models based on land cover grouping schemes with croplands, the best SOFIA models were not related to a certain land cover grouping scheme.

Including human influences as controlling factors in SOFIA models did not improve model performance (Figure 3b). The best models either did not consider human influences or considered human influences through NLDI as global controlling function. However, NLDI did in average not contribute to higher performances. SOFIA models that used population density had on average weaker performance than SOFIA models that used NLDI or that did not consider human influences. The weaker performance of population density as component in SOFIA models could be caused by the general model structure in which

Deleted: SF.124421 with the same predictor variables.

Deleted: model

Deleted: modelling concept

Deleted: model structures

Deleted: structural components of

Deleted: structural components of

Deleted: as components

Deleted: Models

Deleted: that separately considered

Deleted: . Models based on PFTs had on average higher performances than models with less land cover groups. However

Deleted: , i.e. any land cover grouping scheme can potentially be used to regionalize model parameters. These results demonstrate that a PFT-based parameterization provides on average better results but some models based on growth forms can also reach best performances in predicting global burned area

Deleted: model structures

potential burned area equals the total vegetated area: As highly populated areas are usually associated with low vegetation cover, potential burned area is low as well, and thus population density does not provide further information. Although two of the best SOFIA models did not contain any variable for human influences (SF.204422, SF.203512), they however considered the fractional coverage of croplands in the used land cover grouping scheme. Consequently, these two models considered human influence on fire indirectly through the coverage of croplands. These results suggest that human influences on fire activity can be relatively interchangeably described in SOFIA models by the coverage of croplands, NLDI, or population density.

Deleted: , but the combination of these factors does not result in a further improvement in model performance. These results also suggest that more appropriate information and metrics about human fire usage and management are required to significantly improve global fire models

Considering temperature variables in SOFIA models caused on average better model performances than model structures without temperature variables (Figure 3c). However, we also found one model without a temperature control that reached good performance (SF.233210, Table A 2). All of the best performing models included diurnal temperature range or pre-fire annual mean temperature as controlling factors. These results show that temperature-related variables are important predictors in SOFIA.

The consideration of direct wetness effects in SOFIA models had the largest positive impact on model performance (Figure 3d). Models that did not consider direct wetness effects had lower performances than models that used soil moisture, precipitation, or the number of wet days. Especially models based on the number of wet days reached significant higher IoA than models without direct wetness effects (Wilcoxon rank sum test, $p \leq 0.05$). Consequently, direct wetness effects on fire activity were a required component of SOFIA models to predict burned area.

Whether or not including direct vegetation controls did not lead to a significant change in performance of the SOFIA models (Figure 3e). The best models either did not consider direct vegetation effects (SF.324202), used pre-fire FAPAR (SF.204422, SF.124421), or pre-fire VOD (SF.203512). This suggests that precedent FAPAR and VOD conditions did not provide additional information to predict burned area in SOFIA models.

Deleted: of the month before a fire

On the contrary, considering long-term wetness or vegetation effects in SOFIA models caused significantly higher model performances than not considering these effects (Figure 3f). Especially SOFIA models that used pre-fire annual precipitation or VOD reached significantly higher IoA. Models with long-term effects based on soil moisture, the number of wet days, or FAPAR had on average similar performances as models without long-term effects. However, we also found some good models that used long-term conditions of FAPAR (e.g. SF.203512). These results demonstrate that long-term conditions in vegetation productivity (reflected by annual precipitation) or vegetation structure (reflected by VOD or FAPAR) were required components of SOFIA models to predict burned area.

Based on the performances of the different controlling factors and associated predictor variables, the ideal SOFIA model should include NLDI as human influence, one variable to account for temperature effects, the number of wet days as direct wetness effect, and pre-fire annual conditions of precipitation or VOD as long-term wetness/vegetation effects. This ideal model structure is realized in two of the best performing SOFIA models (SF.124421 and SF.324202, Figure 3). The choice of a certain land cover grouping scheme or of a direct vegetation effect are secondary components of SOFIA model structures. The distribution of model parameters in SF.124421 after optimization reflects that parameters for the functional relationships with NLDI, the number of wet days, and VOD were well constrained and thus were the most sensitive parameters within this model to estimate global monthly burned area dynamics. These parameter estimates and distributions could be potentially used as prior parameter estimates to further constrain SOFIA models.

4.3 Global evaluation of burned area from different modelling approaches

4.3.1 Global spatial patterns

The best SOFIA models were applied globally to assess their performance in simulating global and regional spatial-temporal patterns of annual total burned area with respect to random forest models and JSBACH-SPITFIRE. All three model approaches reproduced well the global spatial pattern of mean annual burned area with large burned area in Africa, Australia, and Tropical

Deleted: amounts of

South America, and smaller amounts of burned area in the rest of the world ($0.663 \geq$ IoA ≤ 0.841, Figure 4). However models were often biased in comparison to the observational datasets. The global mean annual burned area was 341 Mha for the GFED dataset, 346 Mha for the CCI dataset, and is estimated much higher (464 Mha) based on assumptions about undetected small fires (Randerson et al., 2012). Although JSBACH-SPITFIRE overestimated global burned area (~32%) in comparison to the GFED and CCI datasets it was however tuned (by adjusting ignitions) to reproduce the burned area estimates including small fires. Results from the SOFIA and random forest models cannot be directly compared to these global burned values because they have gaps both in space and time depending on the missing values in the used predictor variables. Therefore, we masked the GFED and CCI datasets with the spatial-temporal distribution of gaps in all SOFIA and random forest models and recomputed the global mean annual burned area (Figure 4). All SOFIA models underestimated global mean annual burned area (-24 to -40 %, Figure 4). The random forest model RF2 overestimated (~60 %) and the random forest model RF.124421 reached a realistic (3-5% overestimation) global mean annual burned area. Despite the fact that all models reproduced well the global spatial pattern of annual burned area, the maps indicate regional differences especially in extra-tropical regions.

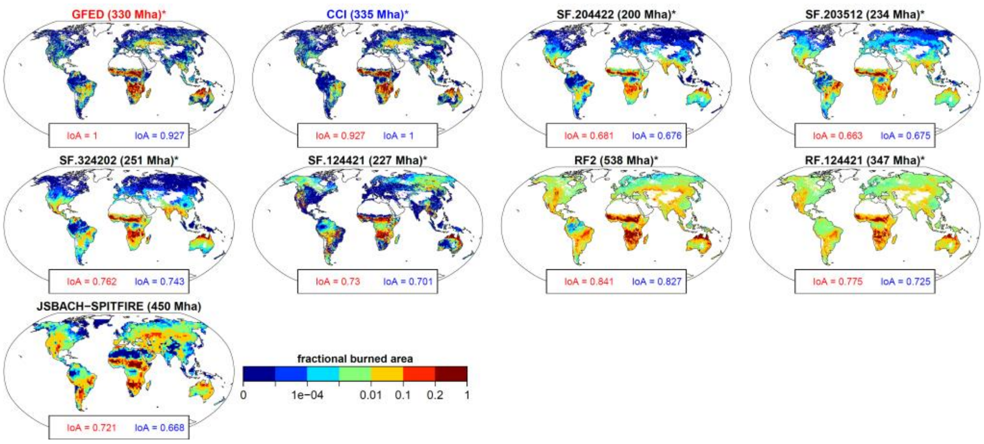

Figure 4: Mean annual fractional burned area in 2005-2011 from observational datasets and global fire models. Numbers in brackets are the global mean annual burned area. In case of * symbol, the computation of global total annual burned area considered the common spatial-temporal occurrence of missing values in all SOFIA and random forest models on the 0.25° grid cells. IoA is shown with respect to GFED (red) and CCI (blue), respectively. All maps were aggregated to the coarsest common spatial resolution (i.e. JSBACH, ~1.875*1.875°) for the computation of IoA and total burned area.

4.3.2 Variability in tundra and boreal forests

Regionally, we found varying performances of SOFIA models, random forest, and JSBACH-SPITFIRE in simulating spatial-temporal and statistical distributions of annual total burned area (Figure 5). In northern regions (boreal forests and tundra), differences between all datasets and models were large: Whereas three SOFIA models produced almost no fire activity and thus had very poor performances, the model SF.124421 reached medium performances (IoA = 0.48 vs. CCI in boreal needleleaf deciduous forests, Figure 5 c). The main difference between these SOFIA models is that SF.124421 used diurnal temperature range and the other three SOFIA models used annual pre-fire temperature as temperature effects on fire activity. Thus the results suggest that mean annual temperature is not an appropriate predictor variable to represent boreal fire activity within a global fire model. Random forest models strongly overestimated mean annual burned area in northern regions.

In the tundra, all models had very low performances but SF.124421 reproduced at least the mean annual burned area from the GFED dataset. However, also the GFED and CCI datasets strongly disagree in the tundra (IoA = 0.17 and FV = -1.91 for CCI vs. GFED, Figure 5 a) while only moderately agreeing in boreal forests. We found that SOFIA and random forest models agreed slightly better with the CCI dataset than with the GFED dataset in northern regions although the GFED dataset was used for training. In boreal needle-leaved evergreen forests, SF.124421 reproduced mean annual burned area and reached the highest IoA of all models (Figure 5 b).

In boreal needle-leaved deciduous forests, the random forest models reached the highest performance (IoA = 0.52 for RF2 against CCI) but overestimated mean annual burned area. SF.124421 and JSBACH-SPITFIRE only slightly overestimated mean annual burned and reached medium performances (IoA = 0.47 for SF.124421 vs. CCI, IoA = 0.31 for JSBACH-SPITFIRE vs. CCI) (Figure 5 c). In summary, although SF.124421 had only moderate performances in northern regions, it reached slightly better performances than random forest models and JSBACH-SPITFIRE. However, these results demonstrate the need to further investigate fire activity in tundra and boreal forests by improving the agreement of satellite datasets and by developing more appropriate empirical and process-oriented fire models.

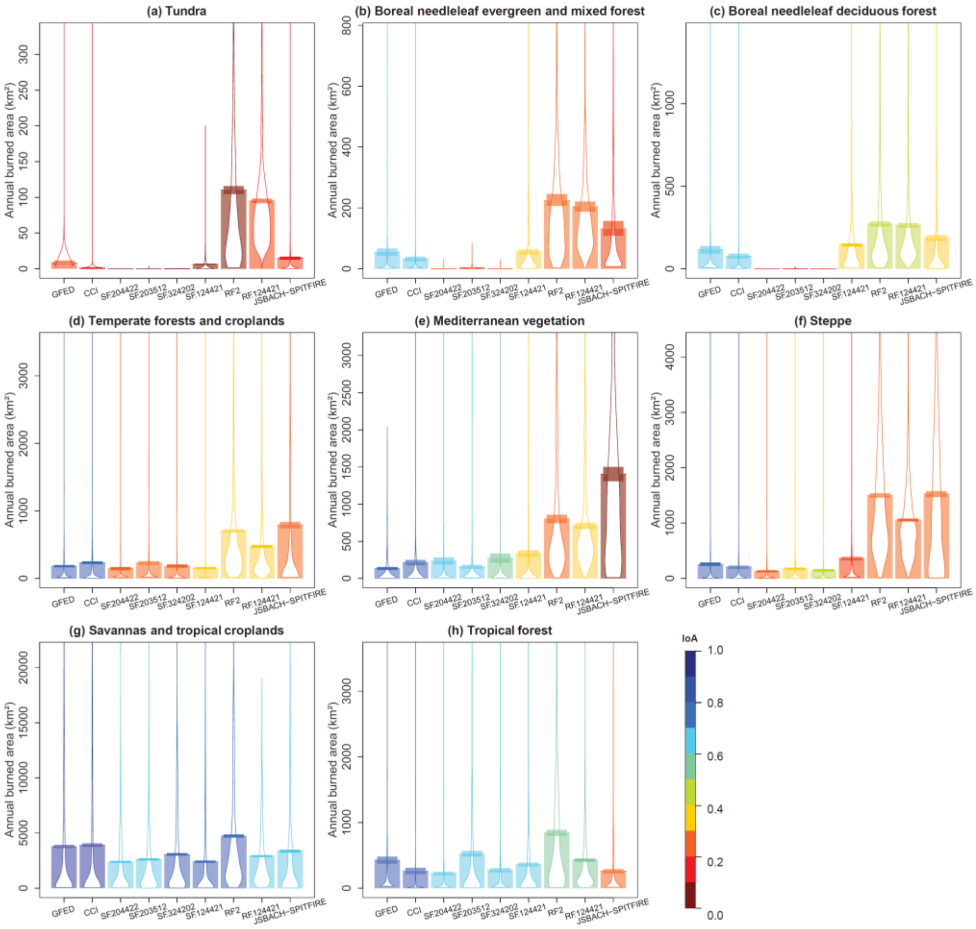

Figure 5: Regional distributions of annual total burned area per 1.875° grid cells from datasets and global fire models for the years 2005-2011. Bars show the mean of the distribution. Horizontal bands at the top of each bar are error estimates for the mean value

(i.e. 95% highest density intervals). Violins show the distribution of values. Colours represent the index of agreement between a model and both (i.e. GFED and CCI) datasets. For GFED and CCI, the index of agreement was computed only with respect to the other observational burned area dataset. The extent of regions is shown in Figure A1 a.

4.3.3 Variability in temperate regions and the Mediterranean

In temperate regions, SOFIA models generally outperformed random forest models and JSBACH-SPITFIRE in reproducing the observed spatial-temporal and statistical distributions of annual total burned area (Figure 5d-f). The random forest models and JSBACH-SPITFIRE overestimated mean annual burned area in all temperate regions.

In temperate forests and croplands, SF.124421 reached the best performance of all models (IoA = 0.43 and FV = -0.2 vs. GFED), whereas the other three SOFIA models had weaker performances (Figure 5 d). Random forest models reached medium IoA (up to 0.4 for RF.124421 vs. GFED) but overestimated mean annual burned area. JSBACH-SPITFIRE had medium IoA and overestimated mean annual burned area in comparison to GFED and CCI.

In the Mediterranean, all SOFIA models had medium to good performances (0.28 ≤ IoA ≤ 0.75) and outperformed JSBACH-SPITFIRE and random forest models **(**Figure 5 e). The performance was usually higher in comparison to the CCI dataset than in comparison to the GFED dataset because GFED contained much fewer very large burned areas and thus had also on average a smaller burned area than the CCI dataset. The models SF.204422 and SF.203512 (both using the GrowthFormCrop scheme and no human influence) had better performances than the models SF.324202 and SF.124421 (both using NLDI). This indicates that the better performance is related to how croplands and human influences are represented in these models.

In the steppes, all SOFIA models reproduced the observed mean annual burned area and some reached medium performances (IoA = 0.48 for SF.324202 vs. CCI, Figure 5 f). These results for temperate regions and the Mediterranean demonstrate that SOFIA models can realistically reproduce observed fire activity.

4.3.4 Variability in tropical regions

In tropical regions, SOFIA models had good performances in reproducing the observed spatial-temporal and statistical distributions of annual total burned area and had comparable or better performances than the random forest models and JSBACH-SPITFIRE (Figure 5g-h). In savannahs and tropical croplands, all SOFIA and random forest models and JSBACH-SPITFIRE had good performances in reproducing the spatial-temporal distribution of annual total burned area (0.63 ≤ IoA ≤ 0.78) but underestimated the variance and extreme fire years (-1.2 ≤ FV ≤ -0.4). This underestimation of very large burned areas in savannahs is the main cause for the underestimation of the mean annual burned area in this region and of the global total burned area by SOFIA models. SF.324202 and SF.124421 had slighter better performances than the other two SOFIA models.

In tropical forests, all SOFIA models had medium to good performances in reproducing the spatial-temporal distribution of annual total burned area (0.61 ≤ IoA ≤ 0.68) but also underestimated the variance and extreme fire years (-1.16 ≤ FV ≤ -0.36, Figure 5 h). However, the FV of all models was usually better in comparison to the CCI dataset than for the GFED dataset. The CCI dataset had less very large burned areas and thus a smaller variance than the GFED dataset in tropical forests (FV = -0.22 for CCI vs. GFED). Random forest models reached moderate but weaker performances than SOFIA models. JSBACH-SPITFIRE had a low performance in reproducing the spatial-temporal variability (IoA = 0.33 vs. GFED) but reproduced mean annual burned area. These results demonstrate that SOFIA models better reproduce observed fire activity in tropical regions than random forests or JSBACH-SPITFIRE.

In summary, we found that all modelling approaches (SOFIA, random forest, JSBACH-SPITFIRE) had relatively good performances in savannahs and tropical croplands. All SOFIA models had relatively good performances in tropical forests and the Mediterranean. Only some SOFIA models reached good performances in temperate forests and croplands (SF.124421) and in steppes (SF.324202). Random forest models and JSBACH-SPITFIRE had generally weaker performances than SOFIA models. The model SF.124421 (Figure 1) had the best performance from all SOFIA models in the tundra, boreal forests, temperate forests and croplands; it had very good performance in savannahs and tropical forests; and it outperformed random forest and JSBACH-SPITFIRE in steppes and the Mediterranean. Consequently, we finally identified SF.124421 as the globally best performing SOFIA model from the tested set of model structures.

4.4 Sensitivity of burned area to climate, vegetation, and human predictor variables

The underlying functional relationships in SOFIA models allow to map the sensitivities of burned area to human, vegetation, and climate variables. To demonstrate such a potential application of a SOFIA model, we mapped mean responses from each functional relationships for the period 1997-2011 from the SOFIA model SF.124421 (Figure 6). Based on this model, human influences (i.e. NLDI) restricted burned area in most parts of Europe and southern Russia, east and south-east Asia, India, central and eastern North America, south-east South America, south Australia and New Zealand (Figure 6 a). These regions correspond to the most populated and developed regions of the world. This pattern was caused by the underlying functional relationship of SF.124421 where NLDI < 1 (i.e. developed regions) restricted and NLDI > 1 (i.e. unpopulated regions or natural ecosystems) allowed fire activity (Figure 1 b). These results indicate a predominant restricting effect of humans on fire activity. Temperature effects in SF.124421, expressed as diurnal temperature range, allowed fire activity mostly in the semi-deserts of western North America, in the Sahel, Australia, and had a moderate restriction effect in tropical forests and the tundra (Figure 6 b). These spatial patterns were caused by the controlling function that had a strong sigmoidal increase of fire activity with diurnal temperature range in shrublands and allowed moderate fire activity in herbaceous vegetation and croplands (Figure 1 c).

Direct wetness effects, expressed as the number of wet days, generally allowed fire activity in all forest regions and moderately restricted fire activity in the rest of the world (Figure 6 c). The underlying controlling function in SF.124421 showed no sensitivity for forests, a weak positive relation in herbaceous vegetation and croplands, and a strong exponential decrease of fire activity with increasing number of wet days in shrublands (Figure 1 d).

As direct vegetation effect, pre-fire FAPAR restricted fire activity in herbaceous vegetation and croplands of central North America, central Asia, in the northern Sahel, the Kalahari, central Australia, and in parts of South America (Figure 6 d). On the other hand, pre-fire FAPAR supported fire activity mostly in the southern Sahel and northern and eastern Australia. These patterns were caused by a general strong restriction of fire activity with pre-fire FAPAR in herbaceous vegetation and croplands and an exponential increase of fire activity with increasing pre-fire FAPAR in shrublands in SF.124421 (Figure 1 e).

As long-term vegetation effect, 12-month precedent mean vegetation optical depth strongly supported fire activity in central North America, central Asia, the Tibetan plateau, the Sahel, parts of India, the Kalahari, in Australia (except interior), and in northern Patagonia (Figure 6 e). In all other regions, annual VOD had a moderate effect on fire activity in SF.124421. The underlying controlling function in SF.124421 showed an exponential increase of fire activity with annual VOD in shrublands, an exponential decrease with annual VOD in herbaceous vegetation and croplands and a strong restriction across all VOD ranges for trees (Figure 1 f). The diverging responses with annual VOD in shrublands and herbaceous vegetation indicate that fire activity increases with higher vegetation density or biomass in shrublands but decreases with increasing vegetation water content in herbaceous vegetation, respectively. Additionally, the general restriction of fire activity with VOD for trees indicates that fire activity is restricted by vegetation density or high vegetation water content in forests.

We further combined the controlling functions of SF.124421 to investigate combined controls on fire activity. Therefore we created a red-green-blue composite map in which the red channel contains the NLDI functional relationship, the green channel contains the mean of the direct (precedent month FAPAR) and long-term vegetation (12 month precedent VOD) effect, and the blue channel contains the climate effects (mean response of functional relationships to number of wet days and diurnal temperature range) from SF.124421 (Figure 6f). Generally, bright colours in this map indicate a strong restriction of fire activity (small burned area) and dark colours indicate that fire activity is allowed (large burned area). Regionally, different

Deleted: and provide in
Deleted: following chapter a demonstration how to apply this
Deleted: to identify controls on fire activity
Deleted: **Application**
Deleted: **SOFIA**
Deleted: **identify controls on fire activity**
Deleted: controlling functions of
Deleted: investigate
Deleted: role of
Deleted: on spatial patterns of fire activity.
Deleted: values of
Deleted: controlling function
Deleted: suppressed fire activity
Deleted: controlling function
Deleted: suppressed
Deleted: suppressing
Deleted: suppression
Deleted: suppressed
Deleted: suppressed
Deleted: suppression
Deleted: in the 12 months before fire
Deleted: .
Deleted: suppression
Deleted: suppression
Deleted: suppressed
Deleted: control function
Deleted: pre-fire
Deleted: pre-fire annual
Deleted: of control functions on
Deleted: suppression
Deleted: with
Deleted: areas
Deleted: , resulting in
Deleted: areas.

combinations of socioeconomic, vegetation and climate factors controlled fire activity. Socioeconomic development dominantly restricted fire activity in western North America, and in populated regions of boreal forests (red colours). Vegetation predominantly supressed fire activity in southern boreal and tropical forests (green colours). Primarily climate conditions and secondly socioeconomic development restricted fire activity in semi-deserts of the northern Sahel, central Asia, the Kalahari, and south-western Australia (purple colours). Socioeconomic development and climate equally supressed fire activity in the Mediterranean, India, eastern Asia, and east South America (pink colour). Both socioeconomic development and vegetation conditions supressed fire activity in most parts of Europe, central and eastern North America, and eastern China (yellow/orange colours). Both climate and vegetation conditions supressed fire activity in the tundra and in central Australia (cyan colours). All factors moderately supported fire activity in boreal forests and strongly support fire activity in large parts of the Sahel, southern Africa, northern Australia, and western North America (dark colours). We want to point out that these sensitivities might look different if SOFIA models with alternative but adequate model structures would be applied for such an analysis. However the results highlight that fire activity is controlled by regionally diverse and complex interactions of human, vegetation and climate factors.

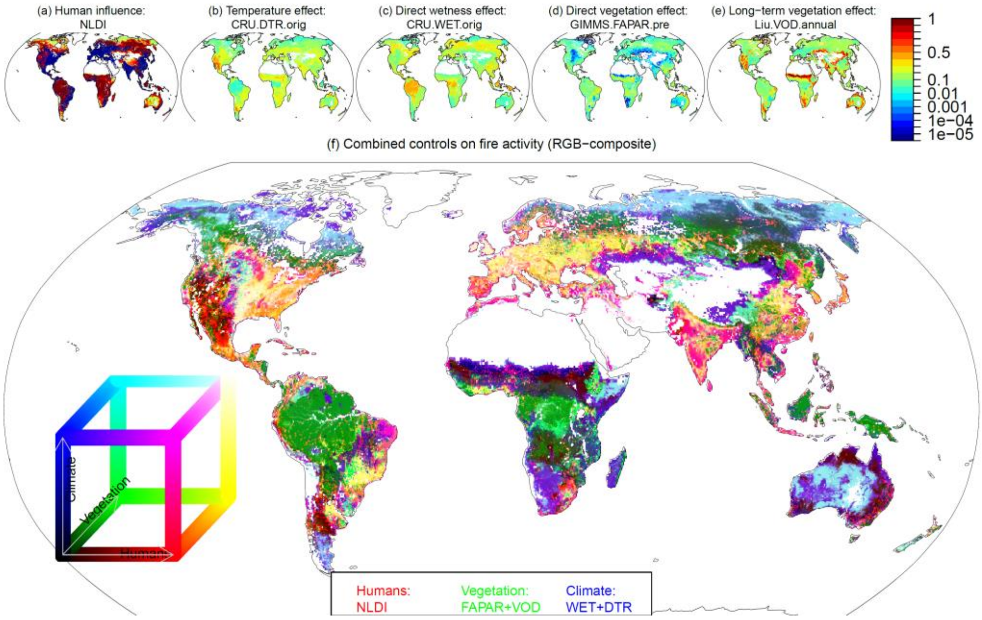

Figure 6: Example of combined climate, vegetation, and human controls on fire activity based on the SOFIA model SF.124421. The maps in (a-e) show the average response value for each functional relationship for the period 1997-2011. High values (1, red) indicate that this factor allows unlimited burning and low values (0, blue) indicate that this factor restricts burning. The map in (f) is a red-green-blue composite of the human influence (map in (a), red channel), the combined direct and long-term vegetation effect (mean of (d) and (e), green channel), and the climate effect (mean of (b) and (c), blue channel). Bright and dark colours indicate a strong restriction and allowance of fire activity, respectively.

5 Discussion and conclusions

5.1 Performance and equifinality of SOFIA models

We developed the SOFIA modelling approach as a framework to explore the importance and the functional relationships between different predictor variables and burned area while relying on relatively simple model structures. The best SOFIA models reached globally average performances but outperformed the state-of-the art process-oriented vegetation-fire model

Deleted: suppressed

Deleted: suppressed

Deleted: In summary,

Deleted: Combined

Deleted: controlling function

Deleted: suppresses

Deleted: suppression

Formatted: Font color: Auto

Deleted: Controls on fire activity

Deleted: required model components

Deleted: concept in order

Deleted: identify required

Deleted: to predict spatial-temporal patterns of burned area.

Deleted: /

JSBACH-SPITFIRE. We interpret the globally medium and regionally varying performances as current upper limits that can be reached with the used predictor datasets and variables because the more flexible and highly adaptive machine learning algorithm random forest did not achieve much higher performance in the evaluation data subset. These upper limits in model performance might be due to several reasons:

1. Uncertainties in the observations for the predictor and response variables inhibit the development of models with high performance. For example, we found regionally partly large differences between the two burned area datasets, especially in northern regions. These uncertainties originate from differences in sensor characteristics and in the ability of the used algorithms to detect small fires.
2. Other processes and variables are important for the spread of fires but cannot be resolved at the used spatial and temporal resolution. For example, on local to regional scales the spread of fire is controlled by landscape structure and topography whereas climatic controls are usually more important on larger scales (Archibald et al., 2009; Liu et al., 2013b; Parisien et al., 2010). Most of the regional controls can likely not be resolved at the used spatial resolution (0.25°) although this resolution is already higher than the resolution of most global vegetation-fire models. Also wind speed and direction is an important control on the spread of fires on short temporal scales but this effect cannot accurately be represented based on monthly data (Bistinas et al., 2014).
3. There is a lack of global observations that directly represent fuel loads, fuel moisture, or modes of human fire usage. For example, all of the used predictor variables are only proxies for fuel loads (FAPAR or VOD) or fuel moisture (surface soil moisture) but do not directly represent such conditions. Similarly, data on population density or socioeconomic development are used as proxies for human effects on fire but cannot represent the complex social, economic, and cultural practices, and policies of human fire use and management.

Formatted: English (United Kingdom)

Field Code Changed

Formatted: English (United Kingdom)

Deleted: /

Deleted: fuel

Deleted: fuel

The four best SOFIA models reached similar performances in savannas and tropical croplands, and in tropical forests which demonstrates the equifinality in fire modelling. Equifinality, i.e. the presence of multiple adequate models and parameter sets that result in very similar responses, is a general problem in environmental modelling (Beven, 2006). General approaches to avoid equifinal models are the use of multiple datasets of the same variable to account for errors or uncertainties in model forcing or reference data, the testing of different cost functions to constrain certain parameters, the inclusion of prior parameter uncertainties in the cost function, or the application of models to new observational data or under different conditions (Beven, 2006; Beven and Binley, 2014; Williams et al., 2009). In our analysis, we were able to rule out three of four initially equifinal SOFIA models based on the application of these models to the global data and by regional comparisons against two burned area datasets. The results from the optimized SOFIA models allow extracting parameter values and ranges for each functional relationship. To give an example, parameters that control the functional relationship to 1) socioeconomic development (NLDI), 2) diurnal temperature range and to the number of wet days in shrublands, and 3) to VOD were well constrained in the SOFIA model SF.124421 (Figure A3). These parameters could be potentially used as prior parameter values in a more constrained analysis in the future. The presence of equifinality in SOFIA model structures suggests to include such prior parameter uncertainties for each functional relationship to better constrain individual SOFIA models. This technique can be applied in future generation of individual SOFIA models by using the current versions as prior parameter estimates and uncertainties.

5.2 Importance of predictor variables and implications for global fire modelling

The derived SOFIA models and the spatial patterns of sensitivities show a sharp decline of burned area with increasing socioeconomic development or population density and thus agree with previous studies that show a primarily negative effect of human activities, population density, or croplands on burned area (Andela et al., 2017; Archibald et al., 2013; Bistinas et al., 2014; Chuvieco and Justice, 2010; Knorr et al., 2014). Strikingly, our results suggest that human effects on global burned area can be expressed by either cropland area, NLDI, or population density but the combination of these factors did not improve the performances of SOFIA models. These variables serve all as proxies for the negative relationship between humans and burned area but do not directly describe human activities of fire use or suppression. For example, regional studies have shown that various information on infrastructure, land use, and other relevant socioeconomic indicators are important to predict fire activity (Archibald et al., 2009; Arndt et al., 2013; Parisien et al., 2016). However such spatially- and temporally-resolved datasets and assessments are missing for the global scale. Certainly, our results do not imply that croplands are unimportant for the global variability of burned area. Agricultural fires account for around 10% of all global fires (Korontzi et al., 2006) and for around 5% of global burned area (Giglio et al., 2013) and are used to remove harvest residues or to fertilize soils. However croplands show more small fires than large fires (Hantson et al., 2015b). As we here used the GFED burned area datasets that was not corrected for small fires (Giglio et al., 2013), small agricultural fires are likely misrepresented in this dataset and thus cannot be accurately analysed within the SOFIA approach. The representation of agricultural fires in a global fire model needs to account for various land use patterns and practices that go far beyond natural climate-vegetation relationships (Le Page et al., 2015; Magi et al., 2012; Rabin et al., 2015). By taking into account this complexity, agricultural fires are often not represented in global vegetation-fire models because they do not directly affect natural vegetation and carbon cycle dynamics (Hantson et al., 2016), unless agricultural fires escape to nearby forests (Cano-Crespo et al., 2015). In summary, an improved representation of human effects on fire in global vegetation-fire models is currently lacking since globally consistent, temporally and spatial resolved, relevant information on infrastructure and socioeconomics is not available.

Direct wetness effects, especially based on the number of wet days, were the component of SOFIA models that contributed most to model performance (Figure 3). These result are in agreement with previous results that identified the number of dry days (the inverse of the number of wet days) as an important variable to predict fire activity (Bistinas et al., 2014). Especially for shrublands, we identified strong exponential relations with the number of wet days and diurnal temperature range. Currently, shrubs are not considered in all ecosystem models (e.g. not in models of the LPJ family, Sitch et al. (2003)) which suggest the need to implement and parameterize shrub PFTs to improve simulations of fire activity. The number of wet days and diurnal temperature range are also used in process-oriented fire models like SPITFIRE to compute the Nesterov index (a fire weather index) and fuel moisture content (Thonicke et al., 2010). Here we confirm that the use of diurnal temperature range and the number of wet days are appropriate predictor variables to simulate fuel moisture conditions and thus fire activity. However, while the Nesterov index is used as fire weather index in many fire modules of global vegetation models (Lasslop et al., 2014; Prentice et al., 2011; Thonicke et al., 2010; Venevsky et al., 2002; Yue et al., 2014), studies on forest fire management rely more often on alternative fire weather indices such as from the Canadian Forest Fire Weather Index (FWI) (Bedia et al., 2012; Stocks et al., 1989). We also show that direct wetness effects can be represented by satellite-derived surface soil moisture. Additionally, several other indices have been derived from satellite data to estimate fuel moisture conditions (Yebra et al., 2013). Consequently, it is necessary to systematically compare the predictive power of fire weather indices, satellite-derived and reanalysis-based surface soil moisture data, and soil moisture schemes of ecosystem models to potentially improve the direct effect of wet conditions on fire activity in global vegetation-fire models.

Long-term vegetation effects contributed strongly to the performance of SOFIA models and thus indicate an important role of vegetation dynamics on the spatial-temporal variability of fire activity. Consequently, global vegetation models require a good representation of vegetation distribution and dynamics to realistically simulate fire activity. Vegetation distribution can be improved either through the prescription of high quality land cover maps in land surface models, or by improving model structures and by constraining model parameters that affect vegetation dynamics in DGVMs. For both approaches, time-variant, e.g. annually resolved, land cover maps would be very valuable to realistically reflect vegetation dynamics. However, it is currently unclear how realistic land cover dynamics are represented for example by the three epochs of the ESA CCI land cover maps or by annual or seasonal maps of the MODIS land cover product (Broxton et al., 2014). Hence intensified efforts are required to check the plausibility of land cover changes in current and upcoming time-variant land cover maps.

Deleted: However, we demonstrated from the ensemble of all candidate SOFIA models that model components on human influences, direct wetness effects, and long-term vegetation effects on fire activity are most important and all need to be accounted for to improve global vegetation/fire models. ¶
Globally, burned area decreases with increasing socioeconomic development and is mainly supressed in croplands and developed regions of the world (Figure 6). Hence our results confirm previous studies that also assign a predominantly suppressing effect of humans in African croplands (Andela and van der Werf, 2014) and a global decrease of burned area with increasing population density (Archibald et al., 2013; Bistinas et al., 2014; Chuvieco and Justice, 2010; Knorr et al., 2014). On the other hand, datasets on population density or socioeconomic development did not improve the performances of the SOFIA models if croplands were already included in the model structure. Consequently, a more detailed analysis and modelling of human-fire interactions is necessary but is currently hampered by the availability of globally available, temporally resolved accurate information on human fire usage and management.¶

Deleted:

Deleted: /

Deleted: .

SOFIA models with a long-term effect of VOD had better performances than models without this effect. The good performance of SOFIA models with VOD as predictor variable likely reflects variability in fuel loads because VOD is sensitive to vegetation density and biomass (Andela et al., 2013; Liu et al., 2015). The importance of VOD suggests that processes such as carbon allocation, turnover and vegetation mortality which all control biomass dynamics need to be carefully assessed in global vegetation models in order to accurately simulate fuel loads and hence fire activity. The finding of a strong restriction of fire activity with VOD in forests corresponds to previous findings that show that woody vegetation tends to restrict burned area either because moist wood is more difficult to ignite than dry grass or litter, or because forests provide generally more moist conditions (Kelley and Harrison, 2014). Fire activity increases with biomass at low vegetation densities and strongly decreases with increasing biomass and very high vegetation densities but the actual fire activity is enhanced or restricted by moisture conditions (Krawchuk and Moritz, 2011; Murphy et al., 2011). Consequently, the SOFIA approach and the identified sensitivities of fire activity with direct wetness effects and with VOD confirm and implement previous conceptual models where fire activity follows a biomass gradient and is modulated by moisture conditions (Krawchuk and Moritz, 2011; Murphy et al., 2011).

5.3 From satellite data to improved global vegetation-fire models

The better performance of SOFIA models compared to JSBACH-SPITFIRE and the generally good performance especially in temperate and tropical regions demonstrate the potential of the SOFIA approach to improve global vegetation-fire models. The SOFIA approach can be potentially adapted to more complex global vegetation-fire models such as SPITFIRE. Thereby the functional relationships in SOFIA models should rely on forcing datasets (e.g. temperature, precipitation) and simulated state variables (e.g. litter and soil moisture, biomass compartments, litter stocks, vegetation structure) of the vegetation models. This allows also to represent feedbacks of changing vegetation conditions on fire activity. By applying the SOFIA approach to forcing and state variables of a process-oriented vegetation model, more adequate predictor variables could be potentially identified and finally model performance could be improved.

In order to represent realistic vegetation/fire interactions, vegetation models need to satisfactorily reproduce observed patterns and dynamics of fuel moisture and vegetation state variables. Consequently, it is necessary to test and improve global vegetation-fire models against multiple observational datasets that cover various aspects of vegetation/fire interactions: For example, satellite datasets on land cover, FAPAR, VOD, biomass (Avitabile et al., 2016; Saatchi et al., 2011; Thurner et al., 2014), and estimates of litter fuels (Pettinari and Chuvieco, 2016) may be useful to constrain vegetation dynamics, biomass allocation, and fuel loads; datasets on surface soil moisture, VOD, and evapotranspiration (Tramontana et al., 2016) may be useful to test hydrological schemes and to constrain fuel moisture; and datasets on burned area, fire size (Hantson et al., 2015b), fire radiative power, fuel consumption (Andela et al., 2016; van Leeuwen et al., 2014), or separations between natural and agricultural fires (Korontzi et al., 2006; Le Page et al., 2010; Magi et al., 2012) may be useful to constrain fire behaviour. Such datasets are currently under-exploited in the development of global vegetation-fire models because #1 they were still missing at the time of model development (Thonicke et al., 2001), #2 there is only little experience of applying formal model-data integration approaches within global fire modelling, or #3 no appropriate model components or observation operators exist that link for example modelled fuel moisture with satellite-derived surface soil moisture or modelled biomass compartments with VOD. For example, it is currently unclear which physiological processes, morphological plant components, and ecosystem structures contribute to a certain VOD signal (Vreugdenhil et al., 2016a). Consequently, it is necessary to better understand the plant and ecosystem controls on VOD to improve global vegetation-fire models.

Previously developed global fire models commonly used observed data for model evaluation but did not undertake a formal model-data integration cycle from the definition of model structures, model parameter estimation, to model evaluation, and potentially back to a re-formulation of model structures by using observational data. In our study we firstly applied the full

Deleted: that
Deleted: the
Deleted: of biomass
Deleted: suppression
Deleted: suppress
Deleted: suppressed
Deleted: concept
Deleted: (Krawchuk and Moritz, 2011; Murphy et al., 2011)
Deleted: 2
Deleted: /
Deleted: demonstrates
Deleted: models
Deleted: /
Deleted: modelling concept
Deleted: applied
Deleted: /
Deleted: in order to identify appropriate model structures.
Deleted: controlling functions
Deleted: concept
Deleted: a best model structure
Deleted: in order to better reproduce observed spatial-temporal dynamics of burned area.
Deleted: /
Deleted: and biomass (Avitabile et al., 2016; Pettinari and Chuvieco, 2016; Saatchi et al., 2011; Thurner et al., 2014)
Deleted: or
Deleted: might
Deleted: /
Deleted: /

model-data integration cycle to derive an optimal structure for an empirical global fire model to predict global burned area. However, in order to apply model-data integration for global process-oriented vegetation-fire models, multiple datasets on vegetation, hydrological, and fire-related variables should be used to realistically constrain vegetation/fire interactions. Hence there is a need to develop appropriate observation operators and to extent currently existing model-data integration frameworks of global vegetation models (Forkel et al., 2014; Kaminski et al., 2013; MacBean et al., 2016; Schürmann et al., 2016) to the corresponding fire modules in order to formally assess model structures and to constrain model parameters. In summary, model-data integration frameworks need to be developed that make use of multiple satellite datasets on vegetation and moisture proxies in order to improve the representation of fire in global vegetation models and thus to better understand interactions of fire with ecosystems and the atmosphere within the Earth system.

Deleted: /

Deleted: (Forkel et al., 2014; Kaminski et al., 2013; MacBean et al., 2016; Schürmann et al., 2016)

Code availability

Formatted: Font color: Auto

The code for this study is organized in several R packages and is available from https://r-forge.r-project.org/R/?group_id=1612. Thereby the package *SOfireA* contains the basic SOFIA model structure and functions to optimize and plot SOFIA models, and the package *ModelDataComp* contains functions for model-data comparison such as model evaluation metrics and comparison plots. The R package *randomForest* was used for random forest fits (Liaw and Wiener, 2002).

Formatted: Font color: Auto

Formatted: Font color: Auto

Data availability

Formatted: Font color: Auto

The used original data is available under the URLs, DOIs, or can be obtained from PIs as indicated in Table 1. The pre-processed (spatially and temporally interpolated) data for the optimization and evaluation data subsets is included as example dataset '*firedata*' in the *SOfireA* R package (https://r-forge.r-project.org/R/?group_id=1612).

Formatted: Font color: Auto

Formatted: Font color: Auto

Appendix

Formatted: Font color: Auto

Table A 1: Land cover to plant functional type conversion table. The units are % coverage of each PFT per land cover class. The conversion factors are based on Poulter et al. (2015a) with some modifications that affect boreal and arctic regions, i.e. to avoid coverage of broadleaved evergreen PFTs in these regions and to reach a total tree cover that is comparable to the MODIS tree cover product (Hansen et al., 2003).

		Plant functional types										
ID	Land cover class	Tree.BE	Tree.BD	Tree.NE	Tree.ND	Shrub.BE	Shrub.BD	Shrub.NE	Herb	Crop	Bare	NoLand
0	No data											100
10	Cropland, rainfed									100		
11	Cropland, rainfed, Herbaceous cover									100		
12	Cropland, rainfed, Tree or shrub cover						50			50		
20	Cropland, irrigated or post-flooding									100		
30	Mosaic cropland (>50%) / natural vegetation (tree, shrub, herbaceous cover) (<50%)	5	5			5	5	5	15	60		
40	Mosaic natural vegetation (tree, shrub, herbaceous cover) (>50%) / cropland (<50%)	5	5			5	10	5	30	40		
50	Tree cover, broadleaved, evergreen, closed to open (>15%)	90				5	5					
60	Tree cover, broadleaved, deciduous, closed to open (>15%)		70				10		20			
61	Tree cover, broadleaved, deciduous, closed (>40%)		80				10		10			
62	Tree cover, broadleaved, deciduous, open (15-40%)		30				20		40		10	
70	Tree cover, needleleaved, evergreen, closed to open (>15%)			70		0	5	5	20			
71	Tree cover, needleleaved, evergreen, closed (>40%)			75		0	5	5	15			
72	Tree cover, needleleaved, evergreen, open (15-40%)			30			5	5	30		30	
80	Tree cover, needleleaved, deciduous, closed to open (>15%)				50	0	15	5	25		5	
81	Tree cover, needleleaved, deciduous, closed (>40%)				70	0	10	5	15			
82	Tree cover, needleleaved, deciduous, open (15-40%)				30		10	5	35		20	

90	Tree cover, mixed leaf type (broadleaved and needleleaved)		35	25	0	0	10	10	15		5	
100	Mosaic tree and shrub (>50%) / herbaceous cover (<50%)	0	15	15	0	0	15	15	40			
110	Mosaic herbaceous cover (>50%) / tree and shrub (<50%)	0	7.5	7.5		0	10	10	60		5	
120	Shrubland					20	30	10	20		20	
121	Shrubland, evergreen					30		30	20		20	
122	Shrubland, deciduous						60		20		20	
130	Grassland								70		30	
140	Lichens and mosses								60		40	
150	Sparse vegetation (tree, shrub, herbaceous cover) (<15%)	0	2	2		0	4	2	5		85	
152	Sparse shrub (<15%)					0	6	4	5		85	
153	Sparse herbaceous cover (<15%)								15		85	
160	Tree cover, flooded, fresh or brakish water	30	30						20			20
170	Tree cover, flooded, saline water	60				20						20
180	Shrub or herbaceous cover, flooded, fresh/saline/brakish water		5	5			10	10	40			30
190	Urban areas		2.5	2.5					15		75	5
200	Bare areas										100	
201	Bare areas, consolidated										100	
202	Bare areas, unconsolidated										100	
210	Water bodies											100
220	Permanent snow and ice											100

Table A 2: Structure and performance of all tested candidate SOFIA models. N denotes the number of model parameters. SSE, AIC, IoA and FV are based on monthly burned area time series in the optimization and evaluation data subsets from the GFED and CCI datasets, respectively. Model experiments are ordered by SSE. The best SOFIA models (IoA ≥ 0.4 and AIC ≤ 200.5) are highlighted in bold font.

Structure of SOFIA models: used control factors and associated variables

Grouping scheme (groups)
- 1 GrowthForm
- 2 GrowthFormCrop
- 3 LeafType
- 4 PFT

Human influence (human)
- 0 no
- 1 PD.med (global)
- 2 NLDI (global)
- 3 NLDI.g (per group)

Direct wetness effect (wet.dir)
- 0 no
- 1 CCI.SM.orig
- 2 (unused)
- 3 GPCC.P.orig
- 4 CRU.WET.orig

Long-term wetness/productivity effect (wetveg.longterm)
- 0 no
- 1 CCI.SM.orig.filter13
- 2 GPCC.P.orig.filter13
- 3 CRU.WET.orig.filter13
- 4 Liu.VOD.orig.filter13
- 5 GIMMS.FAPAR.orig.filter13

Direct vegetation effect (veg.dir)
- 0 no
- 1 Liu.VOD.orig.lagneg1
- 2 GIMMS.FAPAR.orig.lagneg1

Temperature effect (temp)
- 0 no
- 1 CRU.DTR.orig
- 2 CRU.T.orig.filter13

Example: SF.204422 = (2) GrowthFormCrop + (0) no human influence + (4) CRU.WET.orig + (4) Liu.VOD.orig.filter13 + (2) GIMMS.FAPAR.orig.lagneg1 + (2) CRU.T.orig.filter13

Name	Model structure and included variables							Comparison against GFED.BA (1997-2011)						Comparison against CCI.BA (2005-2011)			
								Training (1817 cells, even years) Data used for parameter optimization				Evaluation (1212 cells, uneven years)		Training (even years)		Evaluation (uneven years)	
	N	Groups	Human	Wet.dir	Wetveg.longterm	Veg.dir	temp	SSE	AIC	IoA	FV	IoA	FV	IoA	FV	IoA	FV
SF.204422	48	2	0	4	4	2	2	51.88	199.8	0.44	-1.44	0.39	-1.55	0.42	-1.53	0.41	-1.53
SF.203512	48	2	0	3	5	1	2	52.17	200.3	0.43	-1.45	0.42	-1.54	0.45	-1.49	0.45	-1.51
SF.304522	48	3	0	4	5	2	2	52.92	201.8	0.41	-1.49	0.40	-1.58	0.40	-1.57	0.42	-1.59
SF.324202	39	3	2	4	2	0	2	52.92	183.8	0.41	-1.49	0.37	-1.65	0.39	-1.59	0.35	-1.65
SF.234422	60	2	3	4	4	2	2	52.99	226.0	0.41	-1.49	0.35	-1.63	0.40	-1.58	0.33	-1.64
SF.233210	48	2	3	3	2	1	0	53.10	202.2	0.40	-1.50	0.34	-1.69	0.41	-1.57	0.32	-1.68
SF.124421	39	1	2	4	4	2	1	53.40	184.8	0.40	-1.51	0.39	-1.51	0.39	-1.59	0.41	-1.51
SF.124021	30	1	2	4	0	2	1	54.05	168.1	0.37	-1.56	0.36	-1.56	0.37	-1.64	0.37	-1.57
SF.204501	36	2	0	4	5	0	1	54.09	180.2	0.37	-1.56	0.31	-1.76	0.36	-1.63	0.29	-1.76
SF.314511	51	3	1	4	5	1	1	54.14	210.3	0.37	-1.55	0.34	-1.63	0.35	-1.63	0.34	-1.62
SF.424102	84	4	2	4	1	0	2	54.37	276.7	0.37	-1.55	0.35	-1.63	0.36	-1.63	0.36	-1.63
SF.234421	60	2	3	4	4	2	1	54.40	228.8	0.36	-1.56	0.33	-1.63	0.36	-1.64	0.34	-1.63
SF.314420	39	3	1	4	4	2	0	54.55	187.1	0.36	-1.58	0.32	-1.68	0.33	-1.65	0.32	-1.68
SF.333221	60	3	3	3	2	2	1	54.57	229.1	0.35	-1.57	0.32	-1.71	0.35	-1.64	0.30	-1.69
SF.224211	51	2	2	4	2	1	1	54.59	211.2	0.35	-1.58	0.36	-1.55	0.36	-1.65	0.37	-1.56

Deleted: indicated
Deleted: red
Formatted: Complex Script Font: Times New Roman, 12 pt, Italian (Italy)
Formatted Table
Deleted: N
Formatted: Indent: Before: 0 cm, First line: 0 cm, After: 0 cm
Formatted: Font: Bold, Complex Script Font: Times New Roman, 12 pt
Deleted: veg.dir
Moved down [2]: temp
Deleted: groups
Formatted: Font: Bold, Complex Script Font: Times New Roman, 12 pt
Deleted: human
Formatted: Font: Bold, Complex Script Font: Times New Roman, 12 pt
Deleted: wet.dir
Formatted: Font: Bold, Complex Script Font: Times New Roman, 12 pt
Deleted: wetveg.longterm
Formatted: Font: Bold, Complex Script Font: Times New Roman, 12 pt
Formatted: Font: Bold, Complex Script Font: Times New Roman, 12 pt
Deleted:
Formatted: Font: Bold, Complex Script Font: Times New Roman, 12 pt
Formatted: Font: Bold, Complex Script Font: Times New Roman, 12 pt
Formatted: Font: Bold, Complex Script Font: Times New Roman, 12 pt
Formatted: Font: Bold, Complex Script Font: Times New Roman, 12 pt
Moved (insertion) [2]
Formatted: Font: Bold, Complex Script Font: Times New Roman, 12 pt
Formatted: Centered, Indent: Before: 0.2 cm, After: 0.2 cm
Formatted: Font: Bold, Font color: Auto, Complex Script Font: Times New Roman, 12 pt
Formatted: Font: Bold, Complex Script Font: Times New Roman, 12 pt
Formatted: Font: Bold, Font color: Auto, Complex Script Font: Times New Roman, 12 pt
Formatted: Font: Bold, Complex Script Font: Times New Roman, 12 pt
Formatted: Font: Bold, Font color: Auto, Complex Script Font: Times New Roman, 12 pt
Formatted: Font: Bold, Complex Script Font: Times New Roman, 12 pt
Formatted: Font: Bold, Font color: Auto, Complex Script Font: Times New Roman, 12 pt
Formatted: Font: Bold, Complex Script Font: Times New Roman, 12 pt

SF.204202	36	2	0	4	2	0	2	54.62	181.2	0.35	-1.58	0.35	-1.52	0.35	-1.67	0.36	-1.54
SF.424201	84	4	2	4	2	0	1	54.62	277.2	0.35	-1.58	0.34	-1.61	0.35	-1.66	0.34	-1.61
SF.234102	48	2	3	4	1	0	2	54.64	205.3	0.35	-1.58	0.31	-1.74	0.35	-1.65	0.31	-1.76
SF.321221	51	3	2	1	2	2	1	54.66	211.3	0.35	-1.58	0.32	-1.73	0.35	-1.64	0.29	-1.72
SF.204502	36	2	0	4	5	0	2	54.66	181.3	0.35	-1.59	0.28	-1.80	0.34	-1.66	0.26	-1.80
SF.314201	39	3	1	4	2	0	1	54.77	187.5	0.35	-1.58	0.32	-1.67	0.35	-1.65	0.31	-1.67
SF.314211	51	3	1	4	2	1	1	54.85	211.7	0.35	-1.58	0.30	-1.75	0.34	-1.64	0.30	-1.75
SF.304211	48	3	0	4	2	1	1	54.88	205.8	0.34	-1.61	0.30	-1.70	0.32	-1.68	0.30	-1.70
SF.321021	39	3	2	1	0	2	1	55.12	188.2	0.34	-1.61	0.31	-1.70	0.32	-1.68	0.30	-1.70
SF.214320	39	2	1	4	3	2	0	55.15	188.3	0.33	-1.62	0.32	-1.65	0.32	-1.68	0.33	-1.66
SF.114401	30	1	1	4	4	0	1	55.31	170.6	0.33	-1.61	0.29	-1.69	0.33	-1.68	0.30	-1.68
SF.410311	84	4	1	0	3	1	1	55.57	279.1	0.32	-1.64	0.31	-1.76	0.33	-1.68	0.34	-1.75
SF.203321	48	2	0	3	3	2	1	55.81	207.6	0.31	-1.64	0.31	-1.69	0.32	-1.68	0.34	-1.68
SF.133402	36	1	3	3	4	0	2	55.97	183.9	0.31	-1.64	0.29	-1.60	0.32	-1.70	0.29	-1.59
SF.124002	21	1	2	4	0	0	2	56.35	154.7	0.29	-1.68	0.29	-1.72	0.27	-1.75	0.29	-1.73
SF.424520	84	4	2	4	5	2	0	56.41	280.8	0.29	-1.66	0.22	-1.78	0.28	-1.71	0.20	-1.79
SF.423220	84	4	2	3	2	2	0	56.48	281.0	0.29	-1.67	0.28	-1.71	0.30	-1.72	0.28	-1.72
SF.200211	36	2	0	0	2	1	1	56.49	185.0	0.28	-1.68	0.25	-1.81	0.28	-1.71	0.23	-1.80
SF.201021	36	2	0	1	0	2	1	56.60	185.2	0.28	-1.69	0.28	-1.74	0.28	-1.73	0.30	-1.73
SF.110221	30	1	1	0	2	2	1	56.60	173.2	0.28	-1.69	0.28	-1.74	0.28	-1.73	0.30	-1.73
SF.201412	48	2	0	1	4	1	2	56.65	209.3	0.27	-1.72	0.31	-1.66	0.25	-1.78	0.35	-1.66
SF.303122	48	3	0	3	1	2	2	56.75	209.5	0.24	-1.79	0.23	-1.85	0.25	-1.82	0.24	-1.85
SF.423502	84	4	2	3	5	0	2	56.84	281.7	0.27	-1.69	0.27	-1.73	0.27	-1.75	0.28	-1.73
SF.124222	39	1	2	4	2	2	2	57.05	192.1	0.26	-1.70	0.23	-1.79	0.25	-1.76	0.21	-1.80
SF.103402	27	1	0	3	4	0	2	57.31	168.6	0.25	-1.72	0.24	-1.74	0.26	-1.76	0.25	-1.73
SF.404401	81	4	0	4	4	0	1	57.37	276.7	0.25	-1.73	0.19	-1.83	0.24	-1.78	0.18	-1.84
SF.114102	30	1	1	4	1	0	2	57.37	174.7	0.25	-1.72	0.25	-1.76	0.25	-1.76	0.27	-1.76
SF.103521	36	1	0	3	5	2	1	57.54	187.1	0.24	-1.73	0.25	-1.75	0.25	-1.77	0.26	-1.75
SF.303511	48	3	0	3	5	1	1	57.60	211.2	0.23	-1.76	0.22	-1.82	0.23	-1.78	0.22	-1.82
SF.401301	81	4	0	1	3	0	1	57.66	277.3	0.22	-1.77	0.18	-1.85	0.21	-1.80	0.17	-1.85
SF.203420	36	2	0	3	4	2	0	57.68	187.4	0.24	-1.74	0.24	-1.76	0.24	-1.78	0.24	-1.76
SF.311312	51	3	1	1	3	1	2	57.76	217.5	0.23	-1.76	0.22	-1.84	0.23	-1.78	0.25	-1.82
SF.223520	39	2	2	3	5	2	0	57.77	193.5	0.21	-1.82	0.21	-1.83	0.21	-1.85	0.22	-1.83
SF.224001	27	2	2	4	0	0	1	58.07	170.1	0.22	-1.76	0.22	-1.80	0.21	-1.81	0.24	-1.80
SF.301421	48	3	0	1	4	2	1	58.13	212.3	0.21	-1.79	0.18	-1.86	0.21	-1.81	0.18	-1.85
SF.303301	36	3	0	3	3	0	1	58.21	188.4	0.21	-1.78	0.20	-1.86	0.21	-1.81	0.20	-1.85
SF.321421	51	3	2	1	4	2	1	58.29	218.6	0.22	-1.76	0.17	-1.83	0.22	-1.80	0.16	-1.83
SF.220220	27	2	2	0	2	2	0	58.53	171.1	0.19	-1.81	0.19	-1.83	0.18	-1.85	0.19	-1.84
SF.214112	51	2	1	4	1	1	2	58.62	219.2	0.20	-1.78	0.15	-1.85	0.20	-1.82	0.14	-1.84
SF.211512	51	2	1	1	5	1	2	58.63	219.3	0.19	-1.80	0.20	-1.81	0.19	-1.83	0.20	-1.81
SF.231220	48	2	3	1	2	2	0	58.71	213.4	0.19	-1.80	0.20	-1.76	0.18	-1.86	0.20	-1.77
SF.131201	36	1	3	1	2	0	1	58.81	189.6	0.18	-1.81	0.21	-1.79	0.19	-1.84	0.23	-1.79
SF.333021	48	3	3	3	0	2	1	58.87	213.7	0.18	-1.83	0.16	-1.88	0.18	-1.86	0.17	-1.88
SF.301211	48	3	0	1	2	1	1	58.89	213.8	0.18	-1.82	0.15	-1.89	0.19	-1.84	0.15	-1.89
SF.221512	51	2	2	1	5	1	2	58.92	219.8	0.16	-1.87	0.16	-1.88	0.16	-1.89	0.17	-1.88
SF.130212	36	1	3	0	2	1	2	59.30	190.6	0.16	-1.84	0.17	-1.83	0.15	-1.87	0.18	-1.83
SF.130512	36	1	3	0	5	1	2	59.32	190.6	0.16	-1.84	0.17	-1.84	0.16	-1.87	0.18	-1.85
SF.131500	27	1	3	1	5	0	0	59.38	172.8	0.15	-1.85	0.13	-1.88	0.15	-1.88	0.13	-1.88
SF.310212	39	3	1	0	2	1	2	59.42	196.8	0.15	-1.85	0.13	-1.91	0.14	-1.88	0.13	-1.91
SF.221111	51	2	2	1	1	1	1	59.44	220.9	0.16	-1.84	0.17	-1.84	0.15	-1.87	0.18	-1.84
SF.100322	27	1	0	0	3	2	2	59.47	172.9	0.15	-1.85	0.17	-1.85	0.14	-1.88	0.17	-1.86
SF.311021	39	3	1	1	0	2	1	59.52	197.0	0.15	-1.85	0.14	-1.91	0.14	-1.88	0.14	-1.91
SF.210102	27	2	1	0	1	0	2	59.54	173.1	0.15	-1.86	0.15	-1.90	0.13	-1.89	0.15	-1.90
SF.301120	36	3	0	1	1	2	0	59.58	191.2	0.13	-1.88	0.10	-1.90	0.11	-1.89	0.09	-1.90
SF.421502	84	4	2	1	5	0	2	59.59	287.2	0.15	-1.86	0.15	-1.90	0.14	-1.88	0.16	-1.90
SF.414011	84	4	1	4	0	1	1	59.60	287.2	0.14	-1.86	0.14	-1.91	0.13	-1.88	0.15	-1.91

SF.323502	39	3	2	3	5	0	2	59.61	197.2	0.15	-1.84	0.17	-1.80	0.16	-1.87	0.18	-1.79
SF.111510	30	1	1	1	5	1	0	59.64	179.3	0.13	-1.88	0.11	-1.91	0.12	-1.90	0.11	-1.91
SF.211421	51	2	1	1	4	2	1	59.64	221.3	0.14	-1.86	0.11	-1.92	0.13	-1.88	0.09	-1.92
SF.111502	30	1	1	1	5	0	2	59.68	179.4	0.14	-1.87	0.15	-1.88	0.13	-1.89	0.15	-1.88
SF.133002	27	1	3	3	0	0	2	59.72	173.4	0.14	-1.86	0.15	-1.88	0.14	-1.88	0.16	-1.87
SF.113001	21	1	1	3	0	0	1	59.77	161.5	0.15	-1.82	0.12	-1.88	0.17	-1.85	0.11	-1.88
SF.120510	21	1	2	0	5	1	0	59.81	161.6	0.14	-1.88	0.13	-1.89	0.13	-1.90	0.14	-1.89
SF.210322	39	2	1	0	3	2	2	59.84	197.7	0.13	-1.88	0.12	-1.91	0.12	-1.90	0.12	-1.91
SF.130310	27	1	3	0	3	1	0	59.93	173.9	0.12	-1.89	0.13	-1.91	0.12	-1.91	0.13	-1.92
SF.220510	27	2	2	0	5	1	0	59.94	173.9	0.13	-1.88	0.12	-1.90	0.12	-1.91	0.13	-1.90
SF.220201	27	2	2	0	2	0	1	60.14	174.3	0.11	-1.91	0.12	-1.91	0.10	-1.93	0.12	-1.91
SF.113201	30	1	1	3	2	0	1	60.17	180.3	0.12	-1.88	0.13	-1.93	0.12	-1.90	0.14	-1.93
SF.123512	39	1	2	3	5	1	2	60.23	198.5	0.13	-1.88	0.10	-1.92	0.13	-1.90	0.10	-1.92
SF.201420	36	2	0	1	4	2	0	60.24	192.5	0.10	-1.92	0.09	-1.93	0.09	-1.94	0.09	-1.94
SF.201101	36	2	0	1	1	0	1	60.24	192.5	0.11	-1.90	0.09	-1.92	0.10	-1.91	0.08	-1.92
SF.101320	27	1	0	1	3	2	0	60.33	174.7	0.11	-1.90	0.11	-1.92	0.10	-1.92	0.11	-1.92
SF.300212	36	3	0	0	2	1	2	60.45	192.9	0.11	-1.91	0.14	-1.91	0.11	-1.92	0.16	-1.91
SF.331502	48	3	3	1	5	0	2	60.51	217.0	0.10	-1.91	0.08	-1.94	0.08	-1.93	0.08	-1.94
SF.110120	21	1	1	0	1	2	0	60.67	163.3	0.08	-1.94	0.09	-1.95	0.07	-1.95	0.09	-1.95
SF.120120	21	1	2	0	1	2	0	60.69	163.4	0.08	-1.93	0.09	-1.94	0.08	-1.94	0.09	-1.94
SF.111500	21	1	1	1	5	0	0	60.76	163.5	0.06	-1.96	0.06	-1.97	0.05	-1.97	0.06	-1.97
SF.230101	36	2	3	0	1	0	1	60.91	193.8	0.07	-1.94	0.08	-1.95	0.07	-1.95	0.08	-1.95
SF.333511	60	3	3	3	5	1	1	61.51	243.0	0.03	-1.98	0.02	-1.99	0.02	-1.98	0.02	-1.99
SF.430021	81	4	3	0	0	2	1	61.56	285.1	0.04	-1.98	0.04	-1.98	0.04	-1.98	0.04	-1.98

Table A 3: Performance of the SOFIA model SF.124421 depending on the type of cost function that is used in optimization.

Name	**SOFIA model SF.124421 with different cost functions in optimization:**	**Comparison against GFED.BA (1997-2011)**						**Comparison against CCI.BA (2005-2011)**			
		Training (1817 cells, even years in 1998-2010) Data used for training of RF and for SF parameter optimization				Evaluation (1212 cells, uneven years in 1997-2011)		Training (even years in 2006-2010)		Evaluation (uneven years in 2005-2011)	
		SSE	**AIC**	**IoA**	**FV**	**IoA**	**FV**	**IoA**	**FV**	**IoA**	**FV**
SF.SSE (SF.124421 in Tab. S2)	Default cost function, sum of squared error $Cost = \sum_{i=1}^{i=N}(sim_i - obs_i)^2$	53.40	184.8	0.40	-1.51	0.39	-1.51	0.39	-1.59	0.41	-1.51
SF.KGE	Kling-Gupta efficiency: Euclidean distance in a 3-dimensional space defined by components for correlation, variance, and bias (Gupta et al., 2009) $Cost = \sqrt{(r-1)^2 + \left(\frac{\sigma_{sim}}{\sigma_{obs}} - 1\right)^2 + \left(\frac{\overline{sim}}{\overline{obs}} - 1\right)^2}$ *r* is the Pearson correlation coefficient between *sim* and *obs*	91.28	260.6	0.30	-0.25	0.31	-0.50	0.31	-0.48	0.33	-0.50
SF.IoA-FV	Analogously to KGE, the Euclidean distance in a 2-dimensional space defined by IoA and FV $Cost = \sqrt{(IoA-1)^2 + FV^2}$	90.43	258.9	0.44	0.00	0.45	-0.25	0.45	-0.22	0.46	-0.29
SF.SSE-sqrt	Sum of squared error based on square root-transformed fractional burned area $Cost = \sum_{i=1}^{i=N}(\sqrt{sim_i} - \sqrt{obs_i})^2$	58.15	194.3	0.15	-1.94	0.13	-1.96	0.15	-1.95	0.13	-1.96
SF.SSE-anom	Sum of squared error but with anomalies *x'* included as additional component. $Cost = SSE(sim, obs) + SSE(sim', obs')$ Anomalies defined as the difference to a rolling mean value with a window length of 121 months: $x' = x - rollMean(x)$	57.20	192.4	0.25	-1.73	0.20	-1.81	0.22	-1.78	0.19	-1.82

Formatted: Complex Script Font: Times New Roman, 12 pt, Dutch (Netherlands)

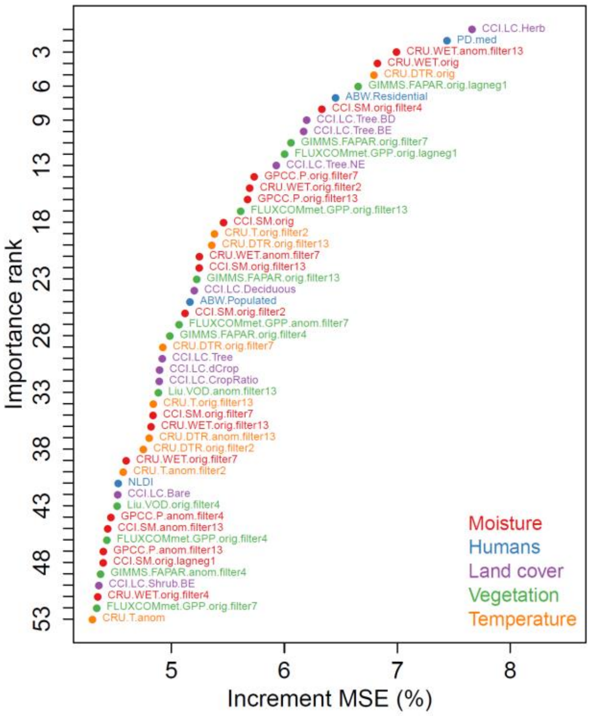

Figure A 1: Importance of several predictor variables to predict monthly burned area using random forest. Importance is expressed as the percentage increment in mean squared error if a certain variable is not included in random forest. Thus, the most important variables cause the largest increment in MSE. Variables that include “orig” or “anom” indicates original absolute values and anomalies (relative to the mean seasonal cycle), respectively. “filterX” indicates mean values over the X precedent months before the actual month for which burned area should be predicted. In total 132 variables were included in this analysis but variables below rank 53 are not shown in this figure).

Formatted: Caption, Don't keep with next

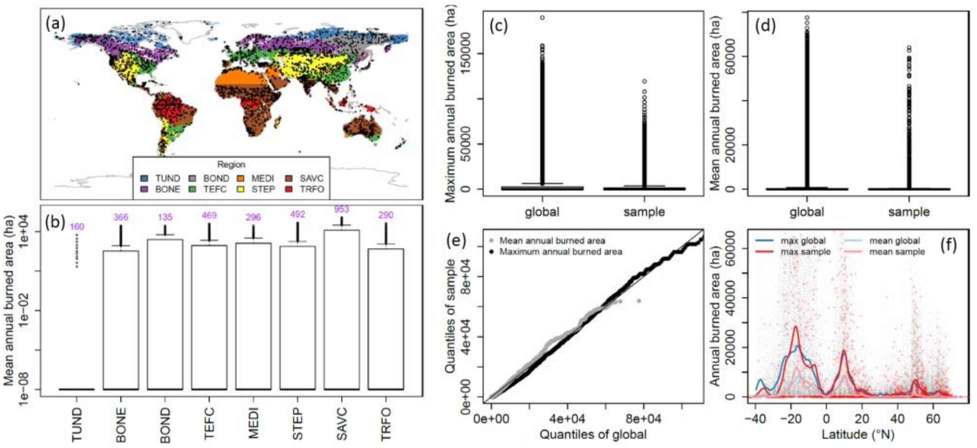

Figure A 2: Representativeness of sampled 0.25° grid cells for global patterns of burned area (based on GFED burned data). (a) Spatial distribution of the grid cells of the optimization and evaluation data subsets and regions for regional analyses of results. Regions are TUND (tundra), BONE (boreal needle-leaved evergreen and mixed forests), BOND (boreal needle-leaved deciduous forests), TEFC (temperate forests and croplands), MEDI (Mediterranean regions), STEP (steppes), SAVC (savannahs and tropical croplands), and TRFO (tropical forests). (b) Distribution of mean annual burned area per region from the sampled grid cells. Numbers indicate the number of grid cells per regions. (c-f) Comparison of mean and maximum annual burned between all global grid cells and the sampled grid cells. (c) and (d) distribution of maximum and mean annual burned. (e) Quantiles of mean and maximum annual burned area. (f) Latitudinal gradients of annual burned area. Latitudinal gradients are smoothing splines fitted to the quantile 0.95 of mean and maximum annual burned area, respectively.

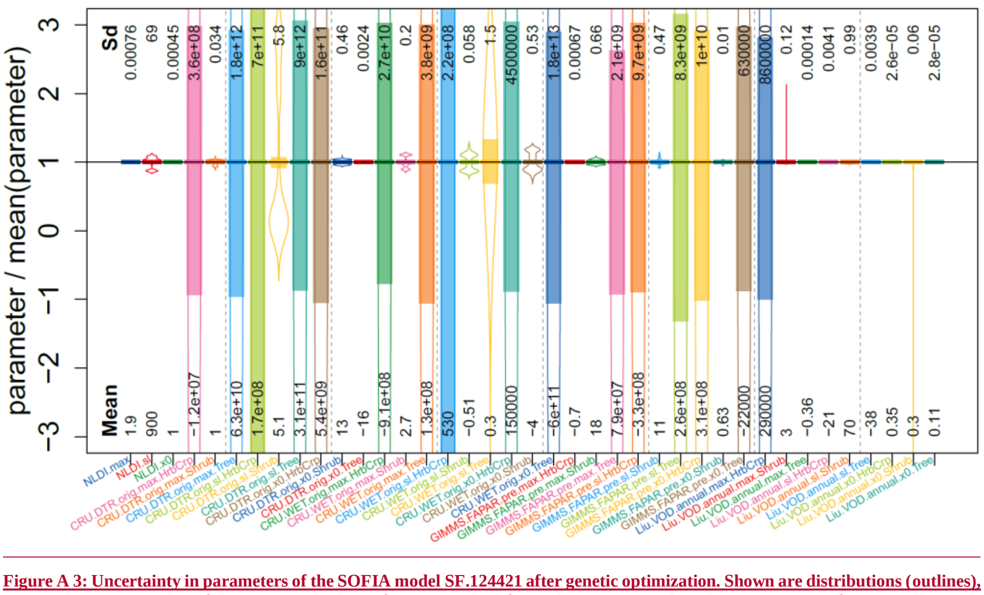

Figure A 3: Uncertainty in parameters of the SOFIA model SF.124421 after genetic optimization. Shown are distributions (outlines), mean values (= 1), and confidence intervals (bars) for mean values for each parameter. Plotted are parameters from equally good-performing parameter sets (i.e. > 0.8 * normalized likelihood NLL, NLL = LL / max(LL) with LL = exp(-SSE)).

Author contribution

Formatted: Font color: Auto

M. Forkel and W. Dorigo designed the study and experimental setup. M. Forkel developed code, carried out the analysis, and mainly wrote the manuscript. I. Teubner contributed with data pre-processing. G. Lasslop performed JSBACH-SPITFIRE model runs. K. Thonicke and E. Chuvieco contributed with conceptual ideas and references. All co-authors discussed results and contributed to the manuscript.

Competing interests

Formatted: Font color: Auto

The authors declare that they have no conflict of interest.

Acknowledgements

Formatted: Font color: Auto

This work was supported by the European Space Agency through a Living Planet Fellowship for M. Forkel (CCI4SOFIE, CCI data for assessing soil moisture controls on fire emissions) and by the TU Wien Wissenschaftspreis 2015, a personal science award assigned to W. Dorigo from the Vienna University of Technology. We further thank the following organisations, projects, portals, and researchers for providing datasets: ESA CCI, GFED, CRU, GPCC, GIMMS, NASA SEDAC, NOAA EOG, and Y. Liu.

References

Formatted: Font color: Auto

Albergel, C., Dorigo, W., Balsamo, G., Muñoz-Sabater, J., de Rosnay, P., Isaksen, L., Brocca, L., de Jeu, R. and Wagner, W.: Monitoring multi-decadal satellite earth observation of soil moisture products through land surface reanalyses, Remote Sens. Environ., 138, 77–89, doi:10.1016/j.rse.2013.07.009, 2013.

Aldersley, A., Murray, S. J. and Cornell, S. E.: Global and regional analysis of climate and human drivers of wildfire, Sci. Total Environ., 409(18), 3472–3481, doi:10.1016/j.scitotenv.2011.05.032, 2011.

Alonso-Canas, I. and Chuvieco, E.: Global burned area mapping from ENVISAT-MERIS and MODIS active fire data, Remote Sens. Environ., 163, 140–152, doi:10.1016/j.rse.2015.03.011, 2015.

Andela, N. and van der Werf, G. R.: Recent trends in African fires driven by cropland expansion and El Nino to La Nina transition, Nat. Clim. Change, 4(9), 791–795, doi:10.1038/nclimate2313, 2014.

Andela, N., Liu, Y. Y., van Dijk, A. I. J. M., de Jeu, R. A. M. and McVicar, T. R.: Global changes in dryland vegetation dynamics (1988–2008) assessed by satellite remote sensing: comparing a new passive microwave vegetation density record with reflective greenness data, Biogeosciences, 10(10), 6657–6676, doi:10.5194/bg-10-6657-2013, 2013.

Andela, N., van der Werf, G. R., Kaiser, J. W., van Leeuwen, T. T., Wooster, M. J. and Lehmann, C. E. R.: Biomass burning fuel consumption dynamics in the tropics and subtropics assessed from satellite, Biogeosciences, 13(12), 3717–3734, doi:10.5194/bg-13-3717-2016, 2016.

Archibald, S., Roy, D. P., Van Wilgen, B. W. and Scholes, R. J.: What limits fire? An examination of drivers of burnt area in Southern Africa, Glob. Change Biol., 15(3), 613–630, doi:10.1111/j.1365-2486.2008.01754.x, 2009.

Archibald, S., Lehmann, C. E. R., Gómez-Dans, J. L. and Bradstock, R. A.: Defining pyromes and global syndromes of fire regimes, Proc. Natl. Acad. Sci., 110(16), 6442–6447, doi:10.1073/pnas.1211466110, 2013.

Avitabile, V., Herold, M., Heuvelink, G. B. M., Lewis, S. L., Phillips, O. L., Asner, G. P., Armston, J., Ashton, P. S., Banin, L., Bayol, N., Berry, N. J., Boeckx, P., Jong, B. H. J., DeVries, B., Girardin, C. A. J., Kearsley, E., Lindsell, J. A., Lopez-Gonzalez, G., Lucas, R., Malhi, Y., Morel, A., Mitchard, E. T. A., Nagy, L., Qie, L., Quinones, M. J., Ryan, C. M., Ferry, S. J. W., Sunderland, T., Laurin, G. V., Gatti, R. C., Valentini, R., Verbeeck, H., Wijaya, A. and Willcock, S.: An integrated pan-tropical biomass map using multiple reference datasets, Glob. Change Biol., doi:10.1111/gcb.13139, 2016.

Balk, D. L., Deichmann, U., Yetman, G., Pozzi, F., Hay, S. I. and Nelson, A.: Determining Global Population Distribution: Methods, Applications and Data, in Advances in Parasitology, vol. 62, edited by A. G. and D. J. R. Simon I. Hay, pp. 119–

156, Academic Press. [online] Available from: http://www.sciencedirect.com/science/article/pii/S0065308X05620040 (Accessed 13 July 2016), 2006.

Balzter, H., Gerard, F. F., George, C. T., Rowland, C. S., Jupp, T. E., McCallum, I., Shvidenko, A., Nilsson, S., Sukhinin, A., Onuchin, A. and Schmullius, C.: Impact of the Arctic Oscillation pattern on interannual forest fire variability in Central Siberia, Geophys Res Lett, 32(14), L14709–L14709, doi:10.1029/2005gl022526, 2005.

Bedia, J., Herrera, S., Gutiérrez, J. M., Zavala, G., Urbieta, I. R. and Moreno, J. M.: Sensitivity of fire weather index to different reanalysis products in the Iberian Peninsula, Nat. Hazards Earth Syst. Sci., 12(3), 699–708, doi:10.5194/nhess-12-699-2012, 2012.

Bistinas, I., Harrison, S. P., Prentice, I. C. and Pereira, J. M. C.: Causal relationships versus emergent patterns in the global controls of fire frequency, Biogeosciences, 11(18), 5087–5101, doi:10.5194/bg-11-5087-2014, 2014.

Bond, W. J.: Large parts of the world are brown or black: A different view on the "Green World"hypothesis, J. Veg. Sci., 16(3), 261–266, doi:10.1111/j.1654-1103.2005.tb02364.x, 2005.

Bowman, D. M. J. S., Balch, J. K., Artaxo, P., Bond, W. J., Carlson, J. M., Cochrane, M. A., D'Antonio, C. M., DeFries, R. S., Doyle, J. C., Harrison, S. P., Johnston, F. H., Keeley, J. E., Krawchuk, M. A., Kull, C. A., Marston, J. B., Moritz, M. A., Prentice, I. C., Roos, C. I., Scott, A. C., Swetnam, T. W., Werf, G. R. van der and Pyne, S. J.: Fire in the Earth System, Science, 324(5926), 481–484, doi:10.1126/science.1163886, 2009.

Bowman, D. M. J. S., Balch, J., Artaxo, P., Bond, W. J., Cochrane, M. A., D'Antonio, C. M., DeFries, R., Johnston, F. H., Keeley, J. E., Krawchuk, M. A., Kull, C. A., Mack, M., Moritz, M. A., Pyne, S., Roos, C. I., Scott, A. C., Sodhi, N. S. and Swetnam, T. W.: The human dimension of fire regimes on Earth, J. Biogeogr., 38(12), 2223–2236, doi:10.1111/j.1365-2699.2011.02595.x, 2011.

Breiman, L.: Random Forests, Mach. Learn., 45(1), 5–32, doi:10.1023/A:1010933404324, 2001.

Burnham, K. P. and Anderson, D. R.: Model selection and multimodel inference a practical information-theoretic approach, Springer, New York. [online] Available from: http://site.ebrary.com/id/10047705 (Accessed 17 December 2013), 2002.

Cai, W., Yuan, W., Liang, S., Liu, S., Dong, W., Chen, Y., Liu, D. and Zhang, H.: Large Differences in Terrestrial Vegetation Production Derived from Satellite-Based Light Use Efficiency Models, Remote Sens., 6(9), 8945–8965, doi:10.3390/rs6098945, 2014.

Chuvieco, E. and Justice, C.: Relations Between Human Factors and Global Fire Activity, in Advances in Earth Observation of Global Change, edited by E. Chuvieco, J. Li, and X. Yang, pp. 187–199, Springer Netherlands, Dordrecht. [online] Available from: http://link.springer.com/10.1007/978-90-481-9085-0_14 (Accessed 24 October 2016), 2010.

Chuvieco, E., Giglio, L. and Justice, C.: Global characterization of fire activity: toward defining fire regimes from Earth observation data, Glob. Change Biol., 14(7), 1488–1502, doi:10.1111/j.1365-2486.2008.01585.x, 2008.

Chuvieco, E., Yue, C., Heil, A., Mouillot, F., Alonso-Canas, I., Padilla, M., Pereira, J. M., Oom, D. and Tansey, K.: A new global burned area product for climate assessment of fire impacts, Glob. Ecol. Biogeogr., 25(5), 619–629, doi:10.1111/geb.12440, 2016.

Dorigo, W., de Jeu, R., Chung, D., Parinussa, R., Liu, Y., Wagner, W. and Fernández-Prieto, D.: Evaluating global trends (1988–2010) in harmonized multi-satellite surface soil moisture, Geophys. Res. Lett., 39(18), L18405, doi:10.1029/2012GL052988, 2012.

Dorigo, W. A., Gruber, A., De Jeu, R. A. M., Wagner, W., Stacke, T., Loew, A., Albergel, C., Brocca, L., Chung, D., Parinussa, R. M. and Kidd, R.: Evaluation of the ESA CCI soil moisture product using ground-based observations, Remote Sens. Environ., 162, 380–395, doi:10.1016/j.rse.2014.07.023, 2015.

Elvidge, C. D., Baugh, K. E., Anderson, S. J., Sutton, P. C. and Ghosh, T.: The Night Light Development Index (NLDI): a spatially explicit measure of human development from satellite data, Soc. Geogr., 7(1), 23–35, doi:10.5194/sg-7-23-2012, 2012.

Forkel, M., Carvalhais, N., Verbesselt, J., Mahecha, M., Neigh, C. and Reichstein, M.: Trend Change Detection in NDVI Time Series: Effects of Inter-Annual Variability and Methodology, Remote Sens., 5(5), 2113–2144, doi:10.3390/rs5052113, 2013.

Forkel, M., Carvalhais, N., Schaphoff, S., v. Bloh, W., Migliavacca, M., Thurner, M. and Thonicke, K.: Identifying environmental controls on vegetation greenness phenology through model–data integration, Biogeosciences, 11(23), 7025–7050, doi:10.5194/bg-11-7025-2014, 2014.

Forkel, M., Migliavacca, M., Thonicke, K., Reichstein, M., Schaphoff, S., Weber, U. and Carvalhais, N.: Codominant water control on global interannual variability and trends in land surface phenology and greenness, Glob. Change Biol., 21(9), 3414–3435, doi:10.1111/gcb.12950, 2015.

Giglio, L., Randerson, J. T., van der Werf, G. R., Kasibhatla, P. S., Collatz, G. J., Morton, D. C. and DeFries, R. S.: Assessing variability and long-term trends in burned area by merging multiple satellite fire products, Biogeosciences, 7(3), 1171–1186, doi:10.5194/bg-7-1171-2010, 2010.

Giglio, L., Randerson, J. T. and van der Werf, G. R.: Analysis of daily, monthly, and annual burned area using the fourth-generation global fire emissions database (GFED4), J. Geophys. Res. Biogeosciences, 118(1), 317–328, doi:10.1002/jgrg.20042, 2013.

Goldewijk, K. K., Beusen, A. and Janssen, P.: Long-term dynamic modeling of global population and built-up area in a spatially explicit way: HYDE 3.1, The Holocene, 20(4), 565–573, doi:10.1177/0959683609356587, 2010.

Grégoire, J.-M., Tansey, K. and Silva, J. M. N.: The GBA2000 initiative: developing a global burned area database from SPOT-VEGETATION imagery, Int. J. Remote Sens., 24(6), 1369–1376, doi:10.1080/0143116021000044850, 2003.

Gupta, H. V., Kling, H., Yilmaz, K. K. and Martinez, G. F.: Decomposition of the mean squared error and NSE performance criteria: Implications for improving hydrological modelling, J. Hydrol., 377(1–2), 80–91, doi:10.1016/j.jhydrol.2009.08.003, 2009.

Hansen, M. C., DeFries, R. S., Townshend, J. R. G., Carroll, M., Dimiceli, C. and Sohlberg, R. a: Global Percent Tree Cover at a Spatial Resolution of 500 Meters: First Results of the MODIS Vegetation Continuous Fields Algorithm, Earth Interact., 7(10), 1–15, doi:10.1175/1087-3562(2003)007<0001:gptcaa>2.0.co;2, 2003.

Hantson, S., Lasslop, G., Kloster, S. and Chuvieco, E.: Anthropogenic effects on global mean fire size, Int. J. Wildland Fire, 24(5), 589–596, doi:10.1071/WF14208, 2015a.

Hantson, S., Pueyo, S. and Chuvieco, E.: Global fire size distribution is driven by human impact and climate: Spatial trends in global fire size distribution, Glob. Ecol. Biogeogr., 24(1), 77–86, doi:10.1111/geb.12246, 2015b.

Hantson, S., Arneth, A., Harrison, S. P., Kelley, D. I., Prentice, I. C., Rabin, S. S., Archibald, S., Mouillot, F., Arnold, S. R., Artaxo, P., Bachelet, D., Ciais, P., Forrest, M., Friedlingstein, P., Hickler, T., Kaplan, J. O., Kloster, S., Knorr, W., Lasslop, G., Li, F., Mangeon, S., Melton, J. R., Meyn, A., Sitch, S., Spessa, A., van der Werf, G. R., Voulgarakis, A. and Yue, C.: The status and challenge of global fire modelling, Biogeosciences, 13(11), 3359–3375, doi:10.5194/bg-13-3359-2016, 2016.

Harris, I., Jones, P. d., Osborn, T. j. and Lister, D. h.: Updated high-resolution grids of monthly climatic observations – the CRU TS3.10 Dataset, Int. J. Climatol., 34(3), 623–642, doi:10.1002/joc.3711, 2014.

Hess, J. C., Scott, C. A., Hufford, G. L. and Fleming, M. D.: El Nino and its impact on fire weather conditions in Alaska, Int. J. Wildland Fire, 10(1), 1–13, doi:10.1071/wf01007, 2001.

Hurtt, G. C., Chini, L. P., Frolking, S., Betts, R. A., Feddema, J., Fischer, G., Fisk, J. P., Hibbard, K., Houghton, R. A., Janetos, A., Jones, C. D., Kindermann, G., Kinoshita, T., Goldewijk, K. K., Riahi, K., Shevliakova, E., Smith, S., Stehfest, E., Thomson, A., Thornton, P., Vuuren, D. P. van and Wang, Y. P.: Harmonization of land-use scenarios for the period 1500–2100: 600 years of global gridded annual land-use transitions, wood harvest, and resulting secondary lands, Clim. Change, 109(1–2), 117, doi:10.1007/s10584-011-0153-2, 2011.

Janssen, P. H. M. and Heuberger, P. S. C.: Calibration of process-oriented models, Ecol. Model., 83(1–2), 55–66, doi:10.1016/0304-3800(95)00084-9, 1995.

Jolly, W. M., Nemani, R. and Running, S. W.: A generalized, bioclimatic index to predict foliar phenology in response to climate, Glob. Change Biol., 11(4), 619–632, doi:10.1111/j.1365-2486.2005.00930.x, 2005.

Kaminski, T., Knorr, W., Schürmann, G., Scholze, M., Rayner, P. J., Zaehle, S., Blessing, S., Dorigo, W., Gayler, V., Giering, R., Gobron, N., Grant, J. P., Heimann, M., Hooker-Stroud, A., Houweling, S., Kato, T., Kattge, J., Kelley, D., Kemp, S., Koffi, E. N., Köstler, C., Mathieu, P.-P., Pinty, B., Reick, C. H., Rödenbeck, C., Schnur, R., Scipal, K., Sebald, C., Stacke, T., van Scheltinga, A. T., Vossbeck, M., Widmann, H. and Ziehn, T.: The BETHY/JSBACH Carbon Cycle Data Assimilation System: experiences and challenges, J. Geophys. Res. Biogeosciences, 118(4), 1414–1426, doi:10.1002/jgrg.20118, 2013.

Kasischke, E. S. and Bruhwiler, L. P.: Emissions of carbon dioxide, carbon monoxide, and methane from boreal forest fires in 1998, J. Geophys. Res. Atmospheres, 107(D1), 8146, doi:10.1029/2001JD000461, 2002.

Keenan, T., Carbone, M., Reichstein, M. and Richardson, A.: The model–data fusion pitfall: assuming certainty in an uncertain world, Oecologia, 167(3), 587–597, doi:10.1007/s00442-011-2106-x, 2011.

Kelley, D. I. and Harrison, S. P.: Enhanced Australian carbon sink despite increased wildfire during the 21st century, Environ. Res. Lett., 9(10), 104015, doi:10.1088/1748-9326/9/10/104015, 2014.

Kelley, D. I., Prentice, I. C., Harrison, S. P., Wang, H., Simard, M., Fisher, J. B. and Willis, K. O.: A comprehensive benchmarking system for evaluating global vegetation models, Biogeosciences, 10(5), 3313–3340, doi:10.5194/bg-10-3313-2013, 2013.

Kloster, S., Mahowald, N. M., Randerson, J. T., Thornton, P. E., Hoffman, F. M., Levis, S., Lawrence, P. J., Feddema, J. J., Oleson, K. W. and Lawrence, D. M.: Fire dynamics during the 20th century simulated by the Community Land Model, Biogeosciences, 7(6), 1877–1902, doi:10.5194/bg-7-1877-2010, 2010.

Knorr, W., Kaminski, T., Arneth, A. and Weber, U.: Impact of human population density on fire frequency at the global scale, Biogeosciences, 11(4), 1085–1102, doi:10.5194/bg-11-1085-2014, 2014.

Krawchuk, M. A. and Moritz, M. A.: Constraints on global fire activity vary across a resource gradient, Ecology, 92(1), 121–132, doi:10.1890/09-1843.1, 2011.

Krueger, E. S., Ochsner, T. E., Engle, D. M., Carlson, J. D., Twidwell, D. and Fuhlendorf, S. D.: Soil Moisture Affects Growing-Season Wildfire Size in the Southern Great Plains, Soil Sci. Soc. Am. J., 79(6), 1567–1576, doi:10.2136/sssaj2015.01.0041, 2015.

Krueger, E. S., Ochsner, T. E., Carlson, J. D., Engle, D. M., Twidwell, D. and Fuhlendorf, S. D.: Concurrent and antecedent soil moisture relate positively or negatively to probability of large wildfires depending on season, Int. J. Wildland Fire, 25(6), 657–668, doi:10.1071/WF15104, 2016.

Langenfelds, R. L., Francey, R. J., Pak, B. C., Steele, L. P., Lloyd, J., Trudinger, C. M. and Allison, C. E.: Interannual growth rate variations of atmospheric CO_2 and its $\delta^{13}C$, H_2, CH_4, and CO between 1992 and 1999 linked to biomass burning, Glob. Biogeochem. Cycles, 16(3), 1048, doi:10.1029/2001GB001466, 2002.

Lasslop, G., Thonicke, K. and Kloster, S.: SPITFIRE within the MPI Earth system model: Model development and evaluation, J. Adv. Model. Earth Syst., 6(3), 740–755, doi:10.1002/2013MS000284, 2014.

Lasslop, G., Hantson, S. and Kloster, S.: Influence of wind speed on the global variability of burned fraction: a global fire model's perspective, Int. J. Wildland Fire, doi:10.1071/WF15052, 2015.

Le Quéré, C., Peters, G. P., Andres, R. J., Andrew, R. M., Boden, T. A., Ciais, P., Friedlingstein, P., Houghton, R. A., Marland, G., Moriarty, R., Sitch, S., Tans, P., Arneth, A., Arvanitis, A., Bakker, D. C. E., Bopp, L., Canadell, J. G., Chini, L. P., Doney, S. C., Harper, A., Harris, I., House, J. I., Jain, A. K., Jones, S. D., Kato, E., Keeling, R. F., Klein Goldewijk, K., Körtzinger, A., Koven, C., Lefèvre, N., Maignan, F., Omar, A., Ono, T., Park, G.-H., Pfeil, B., Poulter, B., Raupach, M. R., Regnier, P., Rödenbeck, C., Saito, S., Schwinger, J., Segschneider, J., Stocker, B. D., Takahashi, T., Tilbrook, B., van Heuven, S., Viovy, N., Wanninkhof, R., Wiltshire, A. and Zaehle, S.: Global carbon budget 2013, Earth Syst. Sci. Data, 6(1), 235–263, doi:10.5194/essd-6-235-2014, 2014.

van Leeuwen, T. T., van der Werf, G. R., Hoffmann, A. A., Detmers, R. G., Rücker, G., French, N. H. F., Archibald, S., Carvalho Jr., J. A., Cook, G. D., de Groot, W. J., Hély, C., Kasischke, E. S., Kloster, S., McCarty, J. L., Pettinari, M. L., Savadogo, P., Alvarado, E. C., Boschetti, L., Manuri, S., Meyer, C. P., Siegert, F., Trollope, L. A. and Trollope, W. S. W.: Biomass burning fuel consumption rates: a field measurement database, Biogeosciences, 11(24), 7305–7329, doi:10.5194/bg-11-7305-2014, 2014.

Lehsten, V., Harmand, P., Palumbo, I. and Arneth, A.: Modelling burned area in Africa, Biogeosciences, 7(10), 3199–3214, doi:10.5194/bg-7-3199-2010, 2010.

Liaw, A. and Wiener, M.: Classification and Regression by randomForest, R News, 2(3), 18–22, 2002.

Liu, Y. Y., Parinussa, R. M., Dorigo, W. A., De Jeu, R. A. M., Wagner, W., van Dijk, A. I. J. M., McCabe, M. F. and Evans, J. P.: Developing an improved soil moisture dataset by blending passive and active microwave satellite-based retrievals, Hydrol Earth Syst Sci, 15(2), 425–436, doi:10.5194/hess-15-425-2011, 2011a.

Liu, Y. Y., de Jeu, R. A. M., McCabe, M. F., Evans, J. P. and van Dijk, A. I. J. M.: Global long-term passive microwave satellite-based retrievals of vegetation optical depth, Geophys. Res. Lett., 38(18), L18402, doi:10.1029/2011GL048684, 2011b.

Liu, Y. Y., Dorigo, W. A., Parinussa, R. M., de Jeu, R. A. M., Wagner, W., McCabe, M. F., Evans, J. P. and van Dijk, A. I. J. M.: Trend-preserving blending of passive and active microwave soil moisture retrievals, Remote Sens. Environ., 123, 280–297, doi:10.1016/j.rse.2012.03.014, 2012.

Liu, Y. Y., van Dijk, A. I. J. M., McCabe, M. F., Evans, J. P. and de Jeu, R. A. M.: Global vegetation biomass change (1988–2008) and attribution to environmental and human drivers, Glob. Ecol. Biogeogr., 22(6), 692–705, doi:10.1111/geb.12024, 2013a.

Liu, Y. Y., van Dijk, A. I. J. M., de Jeu, R. A. M., Canadell, J. G., McCabe, M. F., Evans, J. P. and Wang, G.: Recent reversal in loss of global terrestrial biomass, Nat. Clim. Change, 5(5), 470–474, doi:10.1038/nclimate2581, 2015.

Liu, Z., Yang, J. and He, H. S.: Identifying the Threshold of Dominant Controls on Fire Spread in a Boreal Forest Landscape of Northeast China, PLOS ONE, 8(1), e55618, doi:10.1371/journal.pone.0055618, 2013b.

MacBean, N., Peylin, P., Chevallier, F., Scholze, M. and Schürmann, G.: Consistent assimilation of multiple data streams in a carbon cycle data assimilation system, Geosci. Model Dev. Discuss., 0, 1–44, doi:10.5194/gmd-2016-25, 2016.

Mebane, W. R. and Sekhon, J. S.: Genetic Optimization Using Derivatives: The rgenoud Package for R, J. Stat. Softw., 42(11), 2011.

Moritz, M. A., Parisien, M.-A., Batllori, E., Krawchuk, M. A., Van Dorn, J., Ganz, D. J. and Hayhoe, K.: Climate change and disruptions to global fire activity, Ecosphere, 3(6), 1–22, doi:10.1890/ES11-00345.1, 2012.

Murphy, B. P., Williamson, G. J. and Bowman, D. M. J. S.: Fire regimes: moving from a fuzzy concept to geographic entity, New Phytol., 192(2), 316–318, doi:10.1111/j.1469-8137.2011.03893.x, 2011.

Nemani, R. R., Keeling, C. D., Hashimoto, H., Jolly, W. M., Piper, S. C., Tucker, C. J., Myneni, R. B. and Running, S. W.: Climate-Driven Increases in Global Terrestrial Net Primary Production from 1982 to 1999, Science, 300(5625), 1560–1563, doi:10.1126/science.1082750, 2003.

Page, S. E., Siegert, F., Rieley, J. O., Boehm, H.-D. V., Jaya, A. and Limin, S.: The amount of carbon released from peat and forest fires in Indonesia during 1997, Nature, 420(6911), 61–65, doi:10.1038/nature01131, 2002.

Parisien, M.-A., Parks, S. A., Krawchuk, M. A., Flannigan, M. D., Bowman, L. M. and Moritz, M. A.: Scale-dependent controls on the area burned in the boreal forest of Canada, 1980--2005, Ecol. Appl., 21(3), 789–805, doi:10.1890/10-0326.1, 2010.

Pettinari, M. L. and Chuvieco, E.: Generation of a global fuel data set using the Fuel Characteristic Classification System, Biogeosciences, 13(7), 2061–2076, doi:10.5194/bg-13-2061-2016, 2016.

Pinzon, J. E. and Tucker, C. J.: A Non-Stationary 1981–2012 AVHRR NDVI3g Time Series, Remote Sens., 6(8), 6929–6960, doi:10.3390/rs6086929, 2014.

Poulter, B., Ciais, P., Hodson, E., Lischke, H., Maignan, F., Plummer, S. and Zimmermann, N. E.: Plant functional type mapping for earth system models, Geosci Model Dev, 4(4), 993–1010, doi:10.5194/gmd-4-993-2011, 2011.

Poulter, B., MacBean, N., Hartley, A., Khlystova, I., Arino, O., Betts, R., Bontemps, S., Boettcher, M., Brockmann, C., Defourny, P., Hagemann, S., Herold, M., Kirches, G., Lamarche, C., Lederer, D., Ottlé, C., Peters, M. and Peylin, P.: Plant functional type classification for earth system models: results from the European Space Agency's Land Cover Climate Change Initiative, Geosci Model Dev, 8(7), 2315–2328, doi:10.5194/gmd-8-2315-2015, 2015a.

Poulter, B., Cadule, P., Cheiney, A., Ciais, P., Hodson, E., Peylin, P., Plummer, S., Spessa, A., Saatchi, S., Yue, C. and Zimmermann, N. E.: Sensitivity of global terrestrial carbon cycle dynamics to variability in satellite-observed burned area, Glob. Biogeochem. Cycles, 29(2), 207–222, doi:10.1002/2013GB004655, 2015b.

Prentice, I. C., Kelley, D. I., Foster, P. N., Friedlingstein, P., Harrison, S. P. and Bartlein, P. J.: Modeling fire and the terrestrial carbon balance, Glob. Biogeochem. Cycles, 25(3), GB3005, doi:10.1029/2010GB003906, 2011.

Rabin, S. S., Melton, J. R., Lasslop, G., Bachelet, D., Forrest, M., Hantson, S., Li, F., Mangeon, S., Yue, C., Arora, V. K., Hickler, T., Kloster, S., Knorr, W., Nieradzik, L., Spessa, A., Folberth, G. A., Sheehan, T., Voulgarakis, A., Prentice, I. C., Sitch, S., Kaplan, J. O., Harrison, S. and Arneth, A.: The Fire Modeling Intercomparison Project (FireMIP), phase 1: Experimental and analytical protocols, Geosci. Model Dev. Discuss., 1–31, doi:10.5194/gmd-2016-237, 2016.

Raddatz, T., Reick, C., Knorr, W., Kattge, J., Roeckner, E., Schnur, R., Schnitzler, K. G., Wetzel, P. and Jungclaus, J.: Will the tropical land biosphere dominate the climate--carbon cycle feedback during the twenty-first century?, Clim. Dyn., 29, 565–574, 2007.

Randerson, J. T., Chen, Y., van der Werf, G. R., Rogers, B. M. and Morton, D. C.: Global burned area and biomass burning emissions from small fires, J. Geophys. Res. Biogeosciences, 117(G4), G04012, doi:10.1029/2012JG002128, 2012.

Roy, D. P., Jin, Y., Lewis, P. E. and Justice, C. O.: Prototyping a global algorithm for systematic fire-affected area mapping using MODIS time series data, Remote Sens. Environ., 97(2), 137–162, doi:10.1016/j.rse.2005.04.007, 2005.

Saatchi, S. S., Harris, N. L., Brown, S., Lefsky, M., Mitchard, E. T. A., Salas, W., Zutta, B. R., Buermann, W., Lewis, S. L., Hagen, S., Petrova, S., White, L., Silman, M. and Morel, A.: Benchmark map of forest carbon stocks in tropical regions across three continents, Proc. Natl. Acad. Sci., 108(24), 9899–9904, doi:10.1073/pnas.1019576108, 2011.

Schürmann, G. J., Kaminski, T., Köstler, C., Carvalhais, N., Voßbeck, M., Kattge, J., Giering, R., Rödenbeck, C., Heimann, M. and Zaehle, S.: Constraining a land-surface model with multiple observations by application of the MPI-Carbon Cycle Data Assimilation System V1.0, Geosci. Model Dev., 9(9), 2999–3026, doi:10.5194/gmd-9-2999-2016, 2016.

Seiler, W. and Crutzen, P. J.: Estimates of gross and net fluxes of carbon between the biosphere and the atmosphere from biomass burning, Clim. Change, 2(3), 207–247, doi:10.1007/BF00137988, 1980.

Simon, M., Plummer, S., Fierens, F., Hoelzemann, J. J. and Arino, O.: Burnt area detection at global scale using ATSR-2: The GLOBSCAR products and their qualification, J. Geophys. Res. Atmospheres, 109(D14), D14S02, doi:10.1029/2003JD003622, 2004.

Simpson, I. J., Rowland, F. S., Meinardi, S. and Blake, D. R.: Influence of biomass burning during recent fluctuations in the slow growth of global tropospheric methane, Geophys. Res. Lett., 33(22), doi:10.1029/2006GL027330, 2006.

Sitch, S., Smith, B., Prentice, I. C., Arneth, A., Bondeau, A., Cramer, W., Kaplan, J. O., Levis, S., Lucht, W., Sykes, M. T., Thonicke, K. and Venevsky, S.: Evaluation of ecosystem dynamics, plant geography and terrestrial carbon cycling in the LPJ dynamic global vegetation model, Glob. Change Biol., 9, 161–185, 2003.

Stöckli, R., Rutishauser, T., Baker, I., Liniger, M. a and Denning, a S.: A global reanalysis of vegetation phenology, J. Geophys. Res., 116(G3), G03020–G03020, doi:10.1029/2010jg001545, 2011.

Stocks, B. J., Lawson, B. D., Alexander, M. E., Van Wagner, C. E., McAlpine, R. S., Lynham, T. J. and Dubé, D. E.: The Canadian Forest Fire Danger Rating System: an overview., For. Chron., 65(6), 450–457, 1989.

Tansey, K., Grégoire, J.-M., Defourny, P., Leigh, R., Pekel, J.-F., van Bogaert, E. and Bartholomé, E.: A new, global, multi-annual (2000–2007) burnt area product at 1 km resolution, Geophys. Res. Lett., 35(1), L01401, doi:10.1029/2007GL031567, 2008.

Thonicke, K., Venevsky, S., Sitch, S. and Cramer, W.: The Role of Fire Disturbance for Global Vegetation Dynamics: Coupling Fire into a Dynamic Global Vegetation Model, Glob. Ecol. Biogeogr., 10(6), 661–677, 2001.

Thonicke, K., Spessa, A., Prentice, I. C., Harrison, S. P., Dong, L. and Carmona-Moreno, C.: The influence of vegetation, fire spread and fire behaviour on biomass burning and trace gas emissions: results from a process-based model, Biogeosciences, 7(6), 1991–2011, 2010.

Thurner, M., Beer, C., Santoro, M., Carvalhais, N., Wutzler, T., Schepaschenko, D., Shvidenko, A., Kompter, E., Ahrens, B., Levick, S. R. and Schmullius, C.: Carbon stock and density of northern boreal and temperate forests, Glob. Ecol. Biogeogr., 23(3), 297–310, doi:10.1111/geb.12125, 2014.

Tramontana, G., Jung, M., Schwalm, C. R., Ichii, K., Camps-Valls, G., Ráduly, B., Reichstein, M., Arain, M. A., Cescatti, A., Kiely, G., Merbold, L., Serrano-Ortiz, P., Sickert, S., Wolf, S. and Papale, D.: Predicting carbon dioxide and energy fluxes across global FLUXNET sites with regression algorithms, Biogeosciences, 13(14), 4291–4313, doi:10.5194/bg-13-4291-2016, 2016.

Venevsky, S., Thonicke, K., Sitch, S. and Cramer, W.: Simulating fire regimes in human-dominated ecosystems: Iberian Peninsula case study, Glob. Change Biol., 8(10), 984–998, 2002.

Verbesselt, J., Hyndman, R., Newnham, G. and Culvenor, D.: Detecting trend and seasonal changes in satellite image time series, Remote Sens. Environ., 114(1), 106–115, doi:10.1016/j.rse.2009.08.014, 2010a.

Verbesselt, J., Hyndman, R., Zeileis, A. and Culvenor, D.: Phenological change detection while accounting for abrupt and gradual trends in satellite image time series, Remote Sens. Environ., 114(12), 2970–2980, doi:10.1016/j.rse.2010.08.003, 2010b.

Vinogradova, A. A., Smirnov, N. S., Korotkov, V. N. and Romanovskaya, A. A.: Forest fires in Siberia and the Far East: Emissions and atmospheric transport of black carbon to the Arctic, Atmospheric Ocean. Opt., 28(6), 566–574, doi:10.1134/S1024856015060184, 2015.

Vreugdenhil, M., Dorigo, W. A., Wagner, W., Jeu, R. A. M. de, Hahn, S. and Marle, M. J. E. van: Analyzing the Vegetation Parameterization in the TU-Wien ASCAT Soil Moisture Retrieval, IEEE Trans. Geosci. Remote Sens., 54(6), 3513–3531, doi:10.1109/TGRS.2016.2519842, 2016a.

Vreugdenhil, M., Hahn, S., Melzer, T., Bauer-Marschallinger, B., Reimer, C., Dorigo, W. A. and Wagner, W.: Characterising vegetation dynamics over Australia with ASCAT, IEEE J. Sel. Top. Appl. Earth Obs. Remote Sens., accepted, 2016b.

Wei, Y., Liu, S., Huntzinger, D. N., Michalak, A. M., Viovy, N., Post, W. M., Schwalm, C. R., Schaefer, K., Jacobson, A. R., Lu, C., Tian, H., Ricciuto, D. M., Cook, R. B., Mao, J. and Shi, X.: The North American Carbon Program Multi-scale Synthesis and Terrestrial Model Intercomparison Project – Part 2: Environmental driver data, Geosci. Model Dev., 7(6), 2875–2893, doi:10.5194/gmd-7-2875-2014, 2014.

van der Werf, G. R., Randerson, J. T., Giglio, L., Collatz, G. J., Kasibhatla, P. S. and Arellano Jr, A. F.: Interannual variability in global biomass burning emissions from 1997 to 2004, Atmospheric Chem. Phys., 6(11), 3423–3441, 2006.

van der Werf, G. R., Randerson, J. T., Giglio, L., Collatz, G. J., Mu, M., Kasibhatla, P. S., Morton, D. C., DeFries, R. S., Jin, Y. and van Leeuwen, T. T.: Global fire emissions and the contribution of deforestation, savanna, forest, agricultural, and peat fires (1997–2009), Atmos Chem Phys, 10(23), 11707–11735, doi:10.5194/acp-10-11707-2010, 2010.

Williams, M., Richardson, A. D., Reichstein, M., Stoy, P. C., Peylin, P., Verbeeck, H., Carvalhais, N., Jung, M., Hollinger, D. Y., Kattge, J., Leuning, R., Luo, Y., Tomelleri, E., Trudinger, C. M. and Wang, Y. P.: Improving land surface models with FLUXNET data, Biogeosciences, 6(7), 1341–1359, doi:10.5194/bg-6-1341-2009, 2009.

Yebra, M., Dennison, P. E., Chuvieco, E., Riaño, D., Zylstra, P., Hunt Jr., E. R., Danson, F. M., Qi, Y. and Jurdao, S.: A global review of remote sensing of live fuel moisture content for fire danger assessment: Moving towards operational products, Remote Sens. Environ., 136, 455–468, doi:10.1016/j.rse.2013.05.029, 2013.

Yue, C., Ciais, P., Cadule, P., Thonicke, K., Archibald, S., Poulter, B., Hao, W. M., Hantson, S., Mouillot, F., Friedlingstein, P., Maignan, F. and Viovy, N.: Modelling the role of fires in the terrestrial carbon balance by incorporating SPITFIRE into the global vegetation model ORCHIDEE – Part 1: simulating historical global burned area and fire regimes, Geosci Model Dev, 7(6), 2747–2767, doi:10.5194/gmd-7-2747-2014, 2014.

Zhu, Z., Bi, J., Pan, Y., Ganguly, S., Anav, A., Xu, L., Samanta, A., Piao, S., Nemani, R. and Myneni, R.: Global Data Sets of Vegetation Leaf Area Index (LAI)3g and Fraction of Photosynthetically Active Radiation (FPAR)3g Derived from Global Inventory Modeling and Mapping Studies (GIMMS) Normalized Difference Vegetation Index (NDVI3g) for the Period 1981 to 2011, Remote Sens., 5(2), 927–948, doi:10.3390/rs5020927, 2013.

Deleted: Page Break